



DET TEKNISK-NATURVITENSKAPELIGE FAKULTET

MASTEROPPGAVE

Studieprogram/spesialisering: Offshore teknologi – Offshore systemer	Vårsemesteret, 2009 Åpen
Forfatter: Anne Kathrine Vaagsnes Singelstad (signatur forfatter)
Faglig ansvarlig: Katrine van Raaij Veileder: Eldar Tjelta	
Engelsk tittel på masteroppgaven: Nonlinear analysis of a space frame subjected to loading from dropped objects	
Studiepoeng: 30	
Emneord: Elasto-plastic material behaviour Nonlinear finite element analysis Modelling alternatives for dropped object Work considerations Accidental limit state (ALS)	Sidetall: 94 + vedlegg/annet: 14 Stavanger, 15.06.2009

Summary

There is always a risk of an object being dropped during offshore lifting operations. Any underlying structure or equipment might be severely damaged, and in worst case, lives might be lost. Consequently, structures which might be subjected to an accidental event with an annual probability of 10^{-4} are required to be designed in accidental limit state (ALS). Design in ALS often requires for the structural response to be taken into the plastic range, which means that nonlinear analysis methods must be used.

This master thesis deals with nonlinear structural response. For one specific case, results from hand calculations are compared to results obtained from nonlinear finite element analysis and evaluated as to give an indication of the usefulness of simplified methods to predict nonlinear structural response for the specific structure. The second objective of this master thesis is to compare two different ways of modelling a dropped object scenario in a finite element analysis program. The first, method 1, includes a model of the dropped object where a hyperelastic spring element is introduced to establish contact between the falling object and the underlying structure. In method 2, the node representing the point of impact is given an initial velocity equal to the velocity at impact for the same load scenario as in method 1. The case used for the hand calculations and the nonlinear finite element analyses is a space frame subjected to impact loading from a 6000 kg container dropped from a height of 3 m. The space frame will therefore be analyzed in the accidental limit state (ALS).

The nonlinear (dynamic) analyses have been carried out using the nonlinear finite element software USFOS. The model of the space frame was converted from the structural design and analysis program StaadPro.

It proved difficult to account for the selfweight and live load in work considerations since the dropped object loading is given as energy and the other two as (static) uniformly distributed loads. For a correct evaluation of the suitability of hand calculations the effect of selfweight and live load must be taken into account in the calculations.

Method 1 is, of the methods considered herein, the method which physically simulates a real dropped object scenario most correctly. Modelling alternative No. 2 gave larger maximum displacement than method 1, and results indicate that the actual amount of energy impacting the structure becomes larger for method 2 than for method 1. A possible improvement of method 2 has been suggested in the conclusion.

Preface

This master thesis represents the final part of the master degree in Offshore Technology with specialization in Offshore systems at the University of Stavanger. The work was carried out under the supervision of Professor Katrine van Raaij at the University of Stavanger in the spring 2009. The topic of this work was offered in November 2008 by Fabricom Suez (Stavanger), who also provided facilities and access to software.

I am outmost grateful to Katrine van Raaij who, despite of her tight time schedule this semester, still agreed to be my supervisor at UiS and who has given me valuable support and comments on the manuscript throughout this work.

I would also like to thank Fabricom Suez and Samir Vejzovic for providing me this thesis together with necessary software and working facilities. Finally, I would like to give a special thanks to my supervisor at Fabricom Suez, Eldar Tjelta, for always being available and for taking the time to discuss my many questions.

Stavanger, 15.06.2009

Table of contents

Summary	1
Preface	2
Notation and abbreviations	5
1 Introduction	8
1.1 Background.....	8
1.2 Scope of work.....	8
1.3 Limitations.....	9
1.4 Organization of the work.....	9
2 Rules and regulations	11
2.1 Government principles and regulations.....	11
2.2 Government requirements to safety and risk reduction relating to design of offshore structures.....	12
2.3 Standards.....	14
2.3.1 NORSOK.....	14
2.3.2 Others.....	14
2.4 Accidental loads.....	15
2.4.1 General.....	15
2.4.2 Risk assessment.....	15
2.5 Accidental Limit State (ALS).....	16
2.5.1 Overall requirements.....	16
3 Linear elastic response	17
3.1 Introduction.....	17
3.2 General structural response.....	17
3.3 Elastic analysis and general stress-strain relations.....	17
3.4 Dynamic response.....	19
3.5 Single-degree-of-freedom-systems.....	19
3.6 Dynamic amplification factor (DAF) for a system exposed to rectangular load pulse.....	20
4 Elasto-plastic material behaviour	23
4.1 General.....	23
4.2 Theory of plasticity.....	23
4.2.1 General stress-strain distribution.....	23
4.2.2 Moment distribution and the Mechanism Method.....	29
5 Finite element software	33
5.1 Introduction.....	33
5.2 Theoretical basis.....	33
5.2.1 Continuum mechanics.....	33
5.2.2 Finite element formulation.....	35
5.2.3 Formulation of nonlinear material behaviour.....	36
5.3 Incremental procedures.....	40
5.3.1 General.....	40
5.3.2 Equilibrium iteration.....	40
5.3.3 Plastic hinges.....	40
5.4 Dynamic analysis.....	41
6 Case – Impact loading	43
6.1 Introduction.....	43
6.2 Description of structural model.....	43

6.2.1	Geometry.....	43
6.2.2	Material properties.....	45
6.2.3	Load specifications.....	45
6.3	Cross-section requirements.....	46
6.4	Description of dropped object scenario.....	46
7	Nonlinear finite element analysis of space frame.....	48
7.1	Introduction.....	48
7.2	Method 1: Principle and modelling.....	48
7.3	Method 2: Principle and modelling.....	50
7.4	General dynamic input.....	51
7.5	Features of the hyperelastic spring.....	53
7.6	Damping.....	54
7.7	Repeated plastification/elastic unloading.....	55
8	Hand calculations.....	56
8.1	Work considerations.....	56
8.2	Axial restraint.....	60
8.3	Tensile fracture in yield hinges.....	62
9	Results.....	67
9.1	Method 1.....	67
9.1.1	General.....	67
9.1.2	Maximum displacement.....	67
9.1.3	Plastic utilization and development of plastic hinges.....	69
9.1.4	Beam strain.....	70
9.1.5	Energy.....	71
9.1.6	Γ_y -values.....	73
9.2	Method 2.....	75
9.2.1	General.....	75
9.2.2	Maximum displacement.....	75
9.2.3	Plastic utilization and development of plastic hinges.....	77
9.2.4	Strain.....	78
9.2.5	Energy.....	79
9.2.6	Γ_y -values.....	80
10	Discussion.....	83
10.1	Deflection.....	83
10.2	Collapse mechanism.....	85
10.3	Comparison of method 1 and method 2.....	87
10.4	Approximations to real material behaviour.....	88
10.5	Improvements of the calculations.....	89
10.6	Other considerations.....	90
11	Conclusion.....	91
	References.....	93
	Appendix A – Input files to nonlinear (dynamic) analysis - Method 1.....	95
A.1	Control file.....	95
A.2	Model file.....	96
	Appendix B – Input files to nonlinear (dynamic) analysis - Method 2.....	101
B.1	Control file.....	101
B.2	Model file.....	102
	Appendix C – Input file to static analysis for determination of stiffness.....	107

Notation and abbreviations

Abbreviations

ALARP	As Low As Reasonably Practicable
ALS	Accidental Limit State
BAT	Best Available Technology
DAF	Dynamic Amplification Factor
DAL	Design Accidental Load
DOP	Dropped Object Protection
FEM	Finite Element Method
FMEA	Failure Mode and Effect Analysis
HAZOP	Hazard and Operability Study
HSE	Health & Safety Executive
NPD	Norwegian Petroleum Directorate
NSHD	Norwegian Social and Health Directorate
PSA	Petroleum Safety Authority
RAC	Risk Acceptance Criteria
SDOF	Single Degree Of Freedom
SFT	Norwegian Pollution Control Authority
SJA	Safe Job Analysis
ULS	Ultimate Limit State

Mathematical symbols and operators

f	Function
δ	Variation
Δ	Increment
$\{ \}$	Vector
$[]$	Matrix

Vectors and matrices are also identified by boldface type.

Arabic letters

A	Cross-sectional area
c	Damping (viscous), or nondimensional spring stiffness
c_f	Axial flexibility factor
c_{lp}	Plastic zone length
c_w	Displacement factor
d_c	Characteristic dimension
E	Elasticity modulus
E_k	Kinetic energy
f_y	Yield strength

F	Force
F_D, \mathbf{F}_D	Damping force, matrix of damping forces
F_I, \mathbf{F}_I	Inertia force, matrix of damping forces
F_S	Spring force
F_y	Yield surface
F_b	Bounding surface
g	Acceleration from gravity, equal to 9.81 m/s ²
g_i	Surface normal at node i
H	Potential of external load (Heaviside), or nondimensional plastic stiffness
I	Moment of inertia
k	Stiffness
K	Equivalent elastic, axial stiffness
\mathbf{K}_T	Elastic stiffness matrix
\mathbf{K}_T^{EP}	Elasto-plastic stiffness matrix
L	Length of beam/element, may also be denoted by l
m	Mass
M	Moment
M_y	Yield moment
M_p	Plastic moment capacity
N	Axial force
N_p	Plastic axial capacity
P	Concentrated load
P_c	Collapse load
P_y	Load at to first yield
q	Uniformly distributed load
q_c	Uniformly distributed load at collapse
R_d	Design resistance
\mathbf{R}_{ext}	Matrix of external loads
\mathbf{R}_{int}	Matrix of internal loads
S_d	Design load
\mathbf{S}	Vector of force components
t	Time
t_d	Load duration
t_r	Load rise time
T	Natural period
U	Internal strain energy
u, \mathbf{v}	Displacement of material point, vector of displacements of material point
\mathbf{v}_N	Nodal displacements vector
V	Shear force, or volume
V_p	Plastic shear capacity
w	Deflection of material in the elastic range
w_c	Characteristic deformation

W	Elastic section modulus
W_e	External work
W_i	Internal work
W_p	Plastic section modulus
x	Displacement
\dot{x}	Velocity
\ddot{x}	Acceleration
y_{dyn}	Dynamic deflection
y_{st}	Static deflection

Greek symbols

δ	Displacement or change of deflection
δ_e	Elastic displacement
δ_p	Plastic displacement
ε	Strain
ε_{cr}	Critical strain
ε_y	Yield strain
ε_u	Ultimate strain
Φ	Shape (or interpolation) function matrix
φ	Curvature
Γ_y	Yield function
Π	Total potential
θ	Angle of rotation
σ	Stress
σ_y	Yield stress (strength)
σ_u	Ultimate tensile stress

1 Introduction

1.1 Background

Lifting operations are carried out on a daily basis on most offshore facilities. Containers and other equipment are loaded and unloaded, or simply moved from one location to another. The risk of an object being dropped during a lifting operation is always present, with severe structural damage and loss of human lives as potential consequences.

The objective of dropped object protection (DOP) is to prevent damage to critical equipment, and to protect oil- and gas pipelines from severe damage which might be followed by explosion. Certain parts of a platform such as laydown areas and storage areas are in general required to be reinforced in case of falling objects as to protect any underlying equipment, structure or personnel.

A structure subjected to impact loading from a dropped object shall be designed in accidental limit state (ALS). In order to avoid excessive economical costs or unnecessarily heavy structures, design in ALS normally allows for the structural response to be taken into the plastic range as long as the overall integrity is maintained. The structural design must comply with requirements related to health, safety and environment (the HSE regulations) and to more specific, technical requirements given mainly by the NORSOK or ISO standards. The amount of plastic deformation of a structure subjected to impact loading may be found from work considerations (hand calculations) or by the use of a suitable analysis program.

Nonlinear material behaviour is a relatively complex phenomenon, and many aspects of structural behaviour are difficult to express by mathematical formulas. A certain degree of idealization will always be necessary, both with respect to hand calculations and to more sophisticated computer analysis programs. The accuracy of the results depend upon how well structural effects such as partial end fixity, axial restraint, joint geometry, elasto-plastic material behaviour etc have been accounted for in the calculations or in the computer model. Generally, a nonlinear analysis program provides a more realistic modelling of real structural response. In many cases however, simplified (hand) calculations may give a reasonable estimation of the nonlinear response, with the advantage of being considerably less time-consuming than a nonlinear (dynamic) computer analysis.

1.2 Scope of work

The objective of this master thesis is to compare the results from a nonlinear (dynamic) finite element analysis of a specific space frame subjected to impact loading from a dropped object, with results obtained from hand calculations. Results from the two methods are studied in order to give an indication of the usefulness of hand calculations for the specified case compared to the more realistic, but also more time consuming, computerized nonlinear (dynamic) analysis. A second goal of this master thesis is to study two different ways of modelling a dropped object

scenario. The first, method 1, is a common way of performing a dropped object analysis. The second, method 2, is an alternative and less time consuming way of modelling a dropped object scenario. Basis is taken in a case; a laydown area on the Ekofisk M platform which is to be designed in accidental limit state (ALS) due to the risk of containers being dropped during lifting operations. The analyses are carried out using the nonlinear finite element program USFOS. Hand calculations are performed according to work considerations.

The modelling of a dropped object scenario and analysing the structure in a nonlinear finite element program has been an important part of the work.

1.3 Limitations

Because this work is not primarily a design check, all necessary checks for ALS may not have been accounted for. The space frame representing the case described in Chapter 6 is only analysed, not designed or modified to comply with the ALS criteria. Post accident resistance¹ is therefore not checked. In order to obtain results that are as correct, and thus as suitable, as possible for a comparison between analyses results and hand calculations, effort is put in evaluating one load scenario only. A complete design check would, obviously, have considered all possible load scenarios and various places of impact, including a more thorough check of connections etc.

The space frame described in Chapter 6 was intended to have plates attached later on such that analyses would be carried out for the structure with and without plates. Due to limited time, this has not been done and is therefore not part of this master thesis. Evaluation of failure modes is restricted to plastic collapse only.

In this master thesis, focus has been on deflection of the primary structure for the purpose of comparison between hand calculation and the two different modelling alternatives for computer analysis. Thus, the response of the secondary elements is not considered.

1.4 Organization of the work

The content of this master thesis is organized in 11 chapters of which this chapter is the first. Chapter 2 presents an overview of the regulations relating to petroleum activities on the Norwegian continental shelf, with emphasis on safety and risk reduction. Relevant standards and their requirements to structural design, and accidental limit state design in particular, are also covered.

The basic aspects of linear elastic response are described in Chapter 3. An explanation of the stress-strain curve for steel up to the point of rupture is also included. Chapter 4 gives a brief introduction to plastic material behaviour and kinematical considerations for calculating collapse load and plastic displacement.

¹ The second step of the ALS design check, see NORSOK N-001 (2004) or Chapter 2.5.1 in this master thesis.

Chapter 5 comprises an outline of the basic concepts of the analysis software used in this master thesis, along with a short explanation of certain topics considered relevant for the analyses that have been performed. A description of the case, including the dropped object scenario, is given in Chapter 6, while Chapter 7 explains the modelling and principles of the nonlinear dynamic analyses that have been carried out for the two different modelling alternatives. Chapter 7 also includes a description of the general input necessary to run a dynamic analysis.

Hand calculations are presented in Chapter 8, together with a check of maximum deflection in yield hinges according to NORSOK N-004 (2004). Results from the nonlinear (dynamic) analyses are presented in Chapter 9. A comparison of the results from the computer analyses (Chapter 9) and results obtained from hand calculations (Chapter 8) are given in Chapter 10. This chapter also includes an evaluation of the results that have been obtained, together with a brief discussion of potential improvements of the models and analyses methods. Chapter 11 presents a conclusion.

2 Rules and regulations

2.1 Government principles and regulations

All petroleum activity on the Norwegian continental shelf has to comply with the requirements in Norwegian laws and regulations. The general hierarchical structure of the legal system can be illustrated by Figure 2.1.

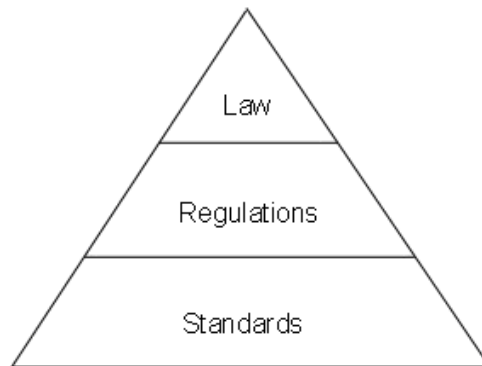


Figure 2.1 Hierarchical structure of the legal system.

For petroleum activity the Petroleum Activities Act is the superior, followed by regulations, guidelines (not legally binding), and supplementary standards such as NORSOK or DNV, as shown in Figure 2.2.

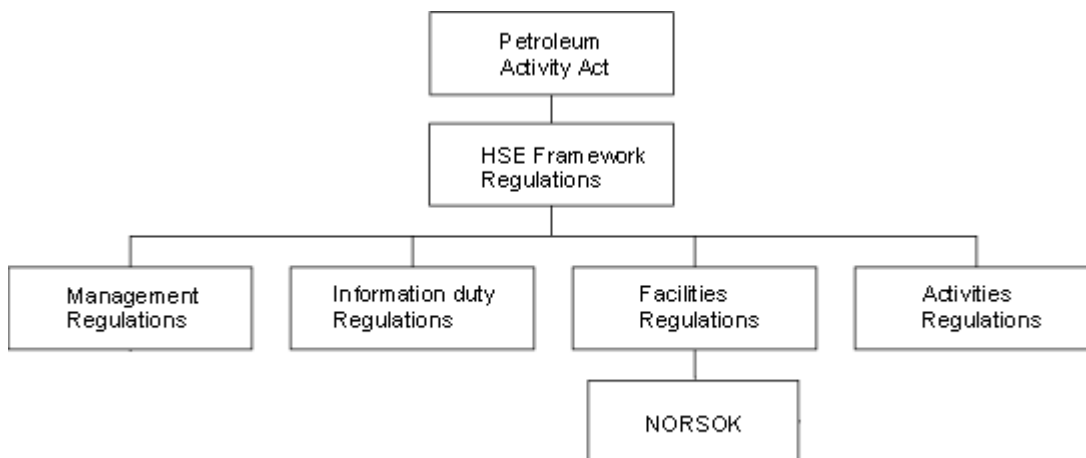


Figure 2.2 Rules and regulations regarding petroleum activity.

The relevant part of the legislation with respect to safety and structural engineering offshore are the offshore HSE regulations. Originally the HSE regulations comprised 25 separate documents. Through collaboration between the Norwegian Petroleum Directorate (NPD)¹, the Norwegian Social and Health Directorate (NSHD), and the Norwegian Pollution Control Authority (SFT) these rules have been reduced to five. The revised offshore HSE regulations entered into force 1 January 2002. They consist of the following five documents:

- The Framework Regulations (Royal Decree)
- The Management Regulations
- The Information duty Regulations
- The Facilities Regulations
- The Activities Regulations

The new regulations attach much importance to risk reduction principles related to health, environment and safety, as a way of reducing the risk of accidents, personal injury, health injury and harm to the environment to the greatest extent possible. Most of the provisions are formulated as functional requirements, i.e. the requirement is a result that must be satisfied, and shows what the government wishes to achieve (Petroleum Safety Authority, 11.02.2008).

To each regulation there is a guideline which recommends solutions in the form of industry standards or international standards such as NORSOK and ISO as a way of fulfilling the requirements. If there is a wish to use another solution than the one recommended by the guideline, it has to be documented that the other solution is as good as or better than the recommended one (Petroleum Safety Authority, 11.02.2008).

Most of the requirements relating to design of offshore structures are found in the Facilities Regulations. In addition, the Framework regulations and the Management regulations state some overall requirements regarding health, environment and safety, and general principles for risk reduction.

2.2 Government requirements to safety and risk reduction relating to design of offshore structures

In addition to the technical part of the design of offshore structures, safety and risk reduction related to health, environment and personnel is a very important aspect which always has to be considered.

The overall government requirements regarding offshore safety are found in the Framework regulations and the Management regulations.

¹ In 2004, the Petroleum Safety Authority (PSA) was established as a new independent regulatory body with the responsibility of technical and operational safety together with the working environment functions, which was previously under the authority of NPD.

Section 9 in the Framework Regulations contains the principles relating to risk reduction. The first part of Section 9 is the ALARP¹-principle: “Harm or danger of harm to people, the environment or to financial assets shall be prevented or limited in accordance with the legislation relating to health, the environment and safety, including internal requirements and acceptance criteria. Over and above this level the risk shall be further reduced to the extent possible. Assessments on the basis of this provision shall be made in all phases of the petroleum activities”. This requirement implies that risk shall be further reduced beyond the established minimum level for health, environment and safety stated in the regulations (Petroleumstilsynet (Ptil), Statens forurensningstilsyn (SFT), & Sosial- og helsedirektoratet (SHdir), 2002; RVK, 2006).

The ALARP-principle is followed by the principle of best available technology (the BAT principle), second paragraph, Section 9: “In effectuating risk reduction the party responsible shall choose the technical, operational or organizational solutions which according to an individual as well as an overall evaluation of the potential harm and present and future use offer the best results, provided the associated costs are not significantly disproportionate to the risk reduction achieved”. This means that the party responsible for the petroleum activities has to base its planning and operation on the technology and methods which, based on an overall evaluation, produce the best and most cost effective results (Petroleumstilsynet (Ptil) et al., 2002; RVK, 2006).

The so-called precautionary principle is expressed in paragraph 3, Section 9: “If there is insufficient knowledge about the effects that use of the technical, operational or organizational solutions may have on health, environment and safety, solutions that will reduce this uncertainty shall be chosen” (Petroleumstilsynet (Ptil) et al., 2002; RVK, 2006).

The 4th paragraph displays a way of thinking where alternative solutions with lower risk level always shall replace solutions with risk potential: “Factors which may cause harm, or nuisance to people, the environment or to financial assets in the petroleum activities shall be replaced by factors which in an overall evaluation have less potential for harm, or nuisance” (Petroleumstilsynet (Ptil) et al., 2002; RVK, 2006).

Another relevant provision in the Framework regulations is Section 11 concerning responsibility of sound health, environment and safety culture (Petroleumstilsynet (Ptil) et al., 2002; RVK, 2006).

Finally, there are two overall requirements to safety and risk reduction in the Management Regulations which also must be considered in relation to design of offshore installations. Section 1 expresses technical requirements regarding risk reduction:

- There shall be chosen technical solutions which reduces the probability that hazardous situations and accidents will occur
- Barriers shall be established to:
 - o prevent development of hazardous situations and accidents
 - o limit possible harm and nuisance (Petroleumstilsynet (Ptil) et al., 2002; RVK, 2006).

¹ ALARP – As Low As Reasonably Practicable

The second provision is related to barriers, Section 2. According to Section 2 there shall be established a strategy for outfitting, use and maintenance of barriers, and it must be known what barriers are already established and which function they are intended to fulfill (RVK, 2006).

For requirements related to risk assessment, see Chapter 2.4.2.

2.3 Standards

2.3.1 NORSOK

The NORSOK standards are the most utilized standards for projects regarding petroleum activity on the Norwegian continental shelf. The NORSOK standards are developed by the Norwegian petroleum industry, and are based on recognized international standards such as ISO and EN. They were developed to fill the needs of the Norwegian petroleum industry which were not already covered by international standards. The NORSOK standards are not legally binding, but they serve as references in the authorities' regulations, see Chapter 2.1. After publication of an international standard which covers the content of a NORSOK standard, the current NORSOK standard will be withdrawn (NORSOK N-001, 2004).

The relevant NORSOK standards for design of offshore structures are:

- N-001 Structural design
- N-003 Actions and action effects
- N-004 Design of steel structures

N-001 is the principle standard for offshore structures. N-003 specifies general principles and guidelines for determination of actions and action effects. N-004 specifies guidelines and requirements for design and documentation of offshore steel structures.

A more thorough description of the code requirements relating to design against accidental loads is given in Chapter 2.5.

2.3.2 Others

Other standards that might be referred to in the government guidelines are DnV, ISO and EN. While NORSOK N-004 is used for checking the capacity of tubular members, Eurocode 3 Part 1-1 is used for capacity check of other types of profiles.

2.4 Accidental loads

2.4.1 General

According to NORSOK N-003 accidental actions are “actions caused by abnormal operation or technical failure” (NORSOK N-003, 2007, p. 33), i.e. actions caused by human or technical error, or by an undesirable external effect. Such actions might be:

- fires and explosions
- impacts from ships
- dropped objects
- helicopter crash
- change of intended pressure difference, or
- unintended distribution of variable deck actions, e.g. ballast

An ALS design check shall be performed for accidental loads with an annual exceedance probability of 10^{-4} . The relevant accidental actions are defined in the risk assessment performed in accordance with NORSOK Z-013 and NORSOK S-001, and are referred to as ‘design accidental load’ (DAL). Relevant design cases are normally defined by the safety discipline and given in a design accidental load specification.

2.4.2 Risk assessment

In relation to any offshore operation the government requires that the probability of accidents is being evaluated and documented. This is done by the use of risk acceptance criteria (RAC) and risk analyses.

The term ‘risk acceptance criteria’ is defined in NORSOK Z-013, p. 7, as “criteria that are used to express a risk level that is considered tolerable for the activity in question”. The risk acceptance criteria shall be defined prior to any risk analysis, and then be compared to the results from the risk analysis in order to decide whether the estimated risk level is acceptable or not. The risk acceptance criteria also form the basis for further risk reduction.

According to the Management Regulations Section 6, risk acceptance criteria shall be established for major accident risk and environmental risk. Section 6 further states that risk acceptance criteria shall be defined for

- the personnel as a whole
- groups of personnel that have particular risk exposure,
- loss of main safety functions,
- the environment, and
- for harm to third party (only relevant for petroleum installations onshore)

The risk acceptance criteria may be both qualitative and quantitative.

The probability of accidents shall be documented based on calculations. This requirement is expressed in the Management Regulations, Section 15, which states that quantitative risk

analyses shall be performed in order to give an understandable and as realistic picture as possible of the risk. In a risk analysis¹ available information is used to identify potential accidental events, and to assess their causes and consequences. Subsequently, the risk with respect to personnel, environment and assets is estimated. The term “quantitative risk analysis”, as required in the regulations, involves a quantification of the probability and the consequences of accidental events such that they may easily be compared to the quantitative risk acceptance criteria (RAC) (NORSOK Z-013, 2001).

2.5 Accidental Limit State (ALS)

2.5.1 Overall requirements

The overall objective of an ALS design check is to ensure that the accidental action does not lead to complete loss of integrity or performance of the structure, and that the main safety functions remain intact. It implies that minor structural damage is accepted for ALS (NORSOK N-004, 2004).

The design check shall be performed in two steps:

- a) First it shall be verified that the structure will maintain its capacity to withstand the defined accidental load.
- b) Secondly, if the resistance has been reduced due to local damage caused by an accidental load as described in a), it shall be verified that the structure will continue to resist defined environmental actions (NORSOK N-001, 2004; NORSOK N-004, 2004).

In connection with the ALS design check it might be necessary to state (some) performance criteria to ensure that the main safety functions of the installation such as escape ways, shelter areas and the global load bearing capacity are not impaired by components of the structure during the accident. These safety functions shall also remain undamaged for a certain time period after the accident (NORSOK N-004, 2004).

For design check in ALS the material coefficient, γ_M , is set equal to 1.0 (NORSOK N-004, 2004).

¹ The term risk analysis covers a wide range of analysis, such as Safe Job Analysis (SJA), Hazard and Operability Study (HAZOP), Failure Mode and Effect Analysis (FMEA) etc.

3 Linear elastic response

3.1 Introduction

Conventional design is based upon the principle of linear elastic material behaviour. It presupposes that maximum capacity of the component is reached at first yield or at first component buckling, i.e. that exceedance of either of the two will lead to failure. This chapter gives a brief introduction to the basic principles of linear elastic material behaviour, without going into detail on the various aspects of the analysis. Chapter 3.3 however, gives a quite thorough explanation of stress-strain relations in the material up to the point of fracture, as this is highly relevant also for elasto-plastic analysis (Chapter 4).

3.2 General structural response

A structure, or a single element, responds to an applied load in different ways depending on the type of loading. A statically applied load may cause elastic or plastic deformations. Dynamic loading may set the structure in motion, causing both vibrations and elastic and possibly plastic deformation. A component subjected to cyclic loading may experience material fatigue, i.e. progressive fracture initiated by small cracks on the surface which ultimately can lead to failure of the material.

3.3 Elastic analysis and general stress-strain relations

A component or structure subjected to external loading will experience internal forces causing deformation of the structure. If the structure regains its original shape after the external load has been removed, the deformation is said to be *elastic*. The relation between loading and deformation forms the basis of structural analysis. In general, structural analysis is performed by checking the elastic capacity of each component to its applied loading, i.e. verifying that the design load S_d is lower than the design resistance R_d :

$$S_d \leq R_d \quad ^1 \quad (3.1)$$

The ultimate limit of resistance of steel in an elastic analysis is referred to as the *yield limit*. It is defined as the point where the outer fibres of the material experience yielding. If the loading exceeds this limit the material behaviour is no longer elastic, and the component will not regain its original shape when unloaded. This behaviour is called plasticity, and is discussed in Chapter 4.

¹ NORSOK N-004 (2004, Section 4).

The relation between load and displacement is often illustrated by a *stress-strain curve* where the vertical axis represents the *stress* σ given in force per unit area (usually N/mm^2), and the *strain* ε which is nondimensional is shown on the horizontal axis, see Figure 3.1.

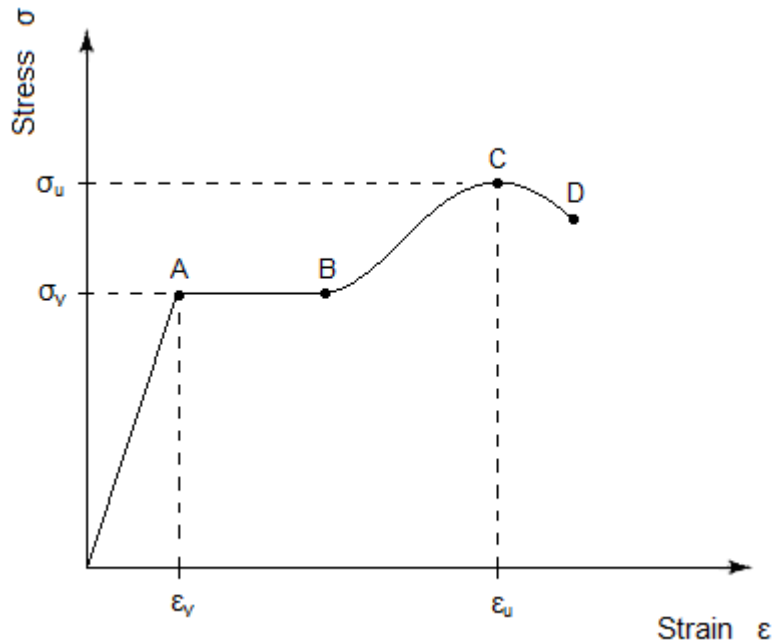


Figure 3.1 Stress-strain curve for mild steel¹.

Up to point A the strain is proportional to the stress (following Hooke's law²), meaning the material behaviour is linearly elastic. At point A the maximum level of stress for which the material behaves elastically is reached, and the steel starts to deform plastically. This limit represents the *yield strength* σ_y ³ of the material, and is defined as the level of stress causing yielding in the outer fibres of the cross-section which experiences most stress. Most ductile materials, i.e. materials experiencing plastic strains before fracture, do not have a well defined yield point so the yield strength (first yield) is typically defined as corresponding to 0,2 % strain ($\varepsilon_y = 0,2 \%$). When point A is reached the strain will continue to increase without any increase in load until a certain point when the material starts *hardening*, meaning the load again must be increased in order to cause further increase in strain. This is represented by point B in Figure 3.1. Point C identifies the maximum stress that occurs in the material before fracture, also referred to as the *ultimate tensile stress* σ_u . From point C the load necessary to maintain elongation decreases, and continued deformation will lead to fracture when the strain has reached the value corresponding to point D. The reduction of cross-section area due to hardening is not accounted for in the curve shown in Figure 3.1 (ESDEP a; Irgens, 1999).

¹ Mild steel is also referred to as ordinary structural steel (Irgens, 1999).

² Hookes law: $\sigma = E \cdot \varepsilon$

³ The index _y denotes (first) yield.

These are the main features of the behaviour of steel with respect to structural design. Other stress-strain curves may differ from the one shown in Fig. 3.1 since the material properties vary depending on the type of steel. Also, the degree of approximation to real material behaviour may vary from one stress-strain curve to another. A typical approximation in structural mechanics is the *engineering stress-strain curve*. The engineering strain is applicable for small strains only. The engineering strain in axial direction of a beam subjected to end forces is expressed as:

$$\varepsilon_x = \frac{\Delta L}{L} \quad (3.2)$$

where L is the initial length of the beam and ΔL is the change in length due to axial forces (Irgens, 1999).

3.4 Dynamic response

A falling object is a dynamic load of short duration, and is therefore often referred to as an impact or impulse load. A dynamic load varies with time, and it may cause the structure to vibrate, or oscillate. The magnitude of these oscillations depends on the eigenperiod¹ of the structure. If the load varies very slowly relative to the eigenperiod, the amplitude of oscillation will be close to zero and the load is considered to be static. However, if the eigenperiod of the load is close to, or smaller than, the eigenperiod of the structure, the amplitudes of motion might be considerable. It is of great importance to consider this dynamic effect during design as a dynamic load may cause considerable damage to the structure if treated as static (Biggs, 1964). The dynamic effect is often represented by a factor called the *dynamic amplification factor (DAF)*, see Chapter 3.6.

3.5 Single-degree-of-freedom-systems

Many practical problems may be idealized by a model consisting of a linear spring connected to a mass m which is restricted to move in only one direction. This is the basic model of a dynamic system, and is called a single-degree-of-freedom-system (SDOF).

The SDOF system contains the basic physical properties of a linearly elastic structural system subjected to dynamic loads; the system mass, its elasticity properties, the damping of the system (energy dissipation) and external loading. A SDOF system is illustrated in Figure 3.2, where the entire mass m of the system is included in a rigid block rolling friction-less on a horizontal plane. The block is attached to a spring with stiffness k , and to a viscous damper with damping coefficient c . The spring is considered to be mass-less, so the entire mass of the system is included in the block (Bergan, Larsen and Mollestad, 1981).

¹ According to Biggs, the eigenperiod is “the time required for the structure to go through one cycle of free vibration, i.e. vibration after the force causing the motion has been removed or has ceased to vary” (1964, p. ix).

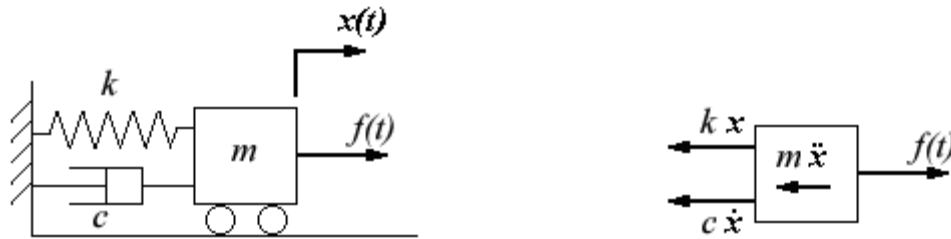


Figure 3.2 Illustration of a single-degree-of-freedom system.

The equation of motion for a SDOF system can be derived by expressing the equilibrium of all forces acting on the mass:

$$F_I + F_D + F_S + f(t) = 0 \quad (3.3)$$

where $F_I = -m \cdot \ddot{x}$ is the inertia force, $F_D = -c \cdot \dot{x}$ is the damping force and $F_S = -k \cdot x$ is the spring force (see Figure 3.2). $f(t)$ is any external force acting on the system.

The general equation of motion of an SDOF system is then found to be the differential equation

$$m \cdot \ddot{x} + c \cdot \dot{x} + k \cdot x = f(t) \quad (3.4)$$

with solutions obtained in the form of equations giving the displacement as a function of time (Bergan et al., 1981; Biggs, 1964).

3.6 Dynamic amplification factor (DAF) for a system exposed to rectangular load pulse

Impact loads may have different impulse shapes. This chapter gives a short description of the DAF in connection with impact loads, using a rectangular load pulse as an example.

The dynamic amplification factor represents the increase in the amplitude of oscillation due to the load being applied dynamically instead of statically. The DAF is thus defined as the ratio of the dynamic deflection at any time to the static deflection (Biggs, 1964):

$$DAF = \frac{y_{dyn}}{y_{st}} \quad (3.5)$$

A suddenly applied constant load with limited duration t_d equals a rectangular load pulse as shown in Figure 3.3.



Figure 3.3 Rectangular load pulse (Singelstad, 2008).

For an undamped system exposed to a load as described above, we get the following expression for the dynamic amplification factor (Biggs, 1964):

$$DAF = 1 - \cos 2\pi \cdot \left(\frac{t}{T} \right) \quad t \leq t_d \quad (3.6)$$

$$DAF = \cos 2\pi \cdot \left(\frac{t}{T} - \frac{t_d}{T} \right) - \cos 2\pi \cdot \left(\frac{t}{T} \right) \quad t \geq t_d \quad (3.7)$$

where T is the natural period of the system.

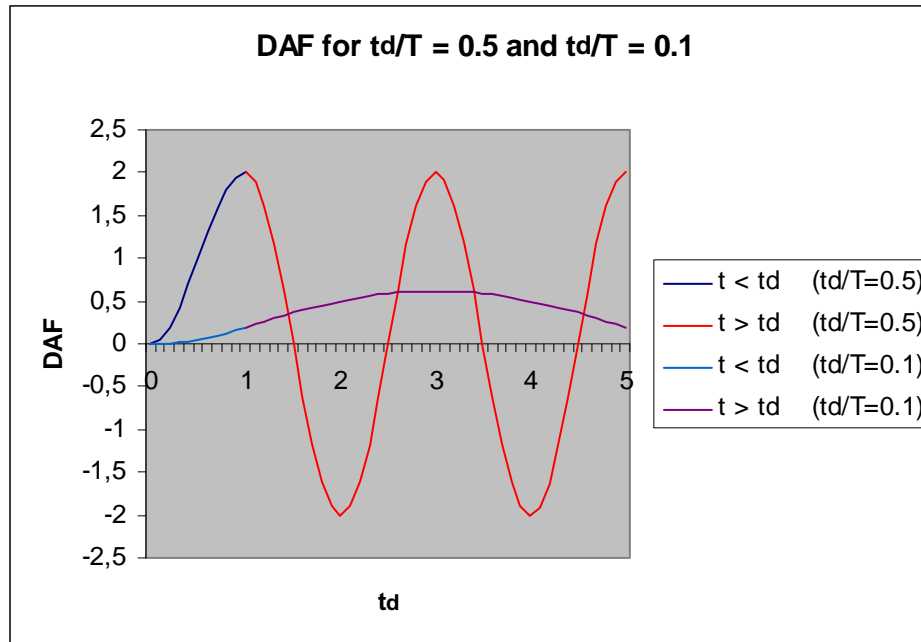


Figure 3.4 Typical response of a rectangular pulse load (Singelstad, 2008).

By simple calculation we find that the highest possible value of DAF for this load situation is two. It means that the largest displacement the system will experience when subjected to a suddenly applied constant load is twice the displacement which would have resulted if the load had been applied statically. DAF_{max} will occur in the time period $0 \leq t \leq t_d$ (Biggs, 1964).

It should be noted that no load can be applied as perfectly rectangular; in reality there will always be a certain rise time¹ t_r . However, if t_r is less than one fourth of the natural period, the effect of the rise time is negligible and the load is considered to be rectangular (Biggs, 1964).

For further details regarding single-degree-of-freedom systems and linear elastic response to impact loads, see Biggs (1964) or Singelstad (2008).

¹ Rise time, t_r , is the time required for the load to reach its maximum value.

4 Elasto-plastic material behaviour

4.1 General

Elasto-plastic analysis, often referred to as nonlinear analysis, is based on the theory of plasticity. While conventional linear elastic design is based upon component checking and first yield, a nonlinear analysis considers the ultimate strength of the structure as *system* allowing for redistribution of stresses and loads over a cross section when some part starts to yield. Elasto-plastic design thus allows for the structure to absorb most of the impact energy from a (dynamic) accidental load through permanent deformation, utilising the plastic capacity of the material. In an elasto-plastic analysis the loads and thus the behaviour of the structure (stress, deformation etc) is highly history dependent.

By applying the method of finite elements (FEM), it is possible to arrive at approximated solutions to any static or dynamic boundary value problem. The structural analysis software USFOS, which has been used to analyse the space frame described in Chapters 6 and 7, is an example of an analysis program based on plasticity theory and the finite element method.

This chapter gives a brief introduction to the theory and principles behind elasto-plastic analysis of steel structures, such that the reader will be able to get a quick and overall understanding of the underlying methods used to solve the problem specified in Chapter 6. Chapter 4.2 briefly describes issues relating to plasticity, emphasizing material behaviour and stress distribution during transition from elastic to plastic state.

4.2 Theory of plasticity

4.2.1 General stress-strain distribution

A component or structure subjected to stress exceeding the yield strength σ_y will experience permanent deformation. This material behaviour is called *plasticity*, and is illustrated by the nonlinear part of the stress-strain curve in Figure 3.1. Plasticification is only possible for ductile materials, e.g. steel or other metals, and makes it possible to redistribute stresses within a single component or within a whole structure utilising more of its actual strength.

To illustrate the principle of stress redistribution and formation of plastic hinges, it is convenient to start with the simplest case of beam failure, namely the simply supported beam under central concentrated loading. As explained in Chapter 3.1 the conventional elastic design criterion is defined as first yield. For a simply supported beam under concentrated loading P first yield is reached in the section just beneath the load where the beam experiences the highest level of stress. Further increase of the load will at a certain load level P_c lead to full plasticification of the cross-section, and a plastic hinge will develop. The stress distribution during transition from elastic to plastic state is shown in Figure 4.1 for a beam of rectangular cross-section. Figure 4.2

illustrates the relation between applied load and central deflection of the beam undergoing the same transition. The beam is assumed to be of Class 2 proportions or better¹ (ESDEP b; Søreide, 1985).

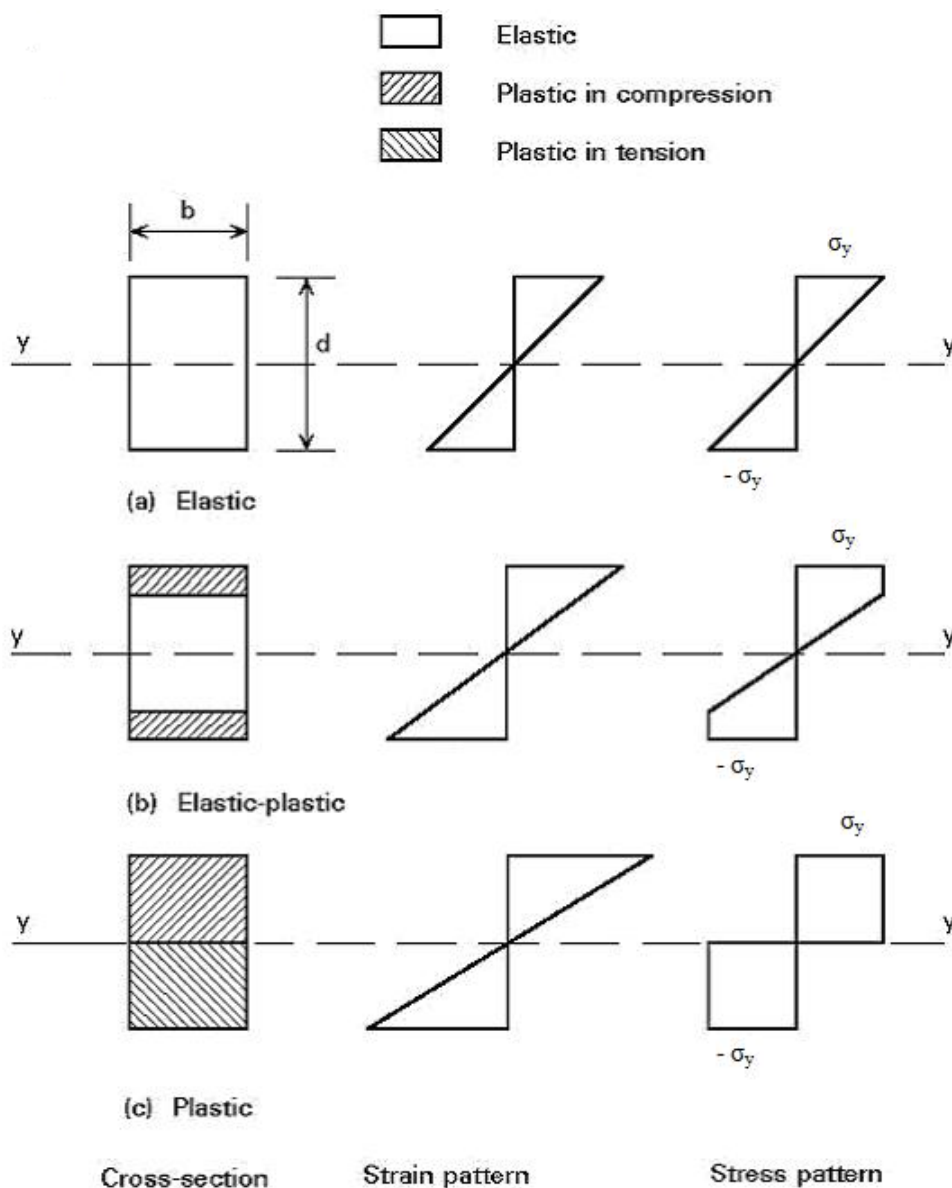


Figure 4.1 Transition from elastic to plastic state of a rectangular cross-section in bending (ESDEP b).

¹ According to NS 3472 (2001) the steel cross-section is required to be of Class 1 or Class 2 in order to be able to distribute the forces or moments within the component and thus forming plastic hinges.

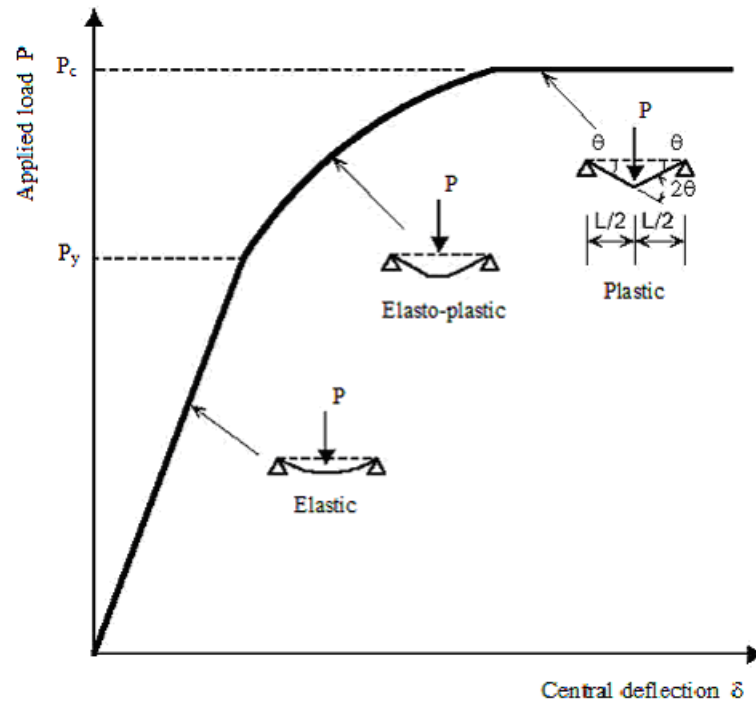


Figure 4.2 Behaviour of a simply supported beam in bending.

As seen in Figures 4.1 and 4.2 the response of the beam is roughly divided in three domains. The first is the *elastic* phase where loading and unloading follows the same path in the stress-strain diagram, meaning the beam will recover its original shape after unloading. The yield stress is not exceeded in any part of the cross-section. When the outer fibres of the beam start to yield at a certain load P_y , the beam enters the *elasto-plastic* domain. The relationship between applied load and central deflection is no longer linear, and as yielding continues the tangent stiffness decreases due to changes of the cross-section. In this domain the response is partly plastic, as shown in Figure 4.1(b). When yielding occurs in the whole cross-section the response is considered *plastic*. In this stage the applied load is close to constant while the deflection continues to increase (ESDEP b; Søreide, 1985).

The *moment-curvature* relation for the simply supported beam is shown in Figure 4.3.

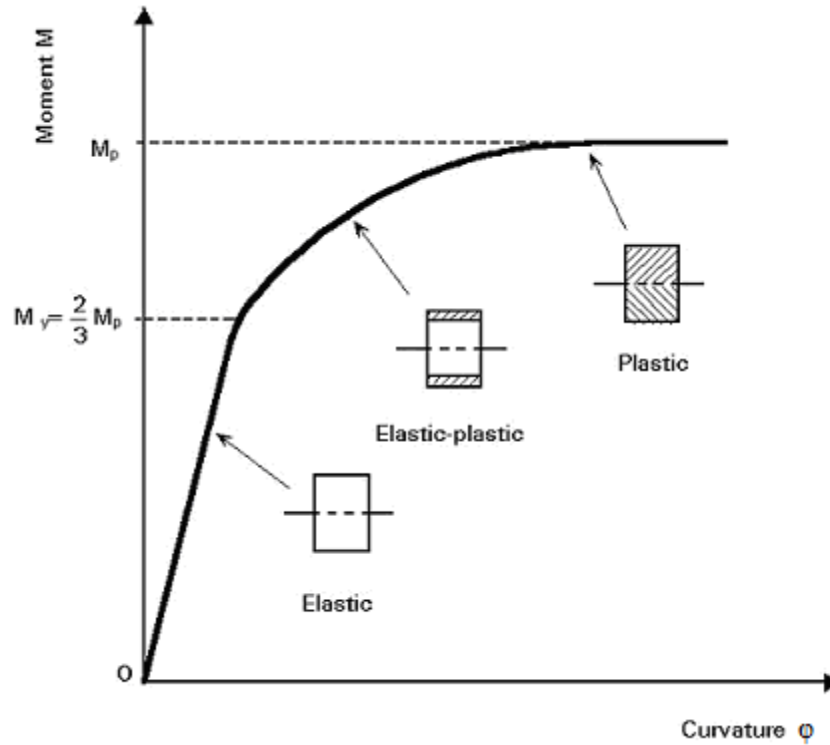


Figure 4.3 Moment-curvature (M - ϕ) relationship for a rectangular cross-section in bending (ESDEP b).

While the beam behaves perfectly linear elastic the curvature in any cross-section is given by the relation

$$\frac{d^2w}{dx^2} = -\frac{M}{EI} \quad (4.1)$$

where w is deflection somewhere on the longitudinal axis (x -axis) of the beam, and M is the bending moment, normally expressed as a function of x (e.g. Irgens, 1999), see Figure 4.4. E and I are the elasticity modulus and moment of inertia, respectively, and the product of the two denotes the elastic bending stiffness of the beam.

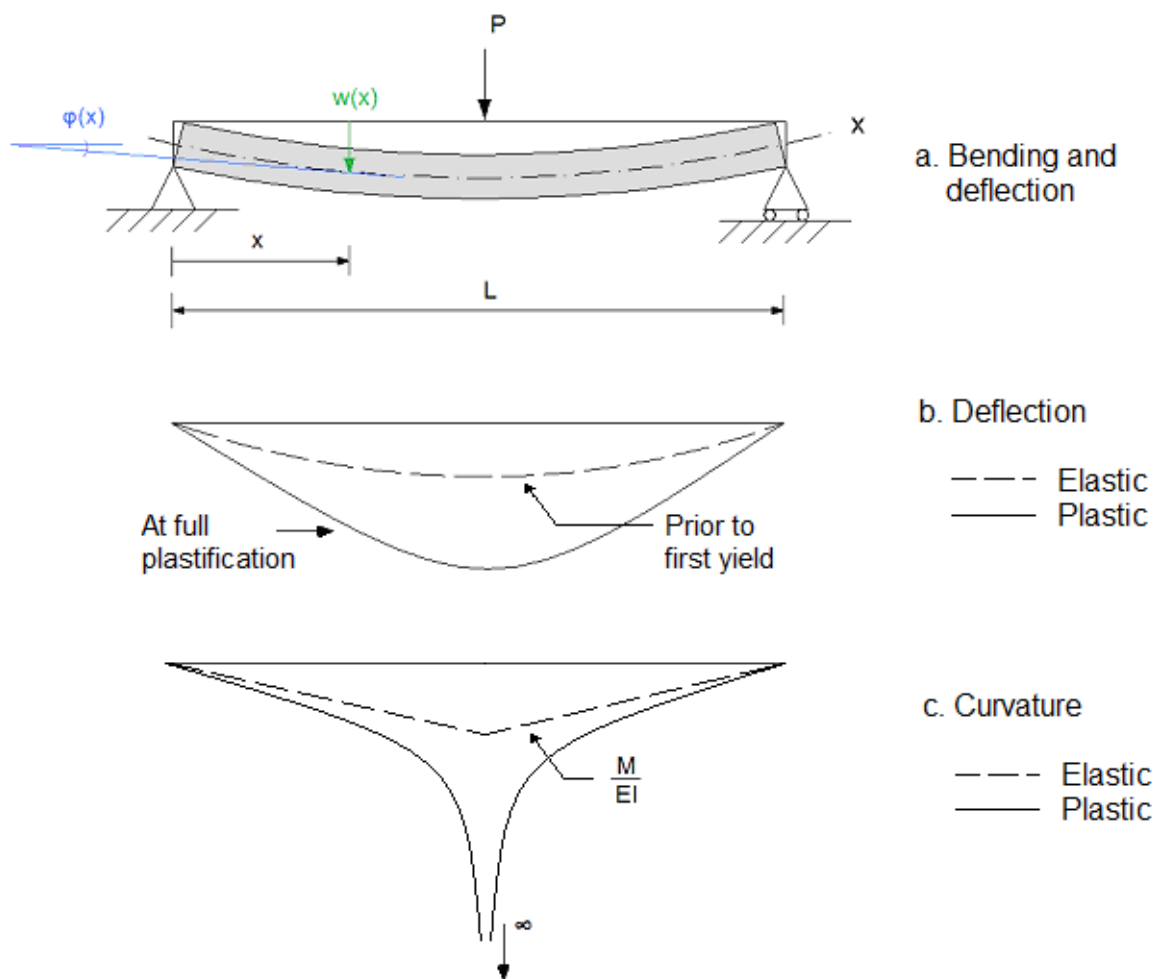


Figure 4.4 Deflection and curvature of a simply supported beam under concentrated loading.

However, when the central region of the beam has reached the yield moment M_y the ratio of moment to curvature is no longer linear in this section. From this point on the slope of the M - ϕ curve decreases towards zero as the moment capacity approaches M_p , illustrated by the second part of the curve in Figure 4.3. As shown in Figure 4.4 the curvature in the cross-section where M_p develops tends towards infinity. When M_p is reached the local bending stiffness in this region is zero, and the beam now acts as if it contains a real hinge, with the difference that the moment in the hinge remains at M_p . A *plastic hinge* has developed, and the beam turns into a mechanism. At this point the beam can take no additional load without causing excessive strain, i.e. it is the limit for which the strain will continue to increase even though no additional load is applied. Exceeding this limit thus results in the real physical collapse of the structure (ESDEP b; Søreide, 1985).

To simplify the highly complicated calculations which would have been necessary to describe the actual behaviour of the material, the stress-strain curve is approximated to different theoretical models. In the *elastic-perfectly-plastic* model the beam is assumed to behave purely elastic or purely plastic, as shown in Figure 4.5.

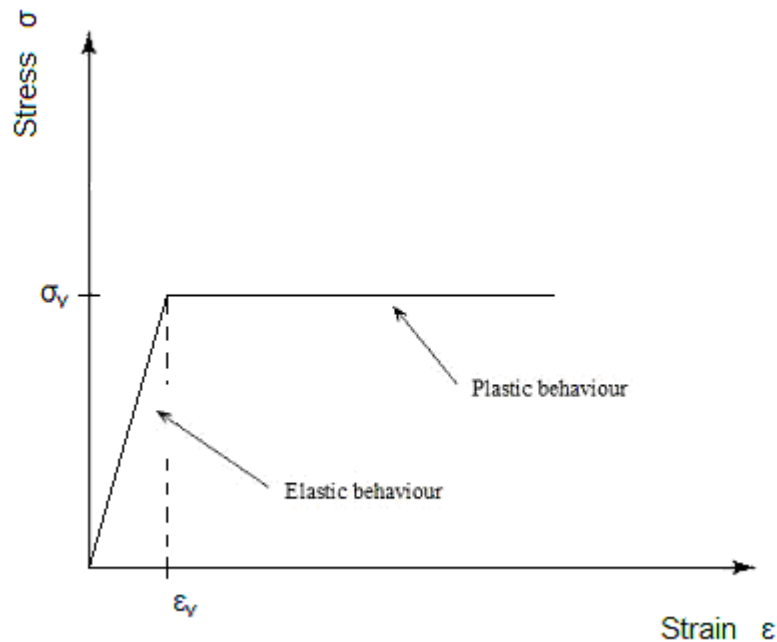


Figure 4.5 Ideal elastic-perfectly-plastic stress-strain curve (ESDEP b).

This means that certain material effects such as upper yield point, strain hardening (see Chapter 3.3) and the Bauschinger¹ effect are neglected. If included, they would only have a very small effect on the resulting analysis for a substantial increase in complexity (ESDEP b; Søreide, 1985).

Another, even more simplified, idealization of material behaviour is the *rigid-plastic* model, illustrated by Figure 4.6. It considers the material behaviour as purely plastic, ignoring the elastic part of the structural response (Horne, 1979).

¹ In plasticity theory it is assumed that the yield stress in tension and compression are the same. In real life however, a specimen deformed plastically beyond yield in tension will when reloaded in compression experience a yield stress that is less than the original yield stress. This is called the Bauschinger effect (Store norske leksikon).

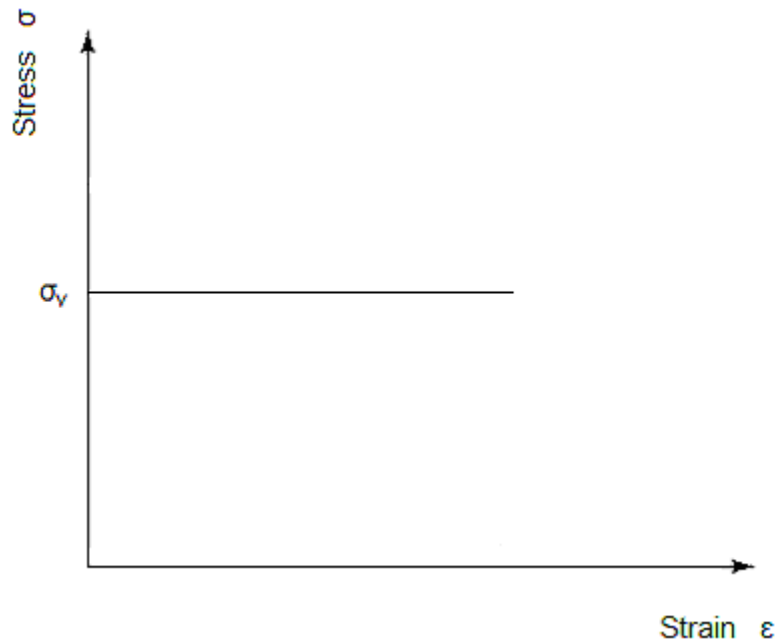


Figure 4.6 Rigid-plastic stress-strain curve

4.2.2 Moment distribution and the Mechanism Method

Chapter 4.2.1 described the material behaviour in the exact section where full plasticity occurs. In the following we will consider the distribution of moments along the beam, and methods for calculating the collapse load.

At load level P_c the central bending moment reaches the plastic moment capacity M_p resulting in a plastic hinge beneath the load. For the case of a simply supported beam this plastic hinge results in a *collapse mechanism*, meaning the limit where no further increase in load is possible. This is illustrated in Figure 4.7 d, together with the change in deflection δ (a so-called increment) at collapse. The load at which the formation of a plastic mechanism occurs is called the *plastic collapse load* P_c which was defined in Chapter 4.2.1 (Søreide, 1985).

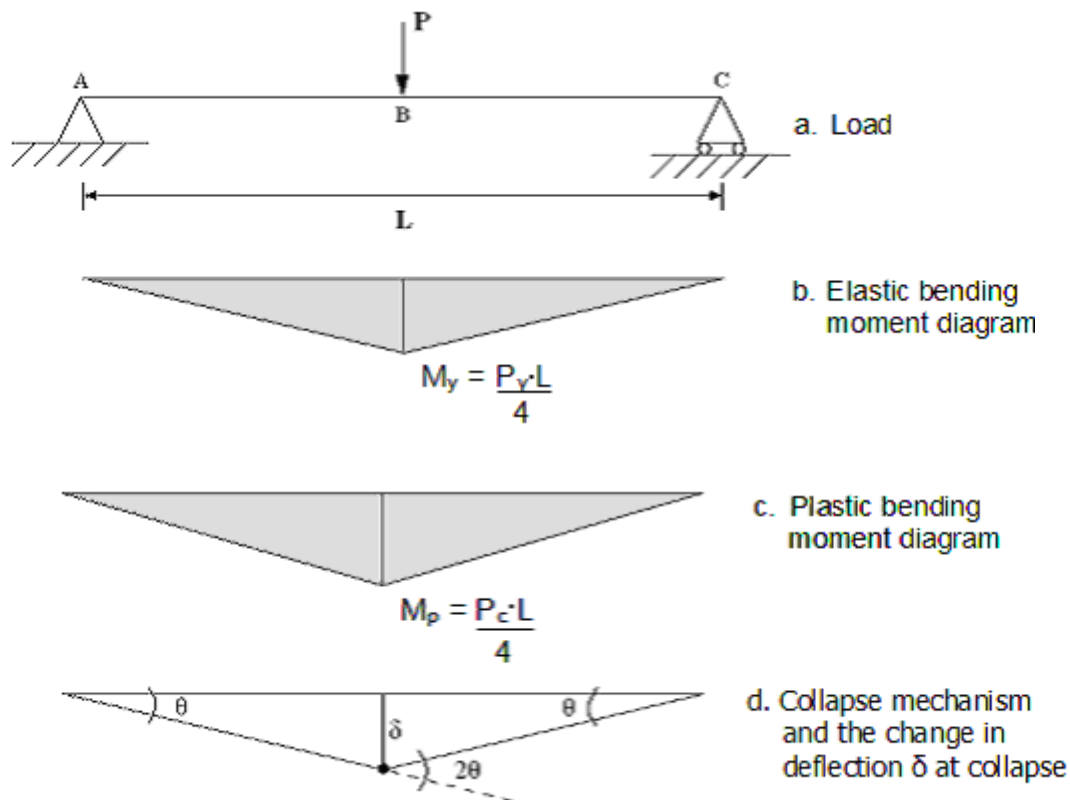


Figure 4.7 Simply supported beam under central concentrated load P .

The load corresponding to M_y is statically determined by taking the moments about B for AB, giving $M_y = P_y \cdot L/4$ or $P_y = M_y \cdot L/4$. With further load increase full plasticity will occur under the load at a value $P_c = M_p \cdot L/4$. It means the moment distribution in this case will be the same for P_y and P_c , as illustrated by Figure 4.7 b and c. For *statically determinate* beams one single plastic hinge will cause failure, which means the plastic collapse load for any statically determinate structure can be obtained by establishing the bending moment diagram and then equating the maximum bending moment to the fully plastic moment. *Statically indeterminate* beams are capable of developing full plasticity in several regions of the beam before collapse due to redistribution of moments, which requires the use of another procedure to be able to find the collapse load (ESDEP b; Søreide, 1985). An example is the single fixed beam illustrated in Figure 4.8.

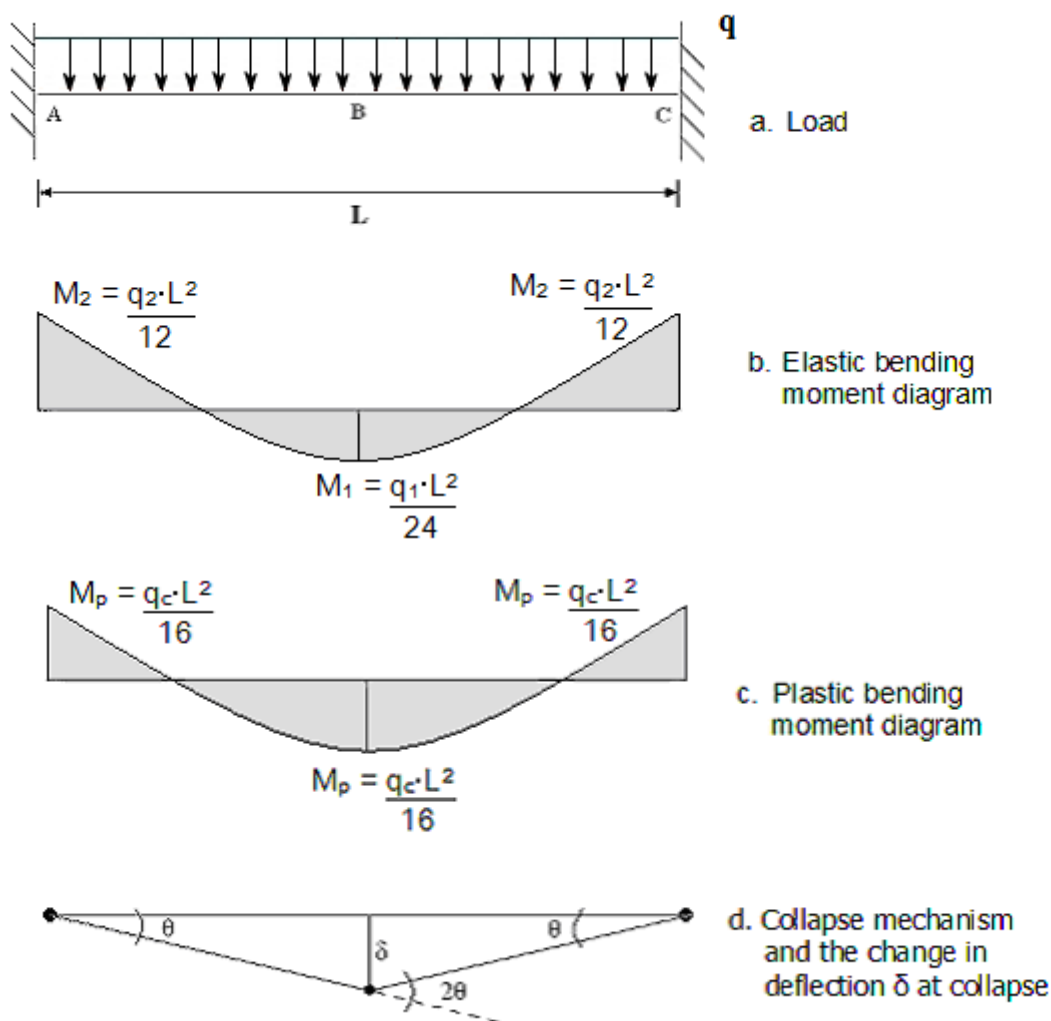


Figure 4.8 Fixed beam under uniform distributed load q .

As shown in Figure 4.8 b and c the plastic moment diagram will differ from that of the elastic moment diagram since the redistribution of moments will cause M_p to be reached at a certain number of places in the beam before failure (collapse mechanism).

Another way of calculating P_c , which is valid for both statically determinate and indeterminate structures, is by *kinematical* considerations, also called the *mechanism method*. This is done by treating the elastic portions of the beam as rigid and equating the work done by the external loads to the energy dissipated by the plastic hinge(s) (see Figures 4.7 d and 4.8 d). The basic principle is thus that external work W_e equals internal work W_i , which for the simply supported beam in Figure 4.7 results in

$$P \cdot \delta = 2\theta \cdot M_p \quad (4.2)$$

Rearranging Equation 4.2 and applying the compatibility relation, $\delta = \theta \cdot L/2$, results in the following expression for the collapse load of a simply supported beam with central concentrated loading

$$P_c = \frac{M_p \cdot L}{4} \quad (4.3)$$

This is exactly the same expression which was found by the static considerations.

For details, reference is made to Søreide (1985).

5 Finite element software

5.1 Introduction

The dynamic analysis of a laydown area exposed to dropped objects on the Ekofisk M platform has been carried out using the nonlinear finite element program USFOS. USFOS has been developed by SINTEF MARINTEK and NTNU¹ for the purpose of advanced nonlinear analysis of offshore structures under extreme loading conditions, up to the point of collapse. It accounts for nonlinear effects such as large structural motions and inelastic deformations. The theoretical basis of the computer code is continuum mechanics and the finite element method with the basic idea that only one finite element represents *one* physical element in the structure. The element formulation is based on the exact solution to the differential equation for a beam subjected to end forces (Skallerud and Amdahl, 2002; USFOS User's Manual: Program Concepts, 1999).

It should be noted that the USFOS formulation is valid for large displacements, but restricted to moderate strains. USFOS applies an elasto-plastic material model with gradual strain-hardening characteristics if nothing else is specified.

Chapter 5.2 gives a brief explanation of the theory behind nonlinear finite element codes. The references upon which Chapter 5.2 is based are USFOS Getting Started (SINTEF GROUP, 2001), Skallerud and Amdahl (2002), and van Raaij (2005).

The main references for Chapter 5.3 and 5.4 are USFOS Theory Manual (Søreide et al., 1993) and USFOS Getting Started (SINTEF GROUP, 2001).

5.2 Theoretical basis

5.2.1 Continuum mechanics

The USFOS computer code is based on *Green strain* (nonlinear), which differs from the traditional engineering strain (linear) by including the effects of large displacements and coupling between lateral deflection and axial strain. The material behaviour is thus represented very accurately, including column buckling and membrane effects.

The Green strain tensor in axial direction (x) for a beam subjected to end forces is defined as

$$\varepsilon_x = v_{x,x} + \frac{1}{2}v_{x,x}^2 + \frac{1}{2}v_{y,x}^2 + \frac{1}{2}v_{z,x}^2 \quad (5.1)$$

¹ The Norwegian University of Science and Technology.

where $v_{x,x}$, $v_{y,x}$ and $v_{z,x}$ denotes the displacements in the directions x, y and z at any location within the beam differentiated with respect to x.

Potential energy considerations lead to the stiffness formulation used in USFOS. The basic principle is that *internal strain energy* U equals the *potential of external load* H , giving the total potential for an elastic element as

$$\Pi = U + H \quad (5.2)$$

with

$$\begin{aligned} U &= \frac{1}{2} \int_V \sigma_x \varepsilon_x dV \\ &= \frac{1}{2} \int_l EA \left(v_{x,x} + \frac{1}{2} v_{y,x}^2 + \frac{1}{2} v_{z,x}^2 \right)^2 dx + \frac{1}{2} \int_l (EI_z v_{y,xx}^2 + EI_y v_{z,xx}^2) dx \end{aligned} \quad (5.3)$$

where σ_x denotes the 2nd Piola-Kirchoff stress in x-direction. The 2nd Piola-Kirchoff stress is the energy conjugate to Green strain, and will for small strains approach the Cauchy stress which is energy conjugate to engineering strain.

$$H = - \sum F_i v_i - \int_l q_x v_x dx - \int_l q_y v_y dx - \int_l q_z v_z dx \quad (5.4)$$

F_i and v_i are the concentrated load and the resulting displacements, respectively. l is the length of the element, and q is the distributed load.

The first variation in total potential is thus given as

$$\delta \Pi = \delta U + \delta H \quad (5.5)$$

which expresses the state of equilibrium in the beam. This formulation is the basis for the equilibrium iteration process (see Chapter 5.4) which is carried out between total internal stresses and total external loads at each level of loading. δ denotes a virtual value/parameter.

The variation of increment in strain energy is then given as

$$\delta \Delta \Pi = \delta \Delta U + \delta \Delta H \quad (5.6)$$

with Δ denoting the increment in displacement between two close configurations.

For details, reference is made to USFOS Getting Started (SINTEF GROUP, 2001), (van Raaij, 2005) or Skallerud and Amdahl (2002).

5.2.2 Finite element formulation

Deformation is a physical phenomenon which can be described in terms of partial differential equations. Together with boundary equations they form a boundary value problem which for very simple geometries can be solved by classical analytical methods. For most structures the method of finite elements must be applied, dividing the structure into elements with a given number of nodes. Since USFOS requires only one finite element per physical element of the structure, structural models for linear analysis can be used directly in the USFOS nonlinear analysis.

By introducing shape or interpolation functions $[\Phi]$ the displacement $\{\mathbf{v}\}$ of any point along the neutral axis of the element can be described by the displacement of the nodes $\{\mathbf{v}_N\}$;

$$\{\mathbf{v}\} = [\Phi]^T \{\mathbf{v}_N\} \quad (5.7)$$

$[\Phi]$ is a matrix, and $\{\mathbf{v}_N\}$ a vector consisting of the displacements in x, y and z-direction. $\{\mathbf{v}_N\}$ may also consist of rotations at the nodes. The shape function Φ is taken as the exact solution to the 4th order differential equation for a beam subjected to end forces.

The displacements for a two node beam element can then be expressed as follows:

$$\begin{aligned} v_x(x) &= \{\phi_x\}^T \{\mathbf{v}_x\} \\ v_y(x) &= \{\phi_y\}^T \{\mathbf{v}_y\} \\ v_z(x) &= \{\phi_z\}^T \{\mathbf{v}_z\} \end{aligned} \quad (5.8)$$

where the nodal displacements \mathbf{v}_x , \mathbf{v}_y and \mathbf{v}_z are the unknowns.

The elastic stiffness matrix $[\mathbf{K}_T]$ is obtained by substituting the expressions in Equation 5.8 into the expression for $\delta\Delta U$, resulting in the following matrix equation;

$$\{\mathbf{S}\} = [\mathbf{K}_T] \begin{Bmatrix} \mathbf{v}_x \\ \mathbf{v}_y \\ \mathbf{v}_z \end{Bmatrix} \quad (5.9)$$

where \mathbf{S} is the vector of force components.

5.2.3 Formulation of nonlinear material behaviour

Plastic behaviour is modelled by yield hinges, inserted at element ends or at element midspan. In the latter case, an extra node is automatically introduced and the element divided into two sub elements.

The behaviour of the hinges is governed by plastic flow theory which briefly consists of the following basic assumptions:

- There exists a *yield condition* which defines when yield occurs (illustrated by an initial yield surface)
- There exists a *flow rule*, relating the plastic strain increment to the stress increment
- There exists a *hardening rule* which describes the relation between the extension of the yield surface to the amount of plastic deformation, i.e. the transition from one plastic state to another.

The *yield condition* is represented by a yield surface or yield function Γ_y based on plastic interaction between element forces. For a multiaxial state the yield function is defined as

$$\Gamma_y = f\left(\frac{N}{N_P}, \frac{V}{V_{yP}}, \frac{V_z}{V_{zP}}, \frac{M_x}{M_{xP}}, \frac{M_y}{M_{yP}}, \frac{M_z}{M_{zP}}\right) - 1 = 0 \quad (5.10)$$

where f is a function of the various force components and the respective plastic capacities. A combination of the force components and plastic capacities giving $\Gamma_y < 0$ states an elastic material, with $\Gamma_y = -1$ being the initial value of a stress-free cross-section. $\Gamma_y = 0$ states that full plastification is occurring in the cross-section. A value of $\Gamma_y > 0$ is not allowed.

Interaction functions for various profiles may be found in Søreide (1985) or other relevant literature.

The *flow rule* defines the relation between plastic strain and stress, and is given by

$$\Delta \mathbf{v}^P = \begin{bmatrix} g_1 & 0 \\ 0 & g_2 \end{bmatrix} \begin{bmatrix} \Delta \lambda_1 \\ \Delta \lambda_2 \end{bmatrix} = G \Delta \lambda \quad (5.11)$$

Equation 5.10 states that the plastic displacement must be normal to a defined plastic potential which for ductile steel materials can be taken as the yield function Γ_y . g_i is the surface normal at node i , and is defined as

$$g_i^T = \frac{\partial \Gamma_y}{\partial S_i} = \left[\frac{\partial \Gamma_y}{\partial N}, \frac{\partial \Gamma_y}{\partial V_y}, \frac{\partial \Gamma_y}{\partial V_z}, \frac{\partial \Gamma_y}{\partial M_x}, \frac{\partial \Gamma_y}{\partial M_y}, \frac{\partial \Gamma_y}{\partial M_z} \right]^T \quad (5.12)$$

where the index i refers to beam end 1 and beam end 2. S_i is the current force state, and together with the surface normal of the yield surface, Δg_i , they define the ‘direction’ of the plastic displacement (plastic elongation vs. plastic shear or plastic rotation). $\Delta \lambda$ is a scalar factor giving the magnitude of the plastic displacements.

The **hardening rule** describes how much the stress increases, or decreases, during plastic flow. When a plastic hinge has developed, the state of forces should move from one plastic state to another, following the yield surface such that $\Gamma_y = 0$. In order for the forces to remain on the yield surface, the following requirement is introduced:

$$\Delta \Gamma_y = g^T \Delta S = 0 \quad (5.13)$$

This is called the consistency criterion, and for an elastic-perfectly plastic material model it can be expressed as

$$\Delta \Gamma_y = \frac{\partial \Gamma_y}{\partial N} \Delta N + \frac{\partial \Gamma_y}{\partial V_y} \Delta V_y + \frac{\partial \Gamma_y}{\partial V_z} \Delta V_z + \frac{\partial \Gamma_y}{\partial M_x} \Delta M_x + \frac{\partial \Gamma_y}{\partial M_y} \Delta M_y + \frac{\partial \Gamma_y}{\partial M_z} \Delta M_z = 0 \quad (5.14)$$

Equation 5.13, together with the elastic stiffness expression for the beam element (Equation 5.8), is used to derive the expression for the elasto-plastic stiffness of the beam, \mathbf{K}_T^{EP} , and to find the value of $\Delta \lambda$.

Partial plastification and strain hardening is accounted for by USFOS through the *bounding surface concept*. This concept is illustrated in Figure 5. 1 for a tubular cross-section subjected to bending moment and axial forces. Two interaction surfaces are employed; the yield surface F_y and the bounding surface F_b which has the same shape as the yield surface. The yield surface defines elastic cross-sectional behaviour, while the bounding surface defines the state of full plastification of the cross-section.

When a cross-section is loaded, the force point will travel through the elastic region towards the yield surface, F_y , as illustrated in Figure 5.1 a. When the force state contacts the yield surface, this state corresponds to first yielding in the cross-section. As further load is applied, the yield surface will translate such that the forces remain on the yield surface, and move towards the

bounding surface (Figure 5.1 b). The bounding surface will also translate, but at a much smaller rate. With further loading the yield surface will eventually reach the bounding surface, representing full plastification of the cross-section (Figure 5.1 c). At this stage $\Gamma_y = 0$, and a plastic hinge is introduced. The force state will from this point on remain on the bounding surface, and both surfaces will translate in contact.

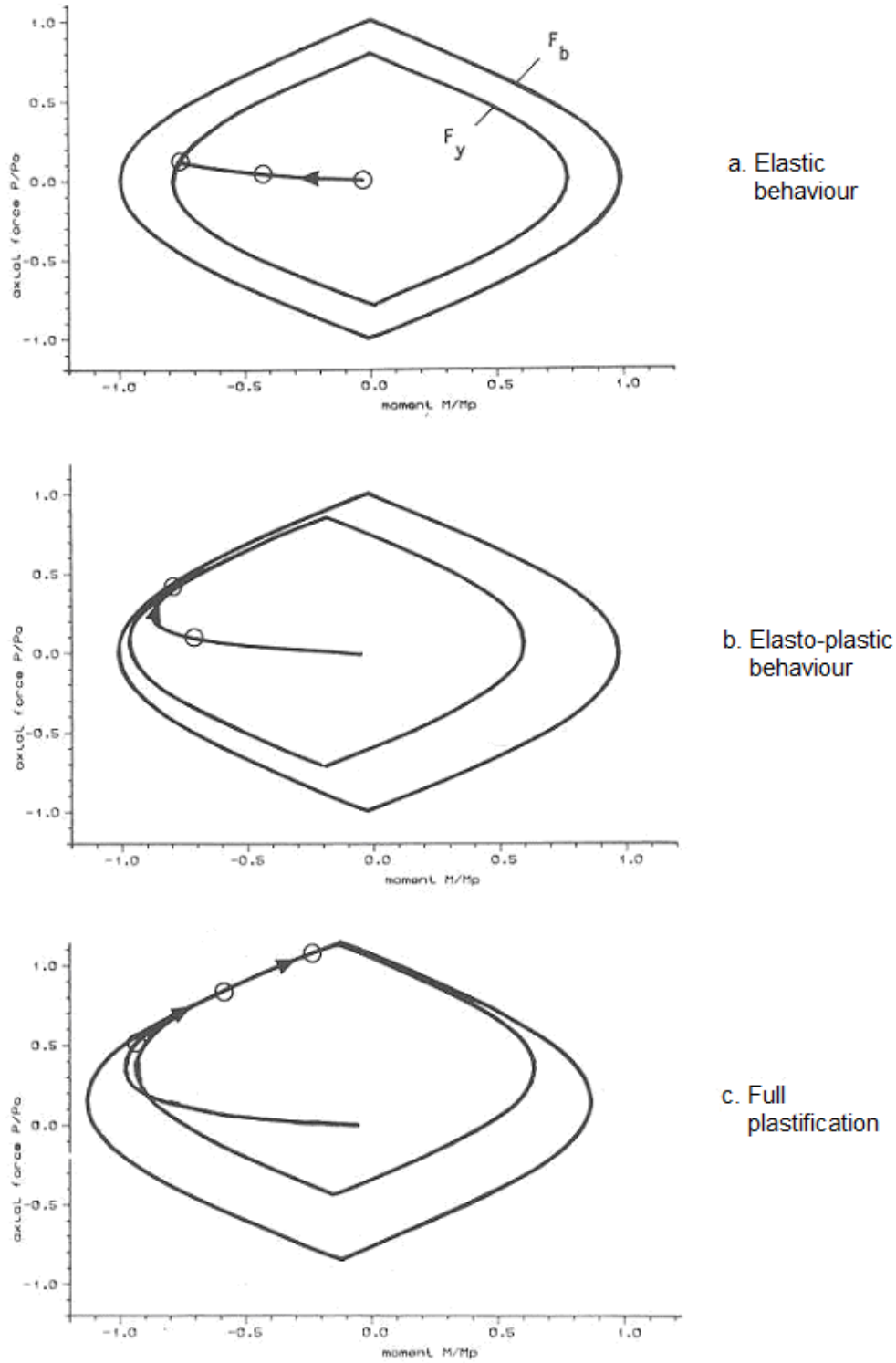


Figure 5.1 Two-surface plasticity model of a tubular cross-section plotted in the m_z - n -plane. A slightly modified figure from USFOS Getting Started (SINTEF GROUP, 2001).

5.3 Incremental procedures

5.3.1 General

In most nonlinear problems, e.g. plasticity, the internal load response is defined by a nonlinear, history dependent function of displacements and rotations. The load is applied in steps (incrementally), and the system stiffness equations are solved at every step. A full analysis is thus performed at each load increment, and the structural configuration – nodal coordinates, element forces etc – is updated. However, after each load step this incremental procedure will lead to an unbalance between internal and external loads which may be corrected for by equilibrium iterations.

5.3.2 Equilibrium iteration

USFOS applies a pure incremental algorithm (the Euler-Cauchy method) which is set as default. When the pure incremental algorithm is implemented, it usually causes a ‘drift-off’ from the ‘true’ solution path. The deviation occurs since each step is a solution to the tangential stiffness matrix and thus will move at a tangent to the ‘true’ curve. This unbalance in equilibrium between external and internal forces after each load step may be adjusted for by implementing equilibrium iterations specified by the user. By iterating within the load step, e.g. using the Newton-Raphson method, the tangent stiffness matrix is updated after each iteration. Iterations are performed until a certain convergence criterion¹ is satisfied.

5.3.3 Plastic hinges

In connection with the introduction of plastic hinges, equilibrium iteration might be important. As the element forces in each increment move at a tangent to the yield surface, the element forces will depart from the yield surface, as illustrated by Figure 5.2. This will result in $\Gamma_y > 0$ which is an illegal value of the yield function.

¹ Iterations are also terminated if the maximum number of iterations is reached, or if a so-called load limit point or bifurcation point is detected.

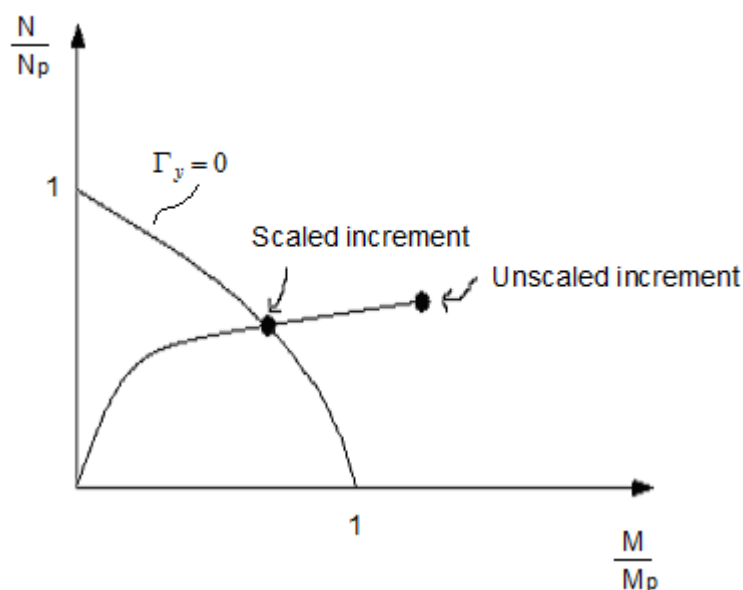


Figure 5.2 Increment scaling due to introduction of plastic hinges.

If the iterative procedure is implemented in addition to the pure incremental algorithm which is set as default, it corrects for the ‘drift-off’ such that the cross-section force state is brought back onto the yield surface. The forces will remain on the yield surface as long as the iteration process converges. However, if the load steps are too large the iteration may not be able to correct for the ‘drift-off’. It is therefore important to apply small load steps in the nonlinear range such that the ‘drift-off’ will be kept as small as possible, and thus making sure that plastic behaviour is accounted for as accurately as possible.

The size of the increments is defined by the input command DYNAMIC (or STATIC), see Chapters 7.4. It may be varied along the deformation path such that large steps are used in the linear range, and smaller steps are used in areas of increasingly nonlinear behaviour.

Since the response of the structure is highly history dependent, the results of different load cases may not be superposed.

5.4 Dynamic analysis

The dynamic equilibrium equation defined in Chapter 3.5 written on matrix form is the basis for dynamic analysis in USFOS:

$$\mathbf{F}_I + \mathbf{F}_D + \mathbf{R}_{Int} = \mathbf{R}_{Ext} \quad (7.1)$$

Equation 7.1 represents the linear elastic case, and corresponds to Equation 3.3. \mathbf{F}_I are the inertia forces, \mathbf{F}_D are the damping forces, \mathbf{R}_{int} the internal forces and \mathbf{R}_{ext} the external forces. The mass

matrix for the system may be given either as a consistent mass or a lumped mass. Material damping is expressed by the viscous damping model, which may be reduced to the Rayleigh damping form. The so-called HHT- α method for time integration is adopted.

For details, reference is made to USFOS Theory Manual (Søreide et al., 1993).

6 Case – Impact loading

6.1 Introduction

In this master thesis a laydown area on the Ekofisk M platform located at the Ekofisk field is studied and analyzed under impact loading using the nonlinear analysis program USFOS (Chapter 7), and compared to hand calculations (Chapter 8) performed according to work considerations and requirements in NORSOK N-004.

A scale inhibitor cabinet and a pump skid will be placed under the laydown area, requiring for the structure to maintain its structural integrity and limited deformations in case of an accidental event. The laydown area will therefore be designed in accidental limit state (ALS).

A model of the laydown area was provided by Fabricom. It was modelled in the structural analysis and design program StaadPro, and converted to USFOS by the converting tool StruMan. As a part of the present project nonlinear analyses of the structure have been performed for two different modelling alternatives, see Chapter 7.

6.2 Description of structural model

6.2.1 Geometry

The model is a 3D frame structure consisting of rectangular hollow sections (RHS) and H-profiles, as illustrated in Figure 6.1.

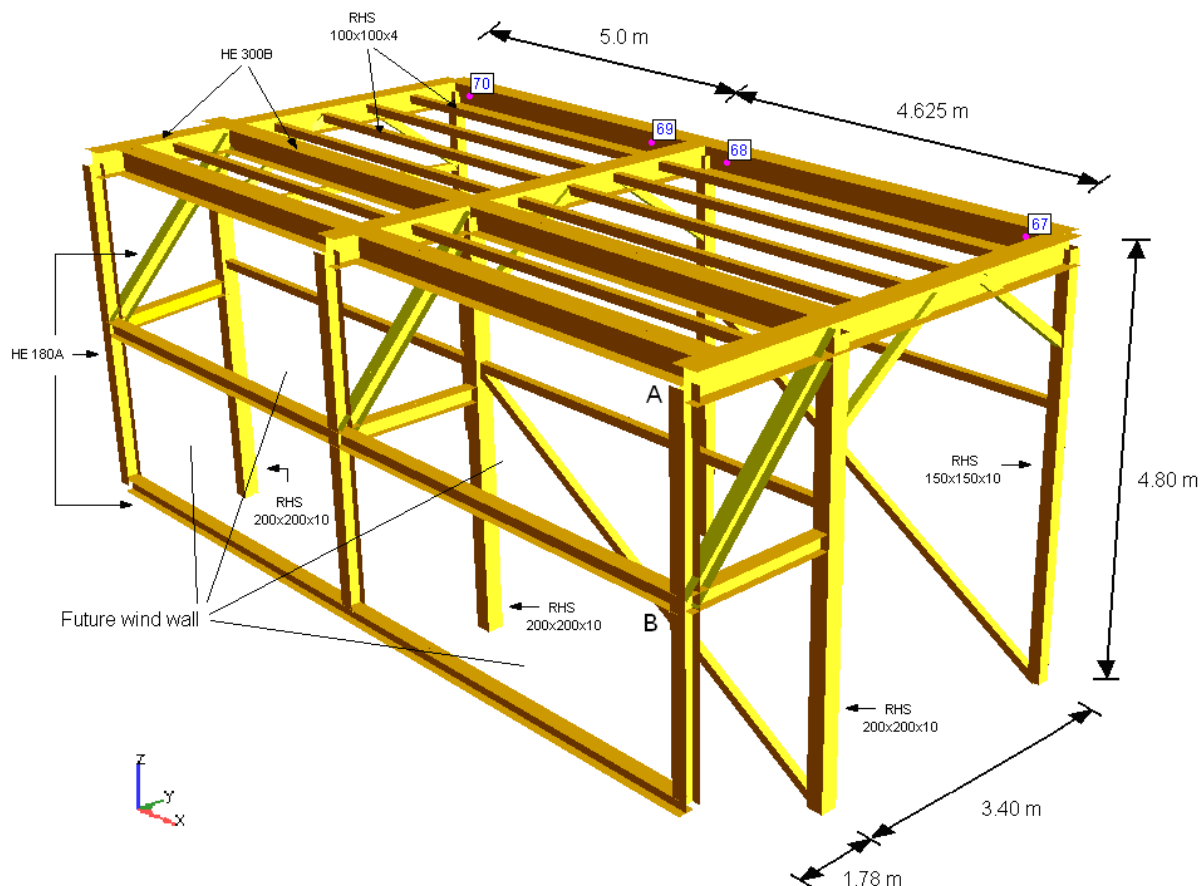


Figure 6.1 Structural model of the laydown area.

The laydown area is in general 9.625 m long divided in two spans of 4.625 m and 5.0 m, respectively. One column is placed ‘outside’ the main frame as to lead any load down into existing load-bearing structure, giving a total length of 10.0 m. The width is 3.40 m plus an additional 1.78 m where wind cladding will be attached to the structure at levels A and B, as shown in Figure 6.1. The total height of the shown structure is 4.80 m. All measures are given as centre-centre.

The other longitudinal side is attached to existing structure in four points (nodes 67, 68, 69 and 70) along the beams in the back, see Figure 6.1. The columns are bolted to the deck of the existing structure, and all joints are welded.

Finally, the structure will have plates on top and on the longitudinal side where the wind wall is indicated, see Figure 6.1. However, plates will not be considered in this master thesis.

The load-bearing part of the structure consists of the following profiles (see also Figure 6.1):

- Beams: HE300B
- Columns in front: RHS 200x200x10
- Columns in the back: RHS 150x150x10

The secondary elements consist of:

- Support for wind wall: HE180A
- Horizontal support for future plates: RHS 100x100x4
- Diagonal braces: RHS 100x100x4

6.2.2 Material properties

The whole structure consists of steel of material quality S 355, i.e. with yield strength of 355 N/mm². The elasticity modulus is $E = 205\,000\text{ N/mm}^2$ for all members.

6.2.3 Load specifications

The laydown area is subjected to the loads given in Table 6.1.

Load type	ALS	
	Relevant loads	Action factors
Dead load:	Selfweight	1.0
Live load:	15.0 kN/m ²	1.0
Wind:	N.A.	N.A.
Accidental action:	Dropped object	1.0

Table 6.1 Current loads and action factors in ALS.

Live load is given according to specifications for laydown areas in NORSOK N-003 (2007). The action factors for ALS are the same offshore as onshore, and are given in NS 3472 (2001).

According to N-003 dead load and live load that are probable to be present at the time of the accidental event shall be accounted for in the analysis, while any environmental load may be neglected unless the accidental action is initiated by it.

The nonlinear analysis of a dropped object action performed in this master thesis thus accounts for the following loads:

- Selfweight
- Live load of 15.0 kN/m²
- Dropped object as specified in Chapter 6.4.

Since the space frame eventually will have plates on top and on the side where the wind wall is indicated (see Figure 6.1), the live load was distributed such that the secondary beams will be assigned a value of 10.2 kN/m each together with the midst horizontal HE300B, and the outward HE300B beams will have to carry half this load, i.e. 5.1 kN/m.

The material factor, γ_m , is set equal to 1.0, according to requirements in NORSOK N-004 (2004) for accidental limit state.

6.3 Cross-section requirements

For nonlinear analyses relevant components must be proportioned to Class 1 requirements defined in NS 3472 or in NS-ENV 1993 1-1 according to NORSOK N-004 (2004). The HE300B beams and the RHS 150x10x10 columns have been checked and approved to Class 1 requirements according to NS 3472 (2001).

6.4 Description of dropped object scenario

An object of 6000 kg dropped from a height of 3 m is considered worst case possible with an annual probability of exceedance of 10^{-4} requiring for design check in ALS. This design criterion is given in the design accidental load specification (DAL) for Ekofisk Area Growth 2/4M. The specified accidental action represents a container dropped from a crane 3 m above the top of the structure.

Since all primary beams are of the same cross-section (HE300B) the worst place for the object to hit is considered to be on the middle of the beam with the longest span, i.e. the point of impact corresponds to node 43, as illustrated by Figure 6.2.

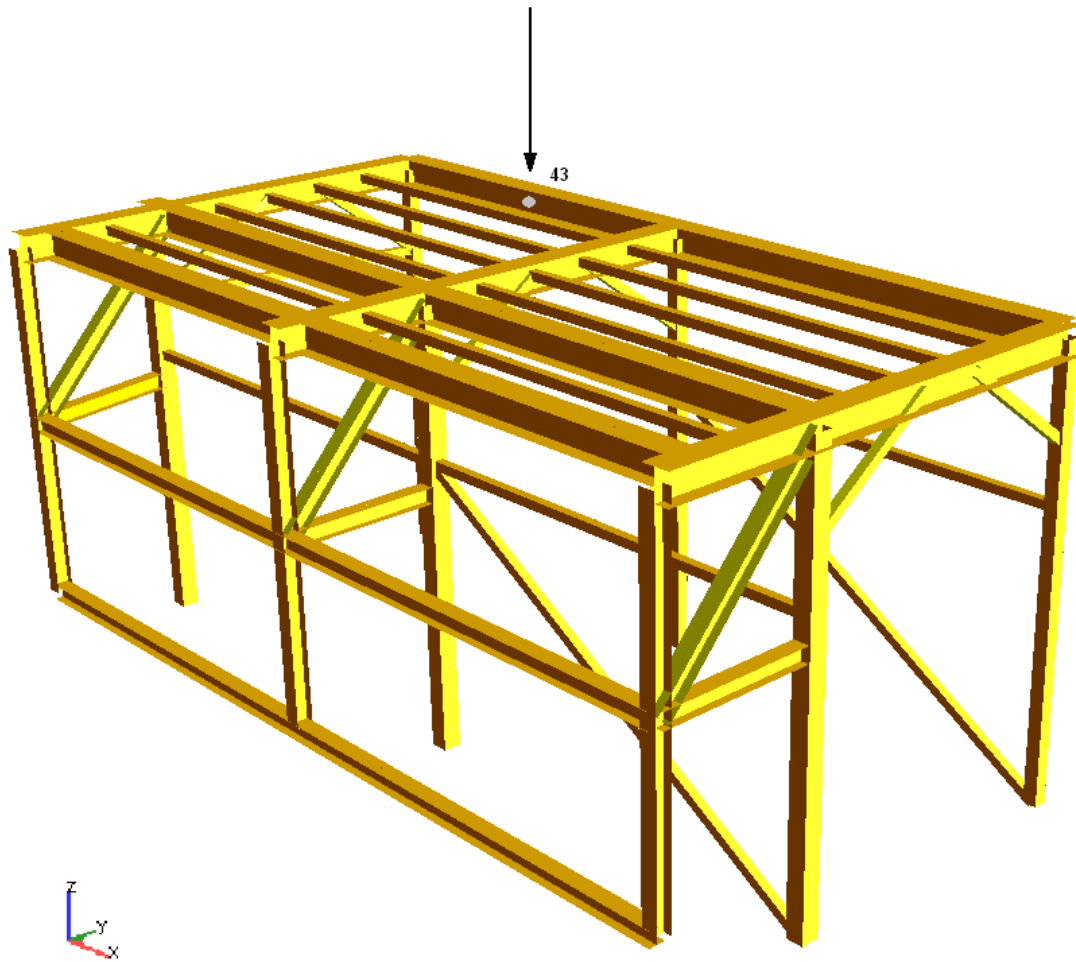


Figure 6.2 Point of impact

Other impact scenarios are possible, and might cause failure such as buckling, torsion buckling etc. Due to reasons explained in Chapter 1.3, other possible scenarios than the one illustrated by Figure 6.2 will not be considered.

7 Nonlinear finite element analysis of space frame

7.1 Introduction

Two text files are required to run an analysis in USFOS; one model file and one analysis control file. The model file is either converted to USFOS from another structural analysis program such as Sesam (Genie), StaadPro etc, or the structure is modelled in USFOS using the structural file format UFO. The head file comprises all analysis control parameters and is created by the analyst.

Two different methods of modelling/analysing a dropped object scenario have been studied. In the first method a beam element attached to a hyperelastic spring is introduced. The new elements were modelled using the structural file format UFO. The drop was activated using the input record USERFRAC which ‘cut’ the beam at a certain time t from its initial position and thus initialized the fall. The load was applied as a nodemass on node 902, see Figure 7.1.

In method 2 the point of impact (node 43) is given an initial velocity, calculated from the principle of energy conservation. The velocity is activated at time t , and a nodemass of 6000 kg has been attached to the same node.

The main reference for this chapter is USFOS Commands: Overview and Description (2008).

7.2 Method 1: Principle and modelling

The dropped object scenario is modelled by introducing the following elements:

- A ***dummy beam***, which intention is to keep the falling object fixed in its initial position until we wish to initialize the fall at time t . The dummy beam has element number 810 and is illustrated in Figure 7.1.
- An ***additional beam*** (element number 820) shall simulate a falling object, see Figure 7.1.
- A ***hyperelastic spring*** element (element number 830) is introduced to establish a contact between the falling beam and the underlying structure, as illustrated in Figure 7.1.

The dummy beam (node 900 to 901), conveniently of small dimensions, is placed vertically at a certain height above the point of impact, see Figure 7.1.

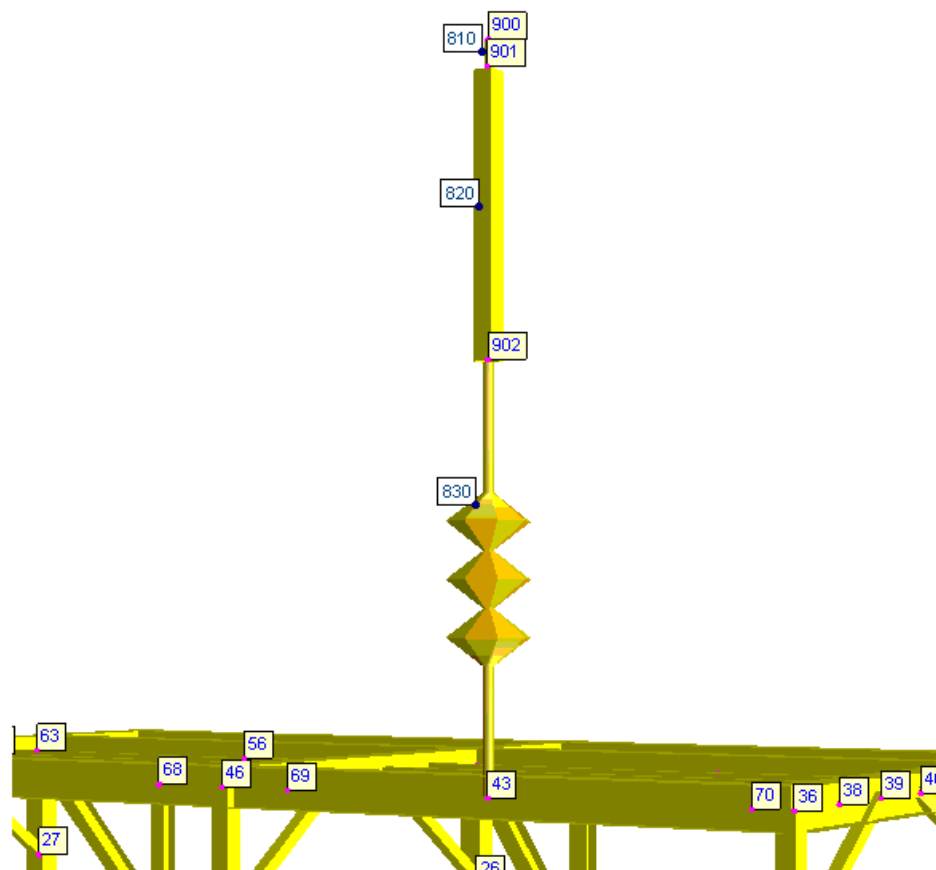


Figure 7.1 Dummy beam, beam and hyperelastic spring attached to the structure in node 43.

The point of impact is assigned node number 43. The top end of the dummy beam is fixed in all degrees of freedom, while the other end is free to move vertically (z-direction). Another beam, of ‘normal’ dimensions, is attached to the dummy beam such that end number 2 of the dummy beam and end number 1 of the other beam are assigned the same node number (901). End 2 (node 902) of the beam is located 3 m above the point of impact according to the design accidental load specification (DAL), see Chapter 6.4.

In order for the analysis program to be able to simulate a movement (fall) of the beam, a contact between the space frame and the falling beam must be made. This is done by introducing a hyperelastic spring, attached to node 902 on the beam and to node 43 of the space frame. A more detailed description of the hyperelastic spring is given in Chapter 7.5.

In order for the beam and the attached nodemass to fall down on the laydown area below, the beam must somehow be disconnected from the dummy beam. This can be done using the input record USERFRAC. USERFRAC forces an element to be fractured, i.e. it cuts the specified element in two. Consequently, half the mass of the dummy beam will be added to the assigned nodemass and the mass of the falling beam, but it is (if not designed extremely large) so small compared to the rest of the mass that it is negligible. The weight of the falling beam is subtracted from the nodemass such that the total mass hitting the structure is 6000 kg.

The whole model is shown in Figure 7.2.



Figure 7.2 Model of laydown area with dropped object (invisible spring).

7.3 Method 2: Principle and modelling

In method 2 the point of impact is given an initial velocity of 7.67 m/s, corresponding to the velocity at impact when an object of 6000 kg falls from a height of 3 m. In this case, the nodemass of 6000 kg is attached to node 43. This will not appear in the model.

7.4 General dynamic input

A dropped object loading is time dependant, i.e. it is a dynamic load. USFOS is designed such that all loads in a dynamic analysis, including permanent loads, must be applied at a certain time t . The input records TIMEHIST and LOADHIST are used to define how loads and load combinations vary with time. DYNAMIC specifies the size of the load step for various time intervals. They are specified in the analysis control file.

TIMEHIST defines the various time histories by relating a scaling factor to time, as shown in Figures 7.3 and 7.4.

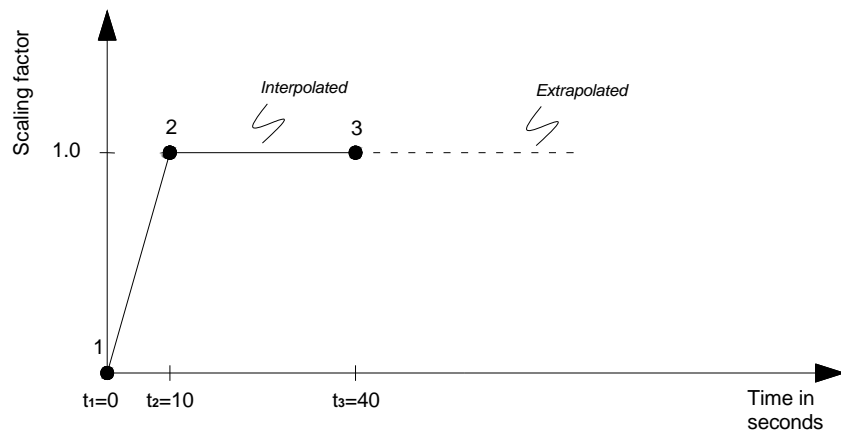


Figure 7.3 Time history used for method 1 and method 2, defined by discrete points.

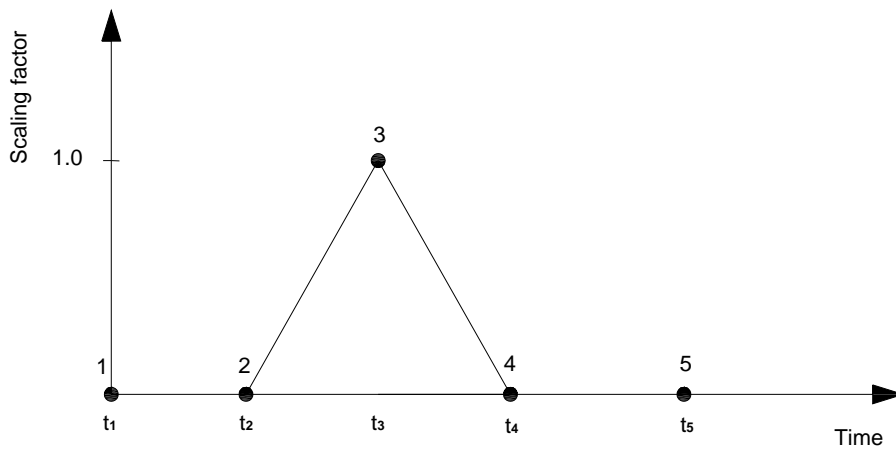


Figure 7.4 Example of time history defined by discrete points (USFOS Commands: Overview and Description, 2008).

Figure 7.3 shows the time history used in the analyses for method 1 and method 2. The scaling factor is placed on the y-axis, and time is given on the x-axis. The scaling factor/time curve is given by defining an adequate number of points as to obtain the desired variation with time. The curve in Figure 7.3 represents the permanent load applied at time $t_1 = 0$ and gradually augmenting to its full size at time $t_2 = 10$ s. The live load is defined according to the same time history. The reason why the loads were applied over such a long period of time was to make sure they would not cause any dynamic effect.

The values between the tabulated points are interpolated, and USFOS uses the last two points to extrapolate the line for times greater than t_3 .

The curve in Figure 7.4 may represent an impact load activated at time t_2 . The load is at its maximum at time t_3 and zero again at time t_4 . It was not necessary to define a time history for the impact loading from the dropped object since this is “incorporated” in the modelling of the dropped object.

The time histories illustrated by Figure 7.3 and 7.4 are defined by discrete points, but other ways of defining time histories are also possible, e.g. as a sine function or as a function for wave loading varying with time, corresponding to a chosen wave theory.

The various load cases are connected to the time history(-ies) by the input record **LOADHIST**. It means that the loads in a dynamic analysis are now activated, deactivated or scaled according to the time history they are connected to by **LOADHIST**. This can be illustrated as follows:

LOAD and **TIMEHIST** = **LOADHIST**

where **LOAD** is a value for scaling the load and **TIMEHIST** defines the variation with time.

For the space frame only one load history was specified, connecting both dead load and live load to the same time history.

The input record **DYNAMIC** defines the load step/increment to be used in various time intervals of the analysis. The input used in the analysis of the laydown area for method 1 is shown below.

	End_Time	D_t	dT_Res	dT_pri
Dynamic	20.00	1.0	5.0	5.0
Dynamic	20.76	0.005	0.1	0.1
Dynamic	20.90	0.0001	0.0002	0.0001
Dynamic	22.00	0.005	0.005	0.005
Dynamic	24.00	0.01	0.1	0.1

First, the end time (End_Time) is specified. It defines the time interval in which a specified load increment will be used. The load increment (Delta_T) is defined after end time. In the analysis of the laydown area large load steps were used in the first time interval, from $t = 0$ to $t = 20.76$ seconds, since the structure was not experiencing any significant load effect in this period. Right

before time of impact, which occurs at $t \sim 20.77$ seconds, much smaller load steps are used to obtain results that are as correct as possible in the nonlinear domain.

The size of the load increment is quite important since it decides how often USFOS analyses the structure. As mentioned in Chapter 5.3 each load increment involves a full update of the structural configuration which means that small load steps generate a lot of information. Plastic hinges are assumed to develop before $t = 22$ seconds, i.e. right after impact, such that for the last time interval large load steps are used to save disc space.

The two last inputs to the record DYNAMIC are:

- time between saving of results to the 'raf'-file (dT_res), and
- a time interval specifying how often the results shall be printed to the terminal.

The control node (CNODES) was chosen as node 43.

7.5 Features of the hyperelastic spring

The nonlinear spring, defined by the input record HypElast, is used to determine contact between the impacting object and the structure. The spring properties (stiffness) are specified by $P - \delta$ curves defined by discrete points as illustrated in Figure 7.5. A beam element is defined as the hyperelastic spring, and is given a material ID referring to the input record MREF. The MREF command automatically refers to material properties for a nonlinear spring, and one $P - \delta$ curve is specified per degree of freedom. Material numbers equal to zero means the spring has no stiffness in the actual degree of freedom. The curve must be linear through origo, and origo should not be specified (USFOS User's Manual: Modelling, 1999).

It is important that the spring stiffness is defined such that it allows for the falling object to hit the structure exactly, i.e. that the falling object do not fall 'through' the structure or stops a distance before the point of impact. This might happen if the $P - \delta$ curve defines a spring that is too stiff before impact, or if the stiffness is very low until a point past the point of impact.

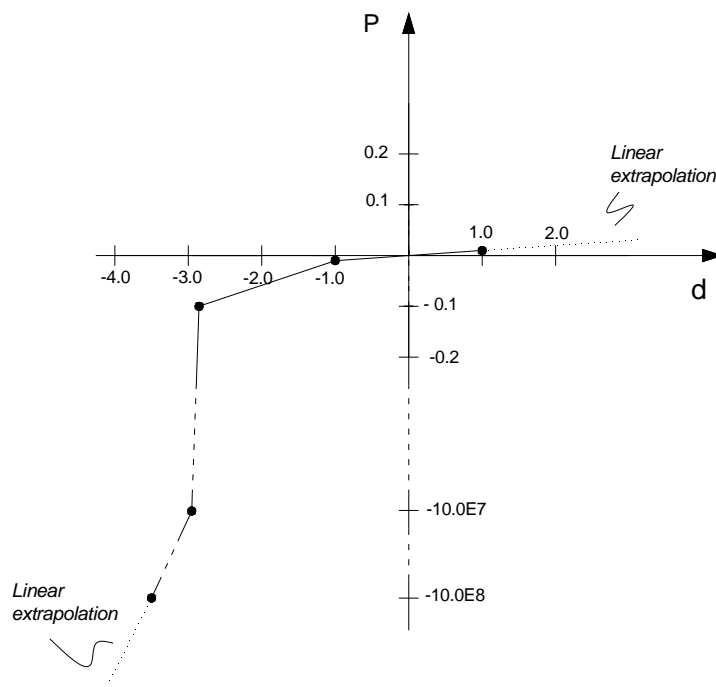


Figure 7.5 P – δ curve for the hyperelastic spring element defined in method 1.

Figure 7.5 shows the P – δ curve defining the stiffness in z-direction for the hyper elastic spring used in method 1. The curve is defined by five discrete points as shown in Figure 7.5, giving a spring with low stiffness from around initial position (0 m) until right before impact (-2.85 m). From the point (-2.85, -0.1) the stiffness is increased considerably, resulting in a very stiff spring just around the point of impact. This is done such that the spring is exactly stiff enough to make the beam fall *onto* the underlying structure.

One might immediately think that the spring, due to it having a stiffness, effects the velocity and acceleration of the falling object. Evaluation of plots showing the velocity and acceleration of the point of impact on the falling beam (node 902) in relation to time indicates that the velocity and acceleration right before impact is as expected, i.e. $v \sim 7.67$ m/s and $a \sim 9.81$ m/s². This may indicate that the resistance in the spring is insignificant or at least very small.

7.6 Damping

Structural damping may be specified by the input records RAYLDAMP according to the Rayleigh damping model and/or by DampRatio. As damping has minor significance when dealing with impact loads, the damping defined in the analysis for the space frame was set equal to a constant value of 2 % according to current practice for dropped object analyses. Also, the USFOS User's Manual: Modelling (1999, p. 3-25 to 3-26) states that "the Rayleigh damping terms will often be of minor importance since the effective damping will be predominated by hysteretic material behaviour in plastic hinges".

7.7 Repeated plastification/elastic unloading

Repeated plastification/elastic unloading is a common problem in USFOS and is referred to as “false on-/off loading”. This may ‘clog up’ the analysis (USFOS Getting Started, 2001).

In the first analysis of the space frame the secondary beams (elements 35-42, 48 and 49) seemed to experience repeated plastification/elastic unloading during the analysis. A maximum number of subsequent load steps were defined by the input command CUNFAL and was set equal to 2. If an element now unloaded/re-plastified in more than 2 subsequent load steps, elastic unloading would be suppressed in the remaining steps. When the element goes through a load step without trying to unload, the restriction is removed (USFOS Commands: Overview and Description, 2008).

8 Hand calculations

8.1 Work considerations

The *kinetic energy* of an object falling in air is given by (NORSOK N-004, 2004):

$$E_k = \frac{1}{2} \cdot m \cdot v^2 \quad (8.1)$$

where the velocity v is defined as

$$v = \sqrt{2 \cdot g \cdot h} \quad (8.2)$$

derived from the principle of energy conservation.
 h is the travelled distance from drop point.

$$m = 6000 \text{ kg} \quad h = 3 \text{ m}$$

$$v = 7.67 \frac{\text{m}}{\text{s}}$$

$$E_k = 176.52 \text{ kNm}$$

All cross-section data are given by the structural program "Section 4.7".

The plastic section modulus for an HE300B is

$$W_p = 1.869 \cdot 10^6 \text{ mm}^3$$

The plastic moment capacity M_p is defined as

$$M_p = \sigma_y \cdot W_p \quad (8.3)$$

where $\sigma_y = 355 \frac{\text{N}}{\text{mm}^2}$

For an **HE300B** the plastic moment capacity is thus

$$M_{p1} = 663.495 \text{ kNm}$$

The columns, RHS 150x150x10, have the following plastic section modulus:

$$W_p = 2.860 \cdot 10^5 \text{ mm}^3$$

The plastic moment capacity for the **RHS 150x150x10** is then given as

$$M_{p2} = 101.53 \text{ kNm}$$

Due to a central concentrated load P (representing the dropped object) the frame will develop three plastic hinges, resulting in the collapse mechanism as shown in Figure 8.1.

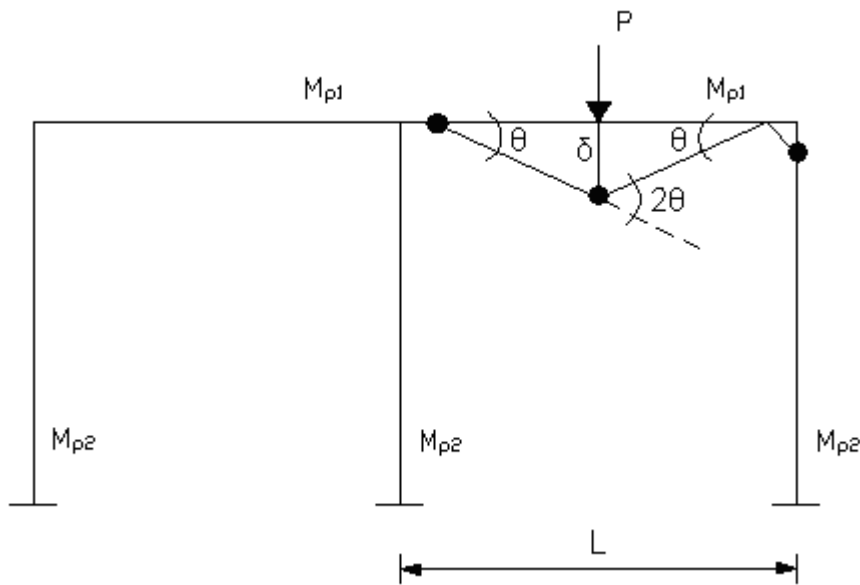


Figure 8.1 Possible collapse mechanism for the portal frame model.

Since only one collapse mechanism is considered to develop in practice, the upper and lower bound theorems which when combined provides the right collapse mechanism, will not be considered.

External work W_e equals internal work W_i :

$$W_e = W_i \quad (8.4)$$

$$P_c \cdot \delta = \theta \cdot M_{p1} + 2\theta \cdot M_{p1} + \theta \cdot M_{p2} \quad (8.5)$$

Compatibility:

$$\tan \theta \approx \theta \quad \text{giving the following relation:}$$

$$\theta = \frac{\delta}{\frac{L}{2}} \quad (8.6)$$

$$L = 5 \text{ m}$$

The number of unknowns in the equation is now reduced to one:

$$P_c \cdot \delta = \frac{\delta}{\frac{L}{2}} \cdot (3 \cdot M_{p1} + M_{p2}) \quad (8.7)$$

$$P_c = 2 \cdot \frac{(3 \cdot M_{p1} + M_{p2})}{L} \quad (8.8)$$

$$P_c = 836.806 \text{ kN}$$

The deflection caused by a mass of 6000 kg falling from 3 m can be found from the following relations:

$$W_e = P_c \cdot \delta = E_k \quad (8.9)$$

$$E_k = \frac{\delta}{\frac{L}{2}} \cdot (3 \cdot M_{p1} + M_{p2}) \quad (8.10)$$

$$\delta = \frac{E_k \cdot L}{2 \cdot (3M_{p1} + M_{p2})} \quad (8.11)$$

$$\boxed{\delta = 211 \text{ mm}}$$

The maximum deflection of the frame is 211 mm when assuming that a plastic mechanism has taken place.

It might be interesting to know how much of the total deflection is elastic displacement and how much is plastic displacement. These values may be found from the method explained in the following.

The elastic deflection w of a fixed beam under central concentrated loading P is given as:

$$w = \frac{P \cdot L^3}{192 \cdot E \cdot I} \tag{8.12}$$

for $\sigma \leq \sigma_y$

where $E = 205000 \frac{N}{mm^2}$ and $I = 2.517 \cdot 10^8 mm^4$ for an HE300B beam.

Assuming elastic-perfectly plastic material behaviour we can get an approximate value for elastic displacement, as illustrated by Figure 8.2.

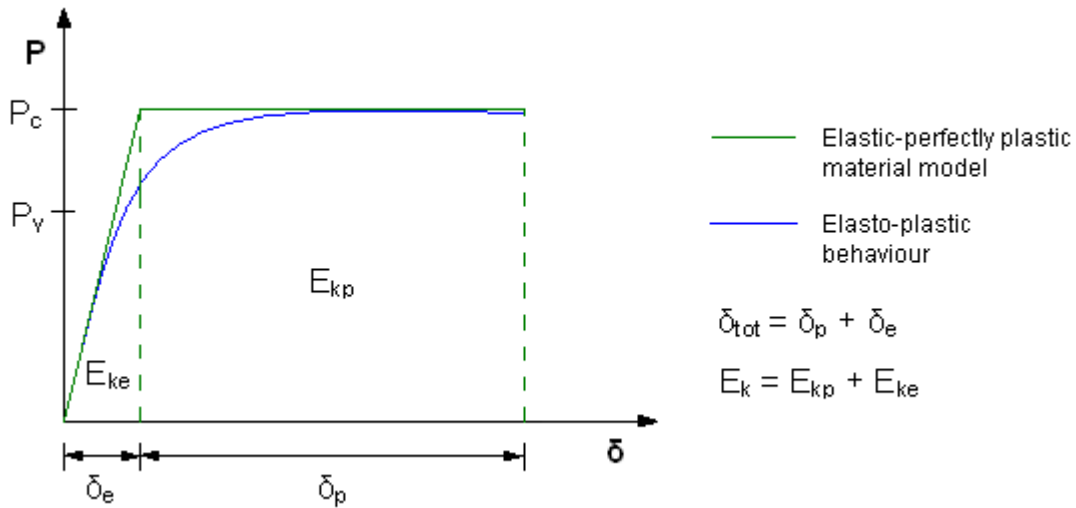


Figure 8.2 Elastic and plastic displacement

P is substituted by P_c into the expression for maximum elastic displacement (Equation 8.12):

$$w = \frac{P_c \cdot L^3}{192 \cdot E \cdot I} \tag{8.13}$$

$$w = 10.6 \text{ mm}$$

The triangular area under the curve in Figure 8.2 gives the amount of the kinetic energy causing elastic displacement, from now denoted δ_e . The rectangular area represents the amount of energy causing plastic displacement, δ_p . The plastic displacement is then found from basic mathematical relations:

$$w = \delta_e = 10.6 \text{ mm}$$

$$E_k = E_{ke} + E_{kp} \quad (8.14)$$

$$E_{ke} = \frac{\delta_e \cdot P_c}{2} \quad (8.15)$$

$$E_{ke} = 4.417 \text{ kNm}$$

$$E_{kp} = E_k - E_{ke} \quad (8.16)$$

$$E_{kp} = 172.103 \text{ kNm}$$

$$E_{kp} = P_c \cdot \delta_p \quad (8.17)$$

$$\delta_p = \frac{E_{kp}}{P_c} \quad (8.18)$$

$$\delta_p = 205.7 \text{ mm}$$

So the elastic displacement, $\delta_e = 10.6 \text{ mm}$, is very small compared to plastic displacement (5.13 %).

8.2 Axial restraint

The elastic elongation of a member subjected to an impact, as well as the axial flexibility of the nodes to which this member is connected, have a significant effect on the development of tensile (membrane) forces. Tensile forces may increase the load carrying capacity substantially, and should therefore be accounted for in the analysis. The effect of these tensile forces depends upon the ability of adjacent members to restrain the impacted member from inward displacement (NORSOK N-004, 2004).

In this case the equivalent elastic, axial stiffness is calculated to find the maximum deformation in yield hinges before tensile fracture (Chapter 8.3). The maximum displacement corresponds to an assumed value for critical strain ε_{cr} given in N-004 (2004). The maximum displacement obtained from the calculations in Chapter 8.3 is compared to the values of displacement found from work considerations in order to evaluate the integrity of the space frame, see Chapter 10.2. The value for critical strain is compared to the maximum beam strain resulting from the nonlinear finite element analyses. The equivalent elastic, axial stiffness may, possibly, be used to calculate the axial force component due to axial restraint.

According to N-004 (2004) an equivalent elastic, axial stiffness may be defined as

$$\frac{1}{K} = \frac{1}{K_{\text{node}}} + \frac{L}{2 \cdot E \cdot A} \quad (8.19)$$

where, in the present case, the elasticity modulus $E = 205\,000 \text{ N/mm}^2$, the member length $L = 5 \text{ m}$ and the cross-sectional area $A = 14\,900 \text{ mm}^2$. K_{node} is the axial stiffness of the node with the considered member removed, and may be found by performing a static analysis of the structure with unit loads introduced at the nodes where the member is removed (NORSOK N-004, 2004).

K_{node} is obtained from the following relation:

$$F = k \cdot x \quad (8.20)$$

where F is the unit load, here defined as 1 kN.
 x is (nodal) displacement.

We get the following nodal stiffness for nodes 36 and 46, respectively (see Figure 7.1):

$$K_{\text{node36}} = \frac{F}{x_1} \quad (8.21)$$

$$K_{\text{node46}} = \frac{F}{x_2} \quad (8.22)$$

$$x_1 = 0.023 \text{ mm} \quad x_2 = 0.004 \text{ mm}$$

x_1 and x_2 are found from static analysis of the space frame (see Appendix C).

$$K_{\text{node36}} = 43478 \frac{\text{N}}{\text{mm}}$$

$$K_{\text{node46}} = 250000 \frac{\text{N}}{\text{mm}}$$

The equivalent elastic, axial stiffness for the two nodes are then found to be:

$$\frac{1}{K_{36}} = \frac{1}{K_{\text{node36}}} + \frac{L}{2 \cdot E \cdot A} \quad (8.23)$$

$$K_{36} = 42017 \frac{\text{N}}{\text{mm}}$$

$$\frac{1}{K_{46}} = \frac{1}{K_{\text{node46}}} + \frac{L}{2 \cdot E \cdot A} \quad (8.24)$$

$$K_{46} = 207469 \frac{\text{N}}{\text{mm}}$$

8.3 Tensile fracture in yield hinges

According to N-004 (2004, Section A.3.10.4) a beam may experience rupture if the deformation in a yield hinge exceeds a value given by the following formula:

$$\frac{w}{d_c} = \frac{c_1}{2 \cdot c_f} \cdot \left(\sqrt{1 + \frac{4 \cdot c_w \cdot c_f \cdot \varepsilon_{cr}}{c_1}} - 1 \right) \quad (8.25)$$

For steel grade S 355 a critical strain value ε_{cr} of 15 % and a non-dimensional plastic stiffness H equal to 0.0034 are suggested (NORSOK N-004, 2004). The parameters L and E are given in Chapter 8.2.

The various factors are defined as follows:

Displacement factor

$$c_w = \frac{1}{c_1} \cdot \left[c_{lp} \cdot \left(1 - \frac{1}{3} \cdot c_{lp} \right) + 4 \cdot \left(1 - \frac{W}{W_p} \right) \cdot \frac{\varepsilon_y}{\varepsilon_{cr}} \right] \cdot \left(\frac{\kappa L}{d_c} \right)^2 \quad (8.26)$$

Plastic zone length

$$c_{lp} = \frac{\left(\frac{\varepsilon_{cr}}{\varepsilon_y} - 1 \right) \cdot \frac{W}{W_p} \cdot H}{\left(\frac{\varepsilon_{cr}}{\varepsilon_y} - 1 \right) \cdot \frac{W}{W_p} \cdot H + 1} \quad (8.27)$$

Axial flexibility factor

$$c_f = \left(\frac{\sqrt{c}}{1 + \sqrt{c}} \right)^2 \quad (8.28)$$

Non-dimensional spring stiffness

$$c = \frac{4 \cdot c_1 \cdot K \cdot w_c^2}{f_y \cdot A \cdot L} \quad (8.29)$$

w_c is characteristic deformation, but is only defined for tubular members and stiffened plating in the current section of N-004. Section A.6.9.2 (NORSOK N-004, 2004) gives a definition of w_c for beams, here defined as characteristic beam height but seem to correspond to the definition of

w_c for stiffened plating in Section A.3.7.2; $w_c = \frac{1.2 \cdot W_p}{A}$, such that it is considered relevant for the use in the calculations also for dropped objects. w_c for beams is defined as follows:

$$w_c = \frac{\alpha \cdot W_p}{A} \quad (8.30)$$

where α may be assigned a value of 1.2 for H or I beams in lieu of more accurate analysis.

$$w_p = 1.869 \cdot 10^6 \text{ mm}^3$$

$$w_c = 151 \text{ mm}$$

For an HE 300B beam with clamped (fixed) ends the remaining parameters have the following values:

$c_1 = 2$ for clamped ends

$\kappa \cdot L \leq 0.5L$ The smallest distance from the point of impact to adjacent joint

$\kappa L = 2500 \text{ mm}$

$W = 1.680 \cdot 10^6 \text{ mm}^3$ Elastic section modulus

$W_p = 1.869 \cdot 10^6 \text{ mm}^3$ Plastic section modulus

$f_y = 355 \frac{\text{N}}{\text{mm}^2}$ Yield strength

$\varepsilon_y = \frac{f_y}{E}$ Yield strain

$\varepsilon_y = 0.00173$

d_c is the characteristic dimension which for symmetric I-profiles shall be taken as equal to the height h :

$d_c = 300 \text{ mm}$

c depends on the equivalent elastic, axial stiffness obtained for the two different nodes; K_{36} and K_{46} .

$$c_{36} = \frac{4 \cdot c_1 \cdot K_{36} \cdot w_c^2}{f_y \cdot A \cdot L} \quad (8.31)$$

$$c_{46} = \frac{4 \cdot c_1 \cdot K_{46} \cdot w_c^2}{f_y \cdot A \cdot L} \quad (8.32)$$

$c_{36} = 0.290$

$$c_{46} = 1.431$$

The previously defined functions have the following values:

$$c_{lp} = 0.208$$

$$c_w = 6.870$$

The following parameters depend upon the equivalent stiffness in the two nodes.

$$c_{f36} = \left(\frac{\sqrt{c_{36}}}{1 + \sqrt{c_{36}}} \right)^2 \quad (8.33)$$

$$c_{f46} = \left(\frac{\sqrt{c_{46}}}{1 + \sqrt{c_{46}}} \right)^2 \quad (8.34)$$

$$c_{f36} = 0.123$$

$$c_{f46} = 0.297$$

Finally, we obtain a maximum displacement in the yield hinge, which will depend on the two different equivalent stiffnesses found for node 36 and node 46:

$$w_{36} = \frac{c_1}{2 \cdot c_{f36}} \cdot \left(\sqrt{1 + \frac{4 \cdot c_w \cdot c_{f36} \cdot \varepsilon_{cr}}{c_1}} - 1 \right) \cdot d_c \quad (8.35)$$

$$w_{46} = \frac{c_1}{2 \cdot c_{f46}} \cdot \left(\sqrt{1 + \frac{4 \cdot c_w \cdot c_{f46} \cdot \varepsilon_{cr}}{c_1}} - 1 \right) \cdot d_c \quad (8.36)$$

$$\boxed{w_{36} = 292 \text{ mm}}$$

$$w_{46} = 660 \text{ mm}$$

The formulas presented in this chapter are defined for accidental loading from ship collisions (NORSOK N-004, 2004), but is considered relevant also for dropped objects since the nature of the load is (more or less) the same.

9 Results

9.1 Method 1

9.1.1 General

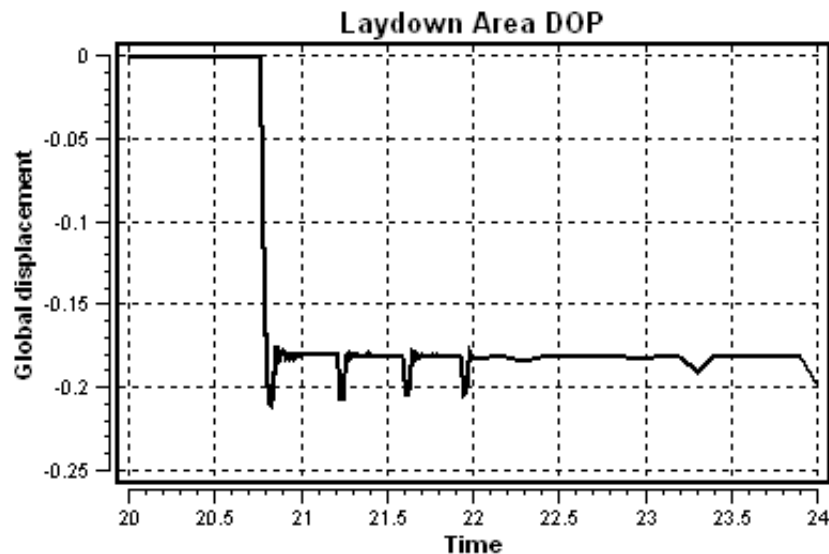
Results from the nonlinear (dynamic) analysis of the space frame modelled as described in Chapter 7.2, are presented in the following.

At first, the analysis was run without performing iterations. This resulted in an exceedance of the Γ_y -values¹ for relevant members. Iteration was specified to obtain the final results presented in this chapter, see Chapter 9.1.6 for further details.

As can be seen clearly from the plots shown in both this chapter and Chapter 9.2, small load steps have been used in the time interval 20.76 – 22.0 seconds and much larger from 22.0 to 24.0 seconds. This was done to save disc space such that the analysis was able to run to the specified end time.

9.1.2 Maximum displacement

Figure 9.1 shows the displacement in z-direction in node 43 as a function of time.



¹ USFOS Getting Started (2001) suggests that the Γ_y -values for a pushover analysis should not exceed 0.05 for primary structures. The first analysis gave a value of 0.067 for one member, thus iterations were 'switched on'. Limit values for a dropped object situation were not found in USFOS Getting Started, therefore the above mentioned limit value was found appropriate.

Figure 9.1 Displacement in z-direction¹ for node No. 43, given in meters.

According to numerical results forming the basis for the graph in Figure 9.1 the maximum displacement in z-direction in node 43 is – 211 mm occurring at time $t \sim 20.8$ s, see Table 9.1.

20.8281	-0.210914
20.8283	-0.210919
20.8285	-0.21092
20.8287	-0.210919
20.8289	-0.210915

Table 9.1 Numerical results for displacement in z-direction for node No. 43 at time $t = 20.8281$ to $t = 20.8289$.

The analysis showed that the dropped beam bounces somewhat up and down on the impacted beam shortly after impact. This can be seen on the graph in Figure 9.1. The plastic displacement is therefore taken as the value of deflection corresponding to where we have asymptotic values on the graph since the dropped beam at this point is ‘in the air’, i.e. the structure is considered unloaded at this point. This gives a plastic deflection of approximately 180 mm.

¹ Only the most relevant part of the graph is shown.

9.1.3 Plastic utilization and development of plastic hinges

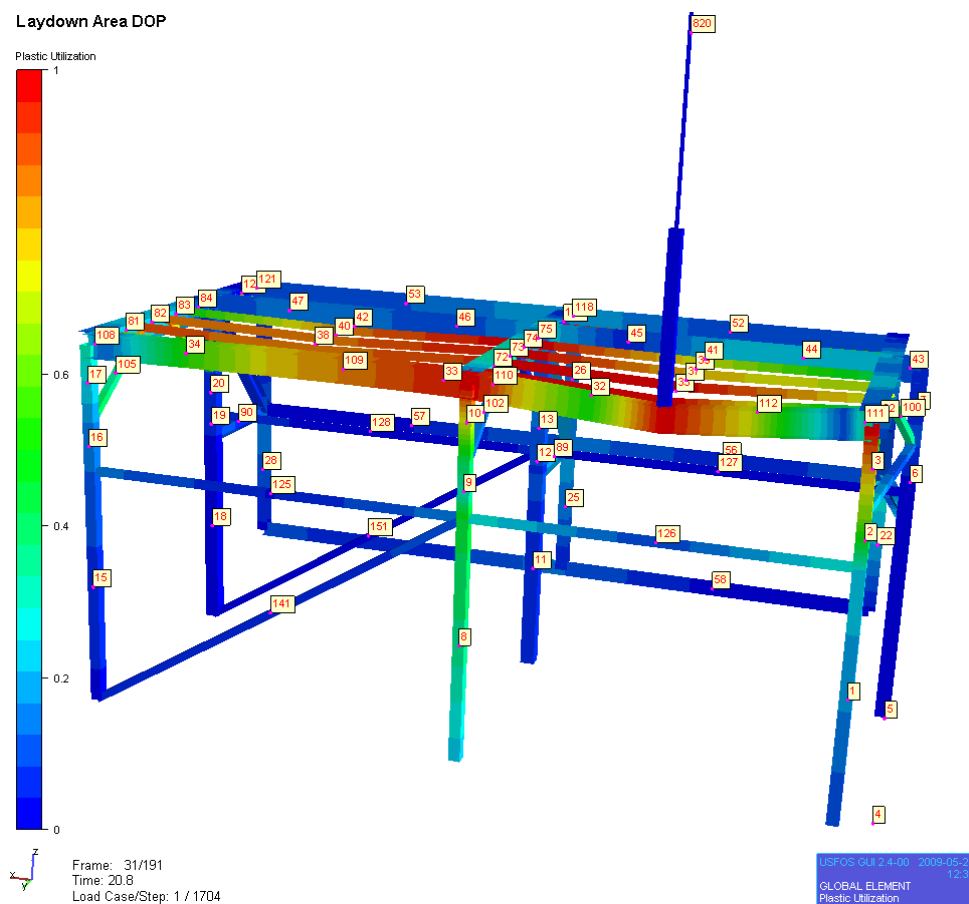


Figure 9.2 Plastic utilization

Figure 9.2 shows how much of the plastic capacity of the space frame is utilized shortly after the time of impact, and gives an indication of where plastic hinges have developed, or are about to be developed. By studying the output file one can find out exactly which beams have reached full plastification. All the (horizontal) secondary beams reach full plastification, but they are not of interest in this case due to reasons explained in Chapter 1.3. Primary elements developing full plastification at some point during the analysis are (given in chronological order):

- 32 end 1
- 112 end 2
- 110 end 2
- 10 end 1
- 3 end 2

End 1 and end 2 of the different elements correspond to the end of the element which in Figure 9.2 is deep red in colour.

Figure 9.2 indicates that element No. 33 (and possibly 109, but 33/109 would ideally have been one element) have, or may, develop a plastic hinge.

9.1.4 Beam strain

NORSOK N-004 (2004) proposes a maximum strain of 15 % for steel grade S 355 in yield hinges. Tensile fracture is assumed to occur at this value, or for the corresponding deflection which might be calculated using formulas defined in Section A.3.10.4 (N-004, 2004).

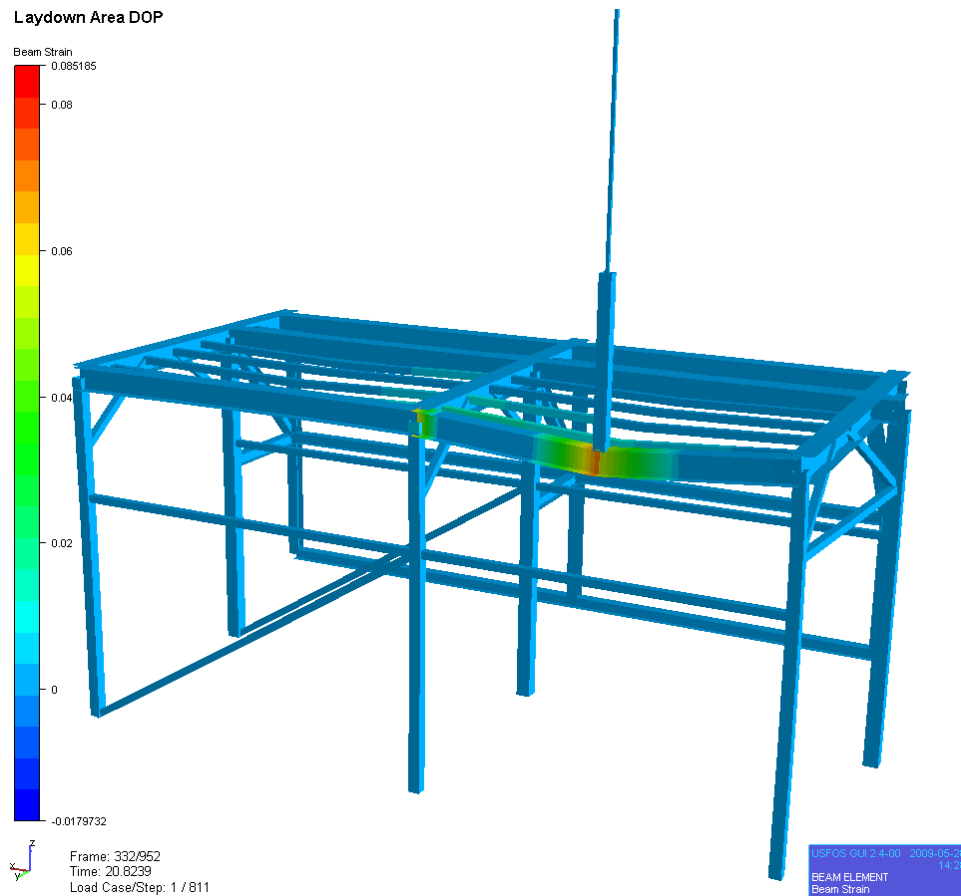


Figure 9.3 Beam strain

As can be seen from Figure 9.3 the maximum (beam) strain occurring in the space frame during the analysis is 8.52 %, which is acceptable.

9.1.5 Energy

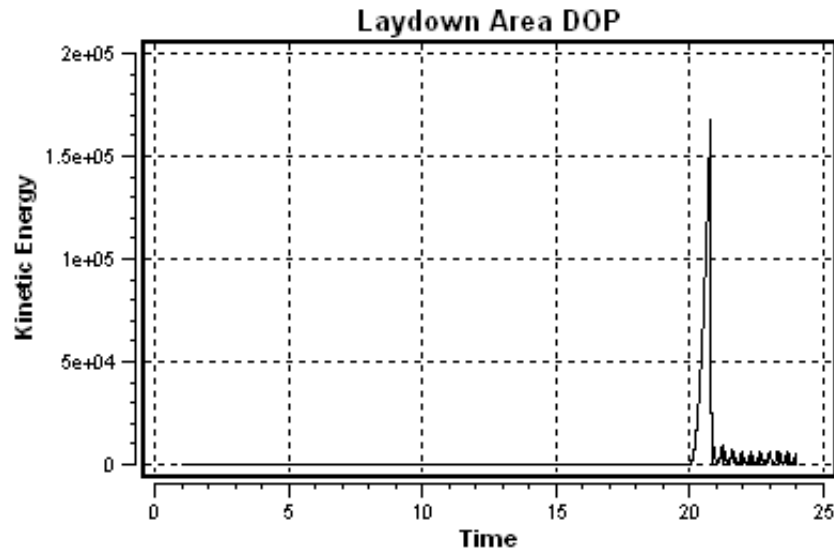


Figure 9.4 Kinetic energy

From Figure 9.4 the maximum kinetic energy seems to be somewhere between 160 and 170 kNm, which is a little lower than the expected maximum kinetic energy of 176.52 kNm, occurring right before impact. Although a plot of the nodal velocity in the end of the falling beam indicates that the velocity at impact is as expected, it is difficult to read an exact value from the graph so it might be somewhat less than 7.67 m/s. Thus, a possible reason for the deviation in expected and resulting kinetic energy might be that some of the kinetic energy from the dropped object is dissipated during the fall caused by a certain resistance in the hyperelastic spring.

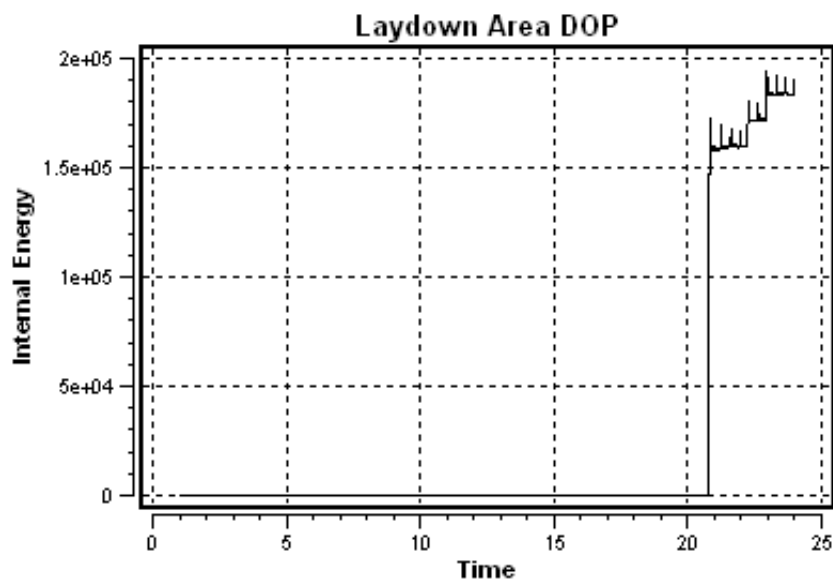


Figure 9.5 Internal energy

An internal energy of approximately 170 – 175 kNm at the time of impact is found from Figure 9.5.

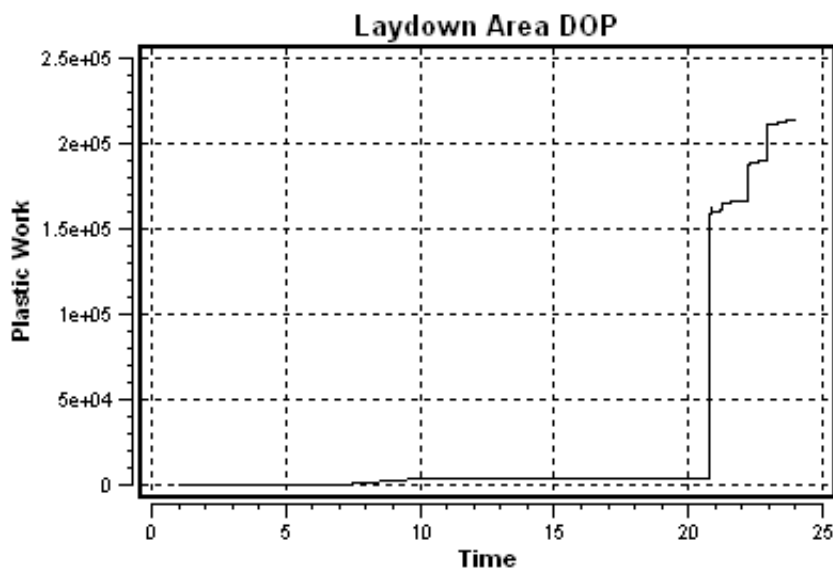


Figure 9.6 Plastic work

Plastic work right after time of impact is somewhere between 160 and 165 kNm according to Figure 9.6. The plot indicates a certain amount of plastic work from $t = 10$ s. It would immediately seem to be an effect from the live load and selfweight since they are defined as fully activated at $t = 10$ s. However, when calculating the maximum deflection for the case of only selfweight and live load using Equation 8.12 (Chapter 8.1), the resulting (elastic) deflection is

0.2 mm. It thus seems reasonable to assume that no, or minor, plastic work should have occurred before impact.

9.1.6 Γ_y -values

As stated in Chapter 5.2.3 Γ_y -values should not exceed 0.0 since it implies that the solution has deviated from the ‘true’ solution. If $\Gamma_y > 0.0$ one might consider the load carrying capacity of that member to have been overestimated by the same value (USFOS Getting Started, 2001). By checking the interaction function at the locations where plastic hinges has been or might be developed, one can find out if the $\Gamma_y = 0.0$ has been exceeded at any point during the analysis.

When a first analysis was performed for the space frame, the interaction values (Γ_y -values) exceeded an acceptable level. In order to try to correct for this problem, iteration was switched on by defining the input record CITER in the analysis control file. This command contains default values for the iteration. The maximum number of iterations may be changed by the input record LITER, but was not considered necessary in this case. The resulting Γ_y -values are described in the following.

For the beam subjected to the dropped object the Γ_y -values are shown in Figure 9.7 for the time period 20.5 s to 24 s.

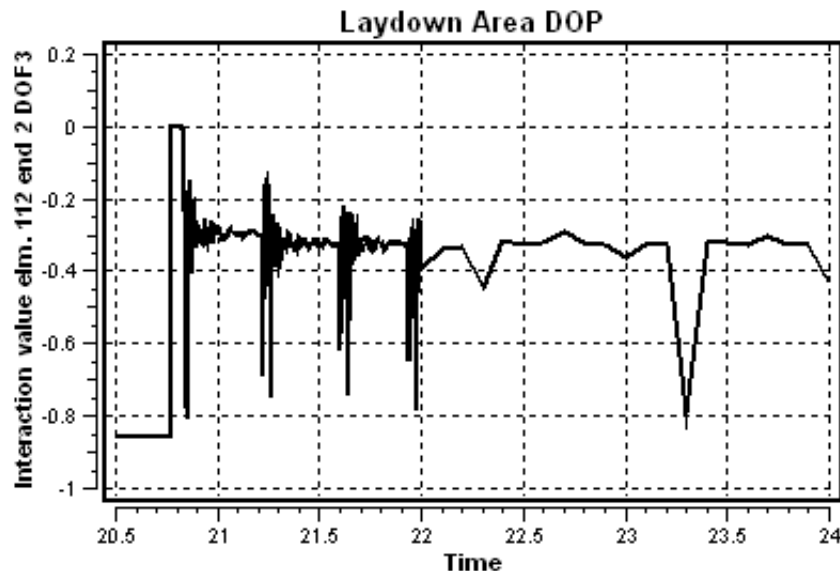


Figure 9.7 Γ_y -values for end 2 of element No. 112 (location of impact).

The graph in Figure 9.7 shows that at time of impact the Γ_y -value is slightly higher than 0.0, which means that the bounding surface is reached and a plastic hinge has been introduced.

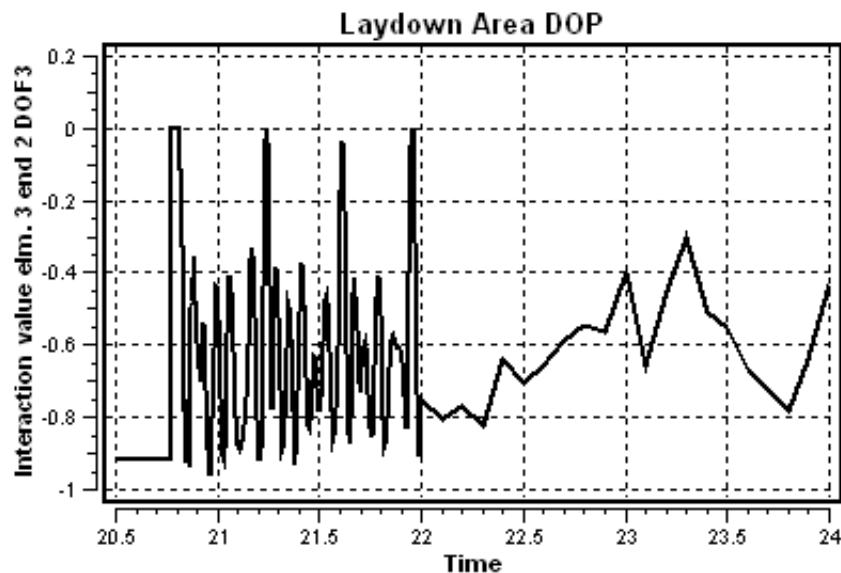


Figure 9.8 Γ_y -values for element No. 3, end 2.

According to Figure 9.8 the maximum Γ_y -value for element No. 3 is (approximately) the same as for element 112. Also, the other primary elements which developed plastic hinges, namely element Nos. 32, 110 and 10, have been checked for exceedance of the Γ_y -values. They showed the same maximum value as seen in Figure 9.7 and 9.8, and these results are therefore only mentioned.

Since element No. 33 according to Figure 9.2 seems to have a plastic utilization of 1.0, the Γ_y -values for this element were also checked. The result is shown in Figure 9.9.

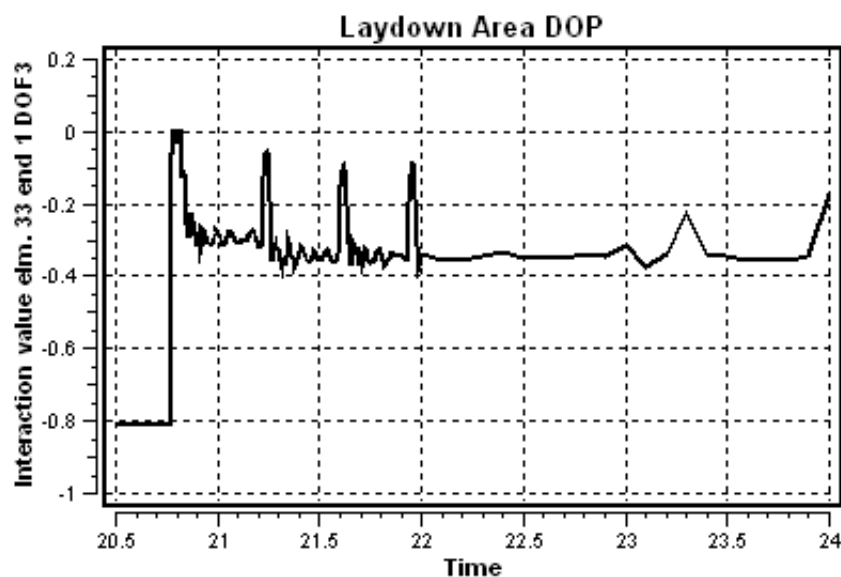


Figure 9.9 Γ_y -values for element No. 33, end 1.

Also this element has reached a Γ_y -value of 0.0, indicating that a plastic hinge has developed.

So, all the primary elements which according to Figure 9.2 show sign of full plastification have been checked for exceedance of the Γ_y -values with acceptable results, indicating that the solution follows the ‘true’ solution.

9.2 Method 2

9.2.1 General

Same load steps that were defined in method 1 were tried for method 2, without success. (The analysis stopped before end time with an error: “Incremental rotations too large...”). After some trial and error it seemed this model did not handle the rather abrupt transition in size of the load steps for the time intervals 20.70-20.90 s and 20.90-22.0 s. A few changes of the load steps in order to get a smoother transition were made, see Appendix B.1.

Results from the nonlinear (dynamic) analysis of the space frame modelled as described in Chapter 7.3, are presented in the following.

9.2.2 Maximum displacement

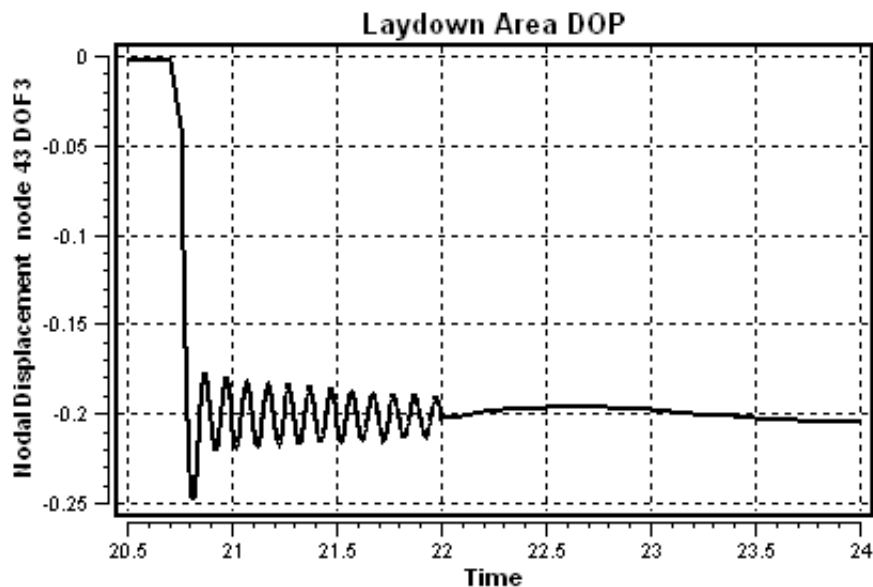


Figure 9.10 Displacement in z-direction for node No. 43, given in meters.

Maximum displacement in z-direction for the point of impact is shown in Figure 9.10.

20.814	-0.248324
20.815	-0.248525
20.816	-0.248596
20.817	-0.248536
20.818	-0.248345

Table 9.2 Numerical results for displacement in z-direction for node No. 43 at time $t = 20.814$ to $t = 20.818$.

According to the numerical results forming the basis of the graph in Figure 9.10, the maximum displacement in z-direction for node No. 43 is 249 mm, occurring right after the time of ‘impact’¹. This value includes both the static and dynamic effect from the loads. Since the mass is attached to the beam (nodemass), it is somewhat difficult to define how much of the total displacement is plastic displacement. One may at least say that the static displacement can be taken as the value corresponding to the axis about which the curve oscillates, i.e. ~ 200 mm which include both elastic and plastic displacement.

¹Corresponding to the activation of initial velocity (at $t = 20.75$ s).

9.2.3 Plastic utilization and development of plastic hinges

Plastic utilization of the space frame right after time of ‘impact’ is shown in Figure 9.11.

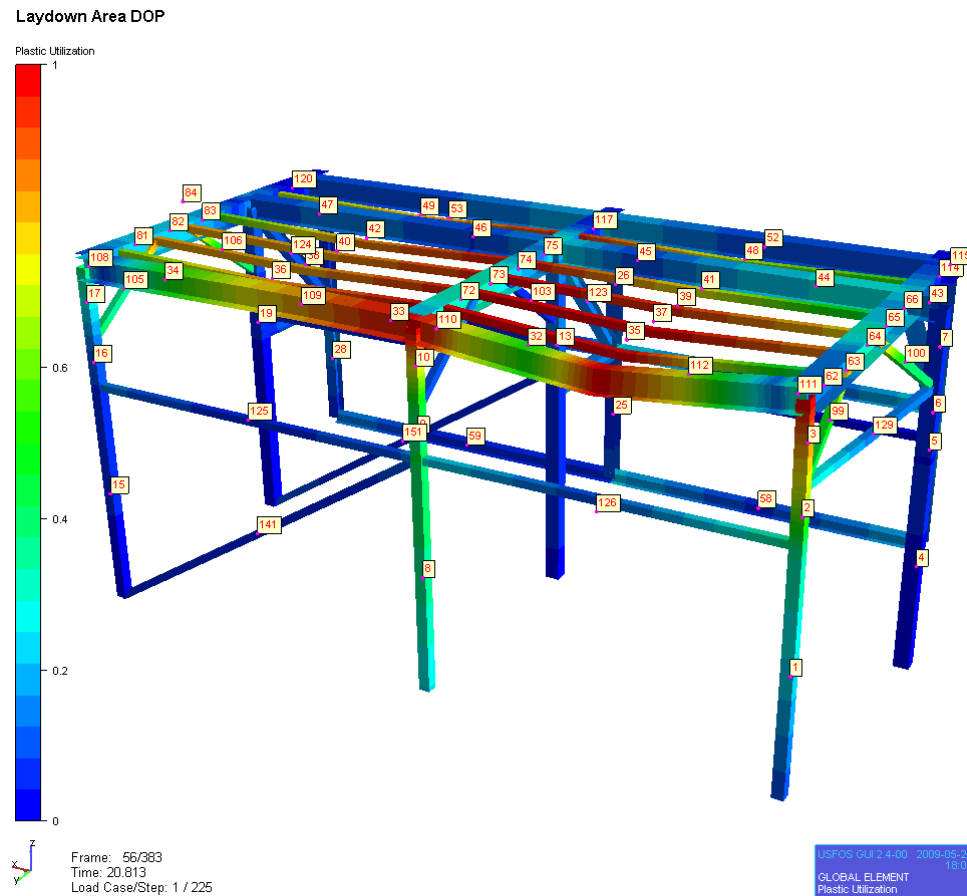


Figure 9.11 Plastic utilization

According to the output-file, following primary elements develop plastic hinges at some point after time of ‘impact’:

- 32 end 1
- 110 end 2
- 33 end 1
- 33 mid
- 110 mid
- 10 end 1
- 112 end 2

End 1 and end 2 of the different elements correspond to the end of the element which in Figure 9.11 is deep red in colour.

End 1 of element No. 32 and end 2 of element No. 112 correspond to the same node; node No. 43 which is the point of impact. Figure 9.11 indicates that element No. 3 also has developed a plastic hinge or is very close to doing so.

9.2.4 Strain

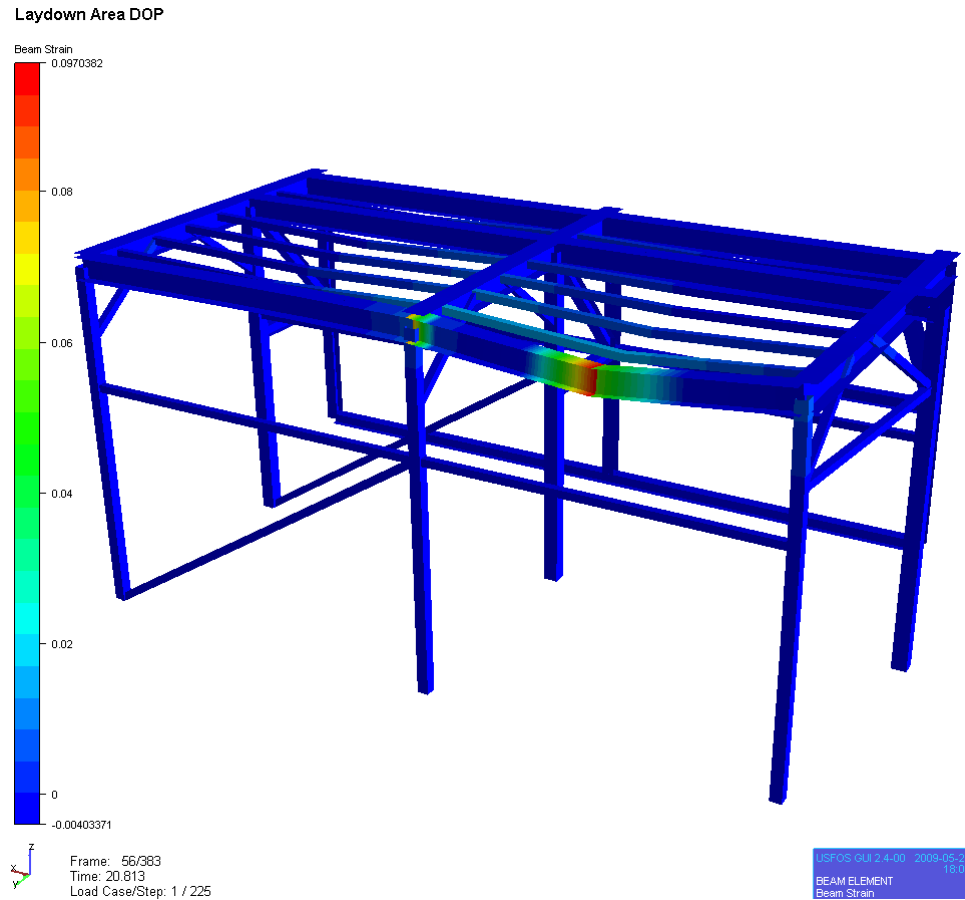


Figure 9.12 Beam strain

Figure 9.12 shows that maximum beam strain is 9.7 % which is acceptable compared to the critical strain value of 15 % (see Chapter 9.1.4).

9.2.5 Energy

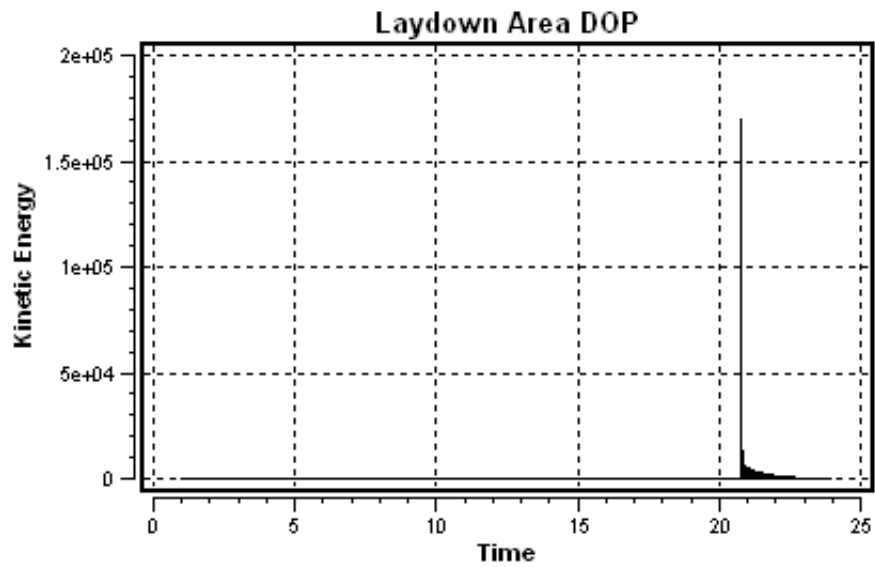


Figure 9.13 Kinetic energy

The kinetic energy is, according to Figure 9.13, approximately 170 kNm at its maximum which occurs right after 'impact'. This is slightly higher than the maximum kinetic energy in method 1.

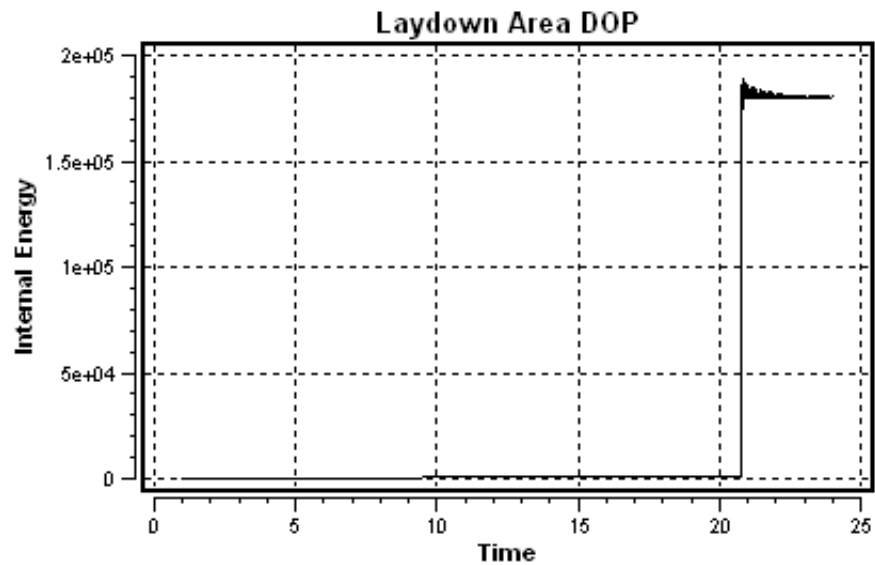


Figure 9.14 Internal energy

Internal energy is approximately 190 kNm, see Figure 9.14. This is around 15 – 20 kNm higher than the resulting maximum internal energy in method 1.

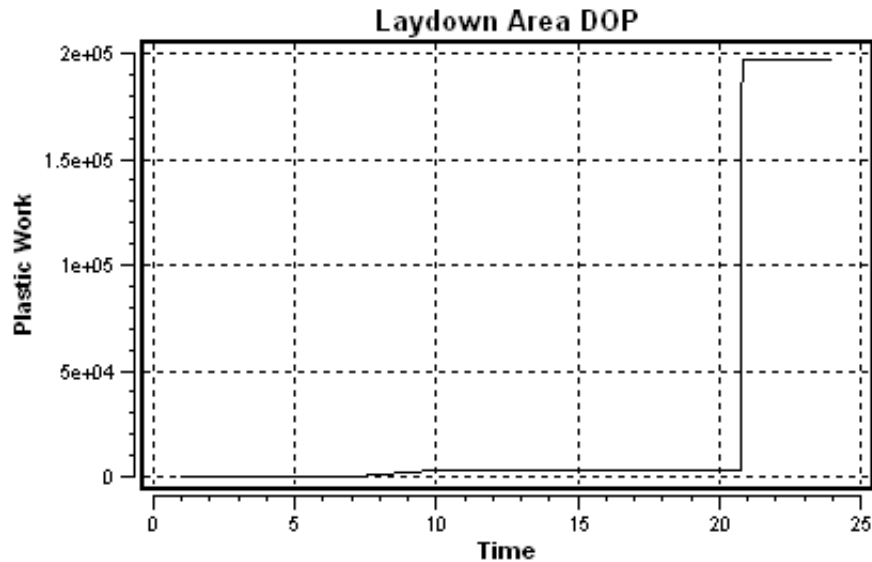


Figure 9.15 Plastic work

According to Figure 9.15 almost all the plastic work is done immediately after 'impact'. Compared to the plot showing plastic work in method 1 (Figure 9.6), it seems there is a significant difference in how the energy is dissipated in the structure between the two methods.

9.2.6 Γ_y -values

Figures 9.16, 9.17 and 9.18 show the Γ_y -values for three of the elements which developed plastic hinges (element Nos. 112, 10 and 32, respectively). The other two, element Nos. 33 and 110 were also checked, with acceptable Γ_y -values.

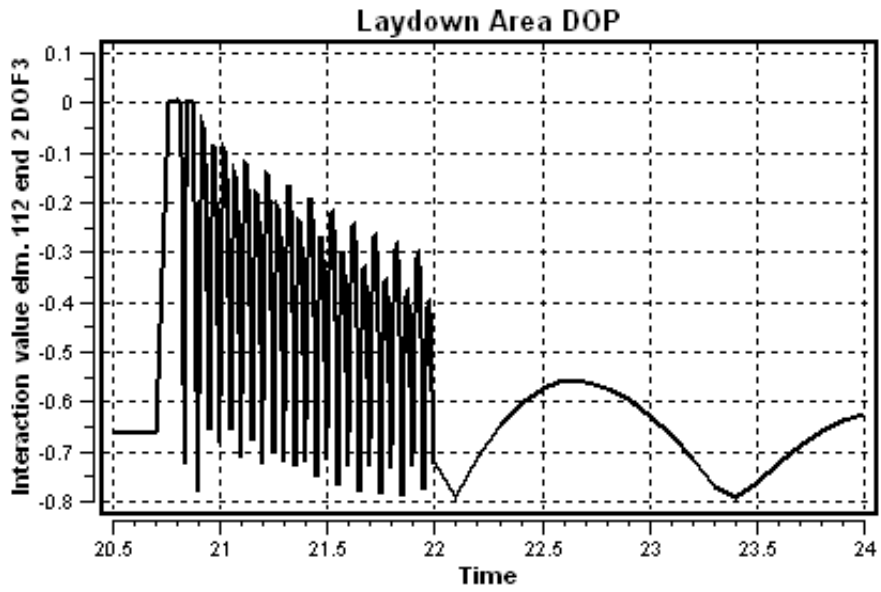


Figure 9. 16 Γ_y -values for end 2 of element No. 112 (location of impact).

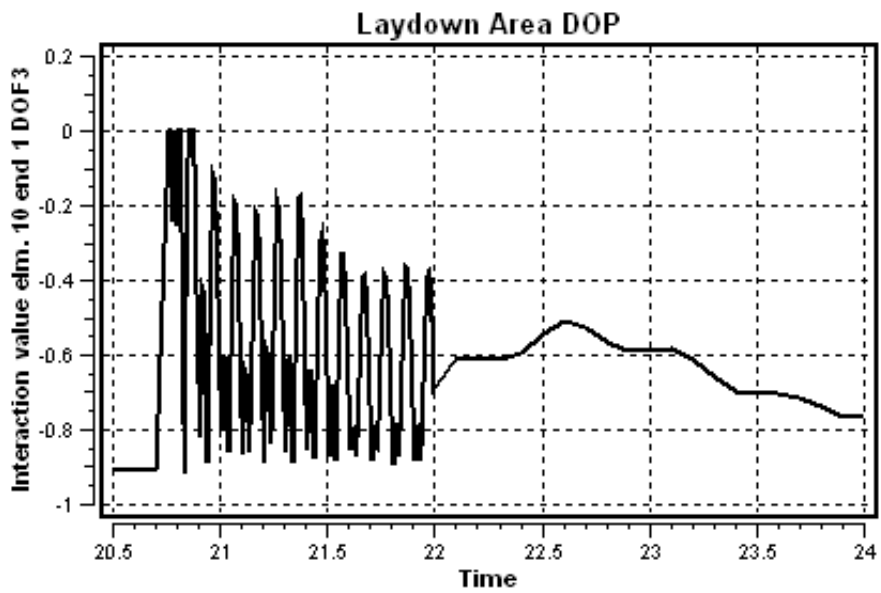


Figure 9. 17 Γ_y -values for element No. 10, end 1.

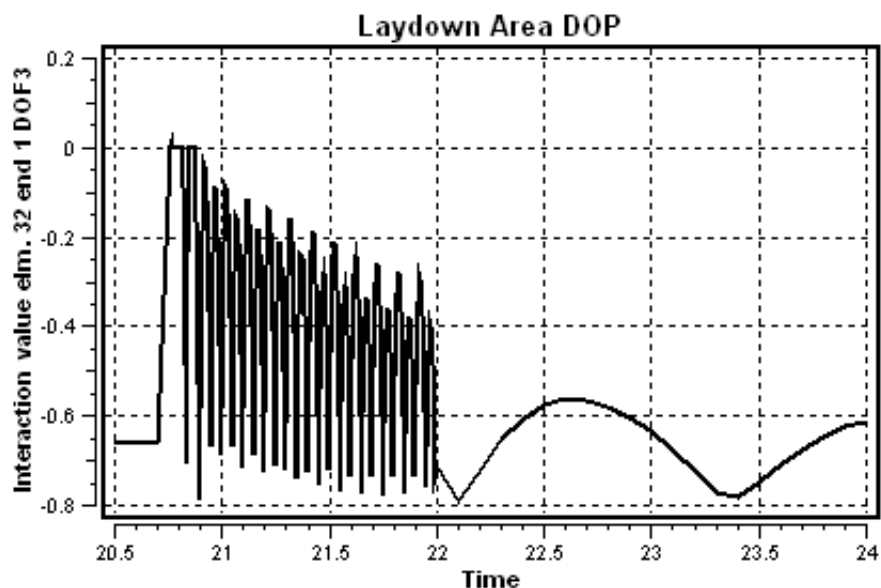


Figure 9.18 Γ_y -values for element No. 32, end 1.

Element nr 32, however, shows a slightly too high Γ_y -value, i.e. approximately 0.03 according to Figure 9.18. As mentioned in Chapter 9.1.1 it should not be higher than 0.02 for primary elements. The consequence is that the load carrying capacity is considered to be overestimated by the same value, see Chapter 9.1.6.

Since element number 3 according to Figure 9.2 seems to have a plastic utilization of 1.0, the Γ_y -values for this element were also checked. The result is shown in Figure 9.19, and indicates that a plastic hinge has developed also in this element.

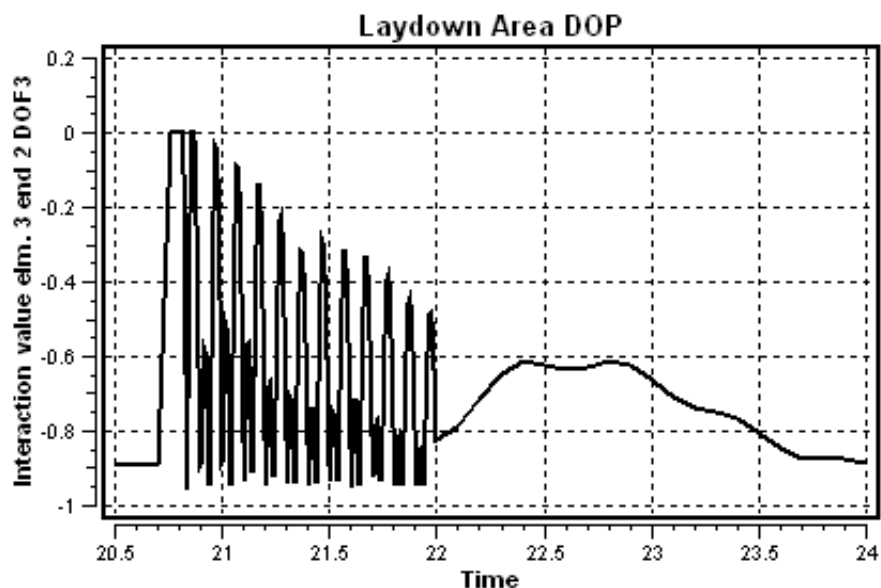


Figure 9.19 Γ_y -values for element No. 3, end 2.

10 Discussion

10.1 Deflection

The plastic displacement obtained from hand calculations was 211 mm and for method 1 approximately 180 mm. For method 2 it was not possible to assume a value for plastic displacement from the results since the impacted structure is never unloaded in the time after ‘impact’. It was, however, possible to specify an approximate value for the static deflection; 200 mm.

To find out how much of the static deflection which is elastic, one might calculate the elastic effect from the dropped object, selfweight and live load using the standard formulas

$$w = \frac{q \cdot L^4}{384 \cdot E \cdot I} \quad \text{for the selfweight and live load, and}$$

$$w = \frac{P \cdot L^3}{192 \cdot E \cdot I} \quad \text{for the dropped object.}$$

The selfweight and live load have a total uniformly distributed load of 6.25 kN/m and the dropped object has a static loading of 58.86 kN. The resulting elastic displacements are 0.20 mm and 0.74 mm for the dropped object and the uniformly distributed loads, respectively. It gives a total elastic deflection of 0.94 mm. Compared to the plastic displacement this value is so small that the total static deflection for method 2 of 200 mm might be considered to be the same as the plastic deflection. Consequently, the total static deflection for method 1 will be the same as the plastic displacement found from Figure 9.1.

A summary of the maximum deflection at the point of impact obtained from the various methods is presented in Table 10.1.

	Nonlinear (dynamic) analysis		Hand calculations
	Method 1	Method 2	Work considerations
Total deflection (exact values) [mm]	211	249	211
Static deflection [mm]	180	200	-
Plastic deflection [mm]	180	200	211 (206) ¹
Elastic deflection [mm]	~ 0	~ 0	(10)

Table 10.1 Summary of the displacement in z-direction at the point of impact from the various methods.

The plastic displacement obtained from work considerations is 31 mm (~ 17 %) larger than the results obtained from the nonlinear (dynamic) analysis of modelling alternative No. 1, see Table 10.1. Method 2, however, shows a plastic displacement of approximately 200 mm which is much closer to the results obtained from hand calculations. The difference in this case is only 11 mm (5,5 %). It is also interesting to see that the dynamic effect in method 2 is larger than in method 1; it is approximately 14.7 % of the total deflection in method 1 and 19.7 % in method 2. The difference in elastic displacement calculated from work considerations (see ¹) and from the nonlinear (dynamic) analyses might be due to the hand calculations assuming an elastic-perfectly-plastic material behaviour while USFOS implements an elasto-plastic material model.

In the hand calculations (Chapters 8.1) selfweight and live load are not accounted for. This is because the impact loading is given as energy, while selfweight and live load are defined as uniformly distributed loads (forces). When dealing with nonlinear material behaviour it is not possible to superpose the loads since the structural response is highly history dependent. It is therefore very difficult to account for various load types when performing hand calculations. One may however, make some considerations as to what influence these loads might have on the deformation of the structure:

- The selfweight and live load are uniformly distributed and will therefore cause a deflection which is only half the value of the resulting deflection if the same load had been acting as a concentrated load.
- Even though the selfweight and live load have a total mass of approximately 20 % of the mass of the dropped object, the fact that they are statically applied loads while the dropped object is dynamically applied increases the effect of the dropped object considerably compared to the selfweight and live load.

¹ The values in parenthesis are approximated values found by the method described in Chapter 8.1.

Most importantly, the selfweight and live load will cause a reduction in the plastic moment capacity prior to the impact from the dropped object.

10.2 Collapse mechanism

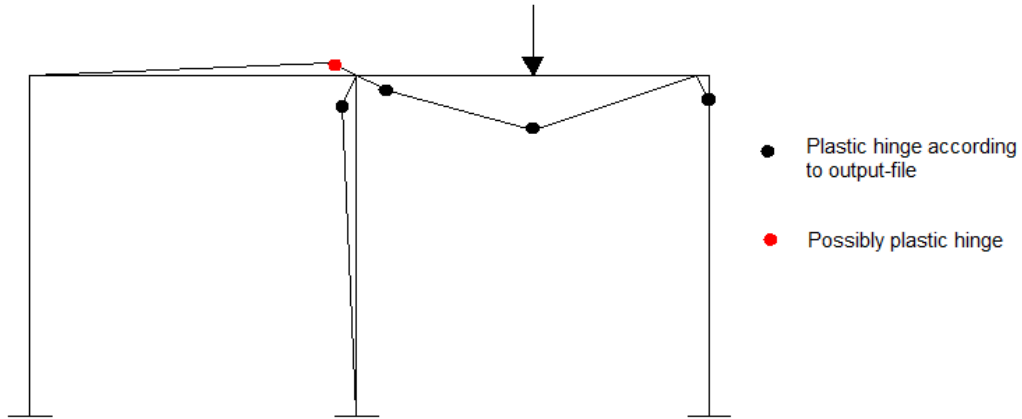


Figure 10.1 Collapse mechanism developed according to nonlinear (dynamic) analysis, method 1.

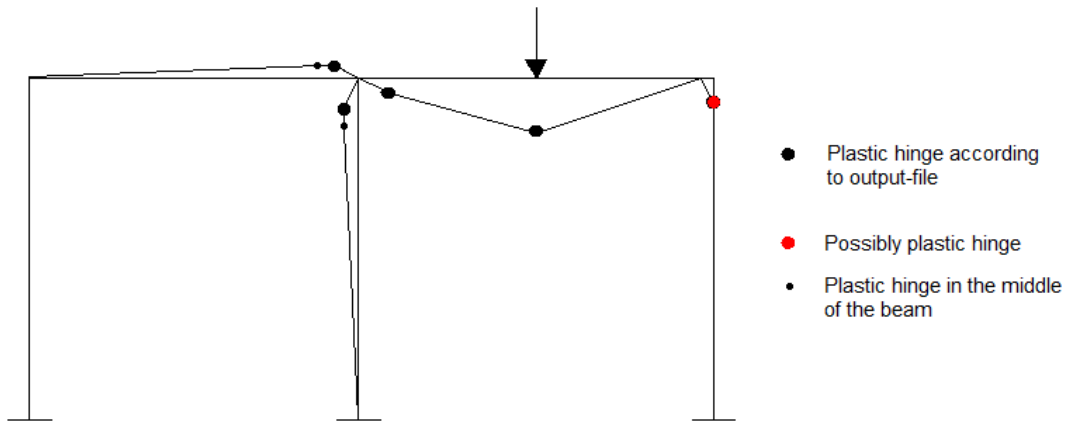


Figure 10.2 Collapse mechanism developed according to nonlinear (dynamic) analysis, method 2.

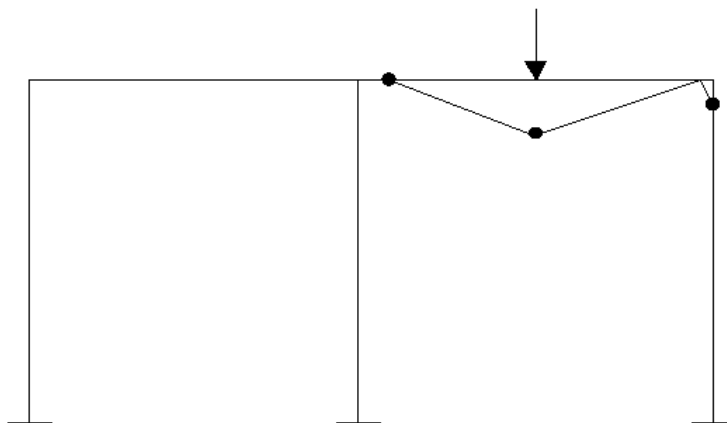


Figure 10.3 Collapse mechanism developed according to work considerations.

As can be seen from Figures 10.1 – 10.3, plastic hinges have developed in almost the same locations as assumed in Chapter 8, but the result is a somewhat different mechanism than expected. The difference is that, in the nonlinear (dynamic) analyses (Figures 10.1 and 10.2), the joint in the middle develop plastic hinges in all three intersecting elements, instead of only in the end of the impacted beam (Figure 10.3). This may be due to the selfweight and live load acting on top of the whole (space) frame in the computer analysis as opposed to in the work considerations which does not account for these loads. The plastic moment capacity is thus somewhat reduced. It may also have something to do with the fact that USFOS considers a redistribution of forces within the structure, while work considerations do not account for this effect. Redistribution of forces is discussed later in this chapter.

In work considerations collapse, whether it is collapse of a single beam or a whole structure, is considered to occur when a sufficient number of hinges has developed to cause a mechanism. When performing calculations of the space frame using work considerations it has been assumed that the impact implies enough energy to cause a mechanism such that the plastic displacement may be estimated. Since the computer analyses confirm that a sufficient number of plastic hinges has developed to cause a mechanism, one might immediately assume that the space frame experiences a collapse. Also, when comparing the two slightly different mechanisms from the computer analyses and hand calculations, it seems likely to assume that a large part of the space frame will collapse instead of only the impacted beam as predicted in the hand calculations, see Figures 10.1 - 10.3. However, a very important difference between the method of work considerations and real life is that a ‘real’ structure subjected to impact loading will be able to distribute the forces throughout the structure (assuming it is redundant), while work considerations only are able to consider redistribution within an element (e.g. the fixed beam with three hinges). Also, the unaffected members in a ‘real’ structure will contribute significantly to restrain the impacted part of the structure from displacement. Therefore, considering the fact that the model in the nonlinear finite element analysis is a space frame (3D) as opposed to the model in the work considerations which is a portal frame (2D), this will have a significant effect on the load carrying capacity of the structure as a whole. An important advantage of USFOS is that it accounts for this redistribution of forces and the effect of adjacent members, which

therefore might be the main reason why the space frame does not collapse even though a sufficient number of plastic hinges has developed.

From an engineering point of view the definition of ‘collapse’ is mainly based on a value for critical strain. NORSOK N-004 (2004) suggests e.g. a critical strain value ε_{cr} of 15 % for tensile fracture in yield hinges for steel quality S 355. This is not necessarily the exact value which will cause fracture, but in a limit state check it is considered as fracture. Thus, if a sufficient number of hinges experience a critical strain of 15 % this might be considered as a collapse of the relevant beam or part of the structure.

The maximum displacement in yield hinges have been calculated according to NORSOK N-004 (2004) and resulted in values of 292 mm and 661 mm for the two different node stiffnesses (see Chapter 8.3). When comparing the lowest value, which is conservative, with the calculated displacement from work considerations (see Figure 10.1), one may conclude that the structure will not experience tensile fracture. This is also confirmed by the computer analyses which show a maximum beam strain of 8.52 % and 9.7 % for method 1 and method 2, respectively (see Chapters 9.1.4 and 9.2.4). The maximum strain value of 15 % suggested by NORSOK N-004 (2004) corresponds to the maximum deflection(s) previously mentioned. One may thus conclude that no part of the structure, including the impacted beam, will experience ‘collapse’ for the specific load scenario.

If a complete design check was to be carried out, other effects such as local buckling and strength of adjacent structure should have been taken into consideration.

Since the integrity of the structure is maintained according to the computer analyses, one may reasonably assume that the structure holds in the first step of an ALS design check. The second step, i.e. checking the resistance in damaged condition (see NORSOK N-001, 2004) has not been considered in this master thesis. If other design criteria were specified, e.g. a maximum value for deflection to ensure that underlying equipment will not be damaged, the resulting maximum deflection from analyses (or from work considerations) should have been checked against this value. In general, deformation (or collapse) of the structure in ALS is accepted as long as it does not cause harm or damage to personnel, assets or environment.

10.3 Comparison of method 1 and method 2

An important difference between the two methods of computer modelling is that in the method where an object (beam) is dropped, the mass is acting *upon* the beam it hits, while in method 2 the mass is attached to the ‘impacted’ beam and follows this up and down causing sinusoidal vibrations. This might have the effect that it *pushes* the beam down instead of *hitting* it like in method 1, with a potential consequence that the impact energy is dissipated somewhat differently in the two methods. It seems possible that the falling mass in method 1 loses more of its energy (at the time of impact) since it *hits* the structure, compared to the mass in method 2 which is only given a corresponding initial velocity and thus does not experience the impact itself. Another way of looking at it is that in method 2 not only the 6000 kg, but also the selfweight, is given an initial velocity of 7.67 m/s since the 6000 kg are defined as nodemass and thus attached to the

‘impacted’ structure. Since the live load is defined as a force, and not as mass, this will probably not include the live load.

If this is the case, method 2 will be applying a larger force to the structure than what a ‘real’ dropped object will do. The fact that kinetic energy, internal energy and plastic work resulting from method 2 are all larger than for method 1, e.g. the internal energy for method 2 is 15 – 20 kNm larger than for method 1, seems to approve to this theory. Also, the graph showing plastic work is quite different for method 1 and method 2, which strongly indicates that there is a difference in the energy (dissipation) in the two methods. This might explain why the resulting maximum displacement (and plastic displacement) is larger for method 2 than for the more authentic modelling in method 1. Based on the fact that method 1 provides a modelling of the dropped object scenario which is closest to reality, this method is considered to give the most accurate results. However, performing analysis of the space frame using method 2 will at least give results to the safe side.

Further study should be carried out in order to obtain a correct answer to the differences between the two modelling alternatives, or to verify the assumptions proposed in this chapter.

10.4 Approximations to real material behaviour

Two important differences between work considerations and nonlinear finite element analyses are to what extent they account for the degree of fixity of the ends of an element and the phenomenon of redistribution of forces within the structure. The latter has also been discussed in Chapter 10.2.

The mechanism method (work considerations) only differs between pinned or fixed ends. It accounts for the properties of the impacted beam, and to some degree it considers the stiffness of the joints, i.e. in conjunction with frames it considers whether a plastic hinge is likely to develop in the end of the beam or in the end of the column, depending on the plastic moment capacity. The nonlinear analysis program (USFOS) however, accounts for the effect of adjacent members; how forces and strains are transferred between elements, axial restraint with development of membrane forces, the actual rotational stiffness etc.

A difference between real structural behaviour and USFOS is that USFOS consider joints that are defined as fixed to be perfectly stiff, i.e. it does not take into account the local stiffness of the joint. In conjunction with the space frame for example, the reduction of the local stiffness caused by the fact that the columns have a width of 150 mm and are connected (welded) to a beam of different width (300 mm), will not be accounted for by USFOS.

Another important aspect is which type of idealized material behaviour that has been assumed. Work considerations presuppose rigid-plastic material behaviour which implies that all of the impact energy is absorbed as rotation of plastic hinges only. The nonlinear analysis program (USFOS) however, implements an elasto-plastic material model which is the closest approximation to real structural behaviour. USFOS also accounts for the important effect of strain hardening, and is, of the methods considered herein, the method that predicts plastic

behaviour most correctly when used by a skilled analyst. However, in many cases the question is if the simple hand calculations provide results that are accurate enough for design so that the more time consuming and more complicated nonlinear (dynamic) computer analysis is unnecessary. Another “disadvantage” of nonlinear finite element analysis programs is that the analyst is required to have a thorough knowledge and understanding of nonlinear methods in order to obtain accurate results.

10.5 Improvements of the calculations

Axial restraint may have a significant influence on the development of tensile forces in a beam in bending, and these forces may contribute considerably to the load-bearing capacity of the beam. Results from the hand calculations could have been made more accurate by taking into account the effect of axial restraint from adjacent members. It requires that an equivalent elastic, axial stiffness is calculated. According to NORSOK N-004 (2004) this is done by performing a static analysis of the structure with the relevant member removed and with unit loads acting in the member axis direction at the end nodes. In conjunction with the check of tensile fracture in yield hinges the equivalent elastic, axial stiffness for the beam subjected to a dropped object was calculated, see Chapter 8.3. This stiffness may be used to find the axial force component N , and it might then be possible to introduce this into work considerations such that the membrane effect is accounted for when calculating maximum deflection or collapse load.

Calculations by the mechanism method consider ends that are either fixed or pinned. It might be possible to define the degree of fixity of a member more accurately by determining the rotational stiffness of the beam ends. The rotational stiffness may be found using the same procedure as defined for equivalent elastic, axial stiffness, with the only difference that unit moments are introduced in the nodes instead of unit loads. This has not been done in this master thesis due to limited time. Also, these improvements imply an increase of the complexity and time consumption of the hand calculations, and it might thus be more reasonable to perform a nonlinear finite element analysis after all.

Method 2 would possibly be more suitable if the mass could have been applied *upon* the beam instead of applying it to the node. In this way the mass would simulate the mass of an actual object more correctly, and only the mass of the ‘impacting object’, not the selfweight, would have been given an initial velocity. It seems likely that the total force affecting the structure would then be closer to reality (and to method 1).

As illustrated in Figure 10.2 (see also Chapter 9.2.3), plastic hinges develop not only in the ends, but also in the middle of two of the adjacent members. This is possible since hinges may be inserted at element ends or at element midspan (USFOS Getting Started, 2001). However, it is not desirable that physical spans are divided in many elements¹ such that we may get plastic hinges on several locations on the span as seen in Figure 10.2. To correct for this, i.e. that USFOS introduces hinges only at locations of impact or in the ends of the physical span, the

¹ In this case the span is divided in four beams due to the space frame being connected to existing structure in two points on each span, see Chapter 6.2.1.

beams may be refined. The span will still be divided in different elements, but without the possibility to develop hinges in ends and midspan of *each* element.

10.6 Other considerations

If this project had been done over again, a few changes of the model would have been done. The falling beam would have been replaced with a rectangular box (e.g. a very short RHS instead of a long one) as to give a more authentic image of the type of dropped object the laydown area could be subjected to, namely a container. Due to time restrictions this was not possible to correct later on. Also, the material density of both the dummy beam and the falling beam would have been set equal to zero instead of subtracting their mass from the total 6000 kg.

One problem with the simulation of the falling object was that it bounces up and down on the impacted beam for some time after impact. By increasing the damping this bouncing was moderated to some extent, but it seems unlikely that a real load of this size (6000 kg) hitting a steel structure would exhibit such behaviour.

Technically, the mass should have been related to a time history in order for the analysis program to understand at which time the mass is activated. By looking at the graphs of displacement, e.g. the graph in Figure 9.10, it seems it is not activated until $t = 20.75$ seconds after all. It may seem that when using the input command `Ini_Vel` the mass is automatically activated at the time specified herein.

11 Conclusion

In this master thesis a space frame subjected to impact loading from a dropped object has been checked in ALS for one specific scenario, and analysed using a finite element analysis software especially developed for nonlinear analysis of offshore structures subjected to extreme loads. The dropped object simulates a container of mass 6000 kg dropped from a crane at height 3 m. The results from the computer analyses have been compared to hand calculations of a portal frame subjected to an impact energy corresponding to the load scenario described above. Hand calculations have been performed using work considerations, and the usefulness of simplified (hand) calculations compared to the more advanced nonlinear (dynamic) analysis has been evaluated for this specific case. Two different modelling alternatives for computer analysis have been carried out and compared to try to assess the suitability of each method. Method 1 includes the modelling of an object of 6000 kg falling from 3 m, connected to the space frame in the point of impact by a hyper elastic spring. In the second modelling alternative, method 2, a nodemass of 6000 kg is attached to the point of impact on the space frame and the corresponding node is given an initial velocity equal to the velocity at impact after a fall of 3 m.

Results show that hand calculations assume a somewhat different collapse mechanism than what is obtained from the computer analyses. This might be due to fact that the nonlinear analysis program takes into account the effect of adjacent members such as axial restraint, partial end fixity and redistribution of forces, which the hand calculations do not consider. When comparing the values for maximum deflection obtained from work considerations and the nonlinear finite element analyses with the maximum deflection in yield hinges calculated according to NORSOK N-004 (2004), one may conclude that the structural integrity is maintained for the specific load scenario and that the structure holds for the first step of an ALS design check.

The influence on the load carrying capacity of the effects mentioned above may to some extent be determined using hand calculations. However, this would result in a more complicated and relatively time consuming task, and the advantage of simplified computational methods compared to advanced nonlinear analysis would then be small.

The work considerations result in larger displacements than the nonlinear finite element analyses, which indicates that the use of hand calculations give a conservative design. It may seem that hand calculations is a reasonable alternative to the more complicated and time consuming nonlinear (dynamic) analyses, assuming that maximum utilization of the structure is not the objective of the design. However, it has not been possible to account for selfweight and live load in the work considerations. Selfweight and live load will cause a reduction in the plastic moment capacity such that yielding will occur for a smaller load when the space frame is subjected to the dropped object. To give a correct evaluation of the suitability of hand calculations for the case of the space frame, the effect of selfweight and live load would have to be accounted for.

Method 2 results in a total displacement which is approximately 18 % larger than what is obtained from method 1. It seems the way the dropped object is modelled in method 2 adds an

extra force to the ‘impacted’ structure compared to method 1. It appears that giving the point of impact an initial velocity do not simulate a real impact as well as hoped.

Modelling alternative No. 1 is a quite complicated and time consuming method, but of the methods considered herein it is the method which physically simulates a real dropped object scenario most correctly. It is therefore assumed that method 1 provides the most accurate structural response, and thus a total displacement which is closest to reality. Except for the modelling of the dropped object scenario, all other conditions are the same for both methods. It therefore seems reasonable to assume that method 2 will give results that are to the safe side. However, further study of method 2 should be done to determine the structural effect of giving the point of impact an initial velocity.

For improvement of method 2, a suggestion is to apply an object *upon* the beam and attach a nodemass equal to that of the dropped object to the end of that beam, then giving this node an initial velocity. In this way, it is only the object impacting the beam which will be given an initial velocity, and this might give a more correct structural response than the method which has been studied in this master thesis.

References

- Bergan, P. G., Larsen, P. K., and Mollestad, E. (1981). *Svingning av konstruksjoner*. Tapir. (In Norwegian).
- Biggs, J. M. (1964). *Introduction to structural dynamics*. McGraw-Hill.
- Cook, R. D., Malkus, D. S., Plesha, M. E., and Witt, R. J. (2002). *Concepts and applications of finite element analysis*. Wiley.
- ESDEP a (European Steel Design Education Programme). *Lecture 2.3.1: Introduction to the Engineering Properties of Steel*. Retrieved 7 April, 2009, from <http://www.esdep.org/members/master/wg02/l0310.htm>
- ESDEP b (European Steel Design Education Programme). *Lecture 7.8.2: Restrained Beams II*. Retrieved 19 March, 2009, from <http://www.esdep.org/members/master/WG07/l0820.htm>
- Horne, M. R. (1979). *Plastic theory of structures*. Pergamon press.
- Irgens, F. (1999). *Fasthetslære*. Tapir.
- NORSOK N-001 (2004). *Structural design*, 4th edition. <http://www.standard.no>.
- NORSOK N-003 (2007). *Actions and action effects*, 2nd edition. <http://www.standard.no>.
- NORSOK N-004 (2004). *Design of steel structures*, 2nd edition. <http://www.standard.no>.
- NORSOK Z-013 (2001). *Risk and emergency preparedness analysis*, 2nd edition. <http://www.standard.no>.
- NS 3472 (2001). *Prosjektering av stålkonstruksjoner – Beregnings- og konstruksjonsregler*, 3rd edition. Norges Standardiseringsforbund (NSF). (In Norwegian).
- Petroleum Safety Authority. (11.02.2008). *The continental shelf*. Retrieved 26.januar, 2009, from <http://www.ptil.no/regulations/the-continental-shelf-article4246-87.html>
- Petroleumstilsynet (Ptil), Statens forurensningstilsyn (SFT), & Sosial- og helsedirektoratet (SHdir). (2002). *Veiledning til Rammeforskriften*. <http://www.ptil.no>. (In Norwegian, available in English).
- RVK (Regelverkskompetanse for petroleumsindustrien) (2006). *Regelverkskompetanse, norsk sokkel; studieguide modularisert opplæringsprogram*. Course material. (In Norwegian).

- Singelstad, A. K. V. (2008). *Response of one-degree systems subjected to impact loads*.
- SINTEF GROUP (2001). *USFOS Getting Started*. Structural Engineering, Marintek, SINTEF GROUP. 'Light version' of the USFOS Theory Manual.
- Skallerud, B. and Amdahl, J. (2002). *Nonlinear Analysis of Offshore Structures*. Research Studies press LTD.
- Store norske leksikon. *Bauschingereffekt*. Retrieved 22 April, 2009, from <http://www.snl.no.ezproxy.uis.no/bauschingereffekt>
- Søreide, T. H. (1985). *Ultimate load analysis of marine structures*. Tapir.
- Søreide, T.H., Amdahl J., Eberg, E., Holmås T., and Hellan, Ø. (1993). *USFOS – A computer program for progressive collapse analysis of steel structures. Theory Manual*. SINTEF Report STF71 F88038, rev. 93-04-02, Trondheim, Norway.
- USFOS Commands: Overview and Description*. (2008). <http://www.usfos.com>.
- USFOS User's Manual: Modelling*. (1999). <http://www.usfos.com>.
- USFOS User's Manual: Program Concepts*. (1999). <http://www.usfos.com>.
- van Raaij, K. (2005). *Dynamic behaviour of jackets exposed to wave-in-deck forces*. Doctoral work, University of Stavanger, Norway.

Appendix A – Input files to nonlinear (dynamic) analysis - Method 1

A.1 Control file

```

HEAD                               Laydown Area DOP
                                U S F O S Dynamic Analysis
                                GEM Install Scale Inh Cab & Pump Skid 2/4M
'
'
'      ncnods
CNODES      1
'      nodex      idof      dfact
          43        3        1.
'
'      End_Time    D_t      dT_Res    dT_pri
Dynamic     20.00    1.0      5.0      5.0
Dynamic     20.76    0.005   0.1      0.1
Dynamic     20.90    0.0001  0.0002  0.0001
Dynamic     22.00    0.005   0.005   0.005
Dynamic     24.00    0.01    0.1      0.1
'
'      Load_case  time_histID
LOADHIST    1      1
LOADHIST    2      1
'
'      TIMEHIST 1  Points
'      Time      Factr
          0.0      0.0
          10.0     1.0
          40.0     1.0
'
'=====  
Cut of dummy element  
=====
'
'      ElmID  Type  {Crit.}
USERFRAC    Element  Time 20 810
'
'=====  
=====
'
'      Rat1  Rat2  Freq1 [Hz]  Freq2 [Hz]
DampRatio   0.02  0.02    0.01    20.0
'
'
Dynres_G    Wt
Dynres_G    Wk
Dynres_G    Wi
Dynres_G    Wext
Dynres_G    Wplast
Dynres_N    vel      902  3
Dynres_N    vel      902  1
Dynres_N    Acc      902  3
Dynres_N    Acc      902  1
Dynres_E    Force    110  2    1
Dynres_E    Disp     110  2    1

```



```
'
      Type (=Local)
Eq_corr Local

CITER
'
      max_on/off
CUNFAL      2
```

A.2 Model file

HEAD FE Model Created from STAAD model

```
'
      Node ID      X      Y      Z      Boundary code
NODE      1      10.000  -12.650  0.000  1 1 1 0 0 0
NODE      2      10.375  -9.250  0.000  1 1 1 0 0 0
NODE      3      15.000  -9.250  0.000  1 1 1 0 0 0
NODE      4      15.000  -12.650  0.000  1 1 1 0 0 0
NODE      5      20.000  -9.250  0.000  1 1 1 0 0 0
NODE      6      20.000  -12.650  0.000  1 1 1 0 0 0
NODE      8      15.000  -14.430  0.850
NODE      9      20.000  -14.430  0.850
NODE     10      10.000  -12.650  2.850
NODE     11      10.375  -14.430  2.850
NODE     12      15.000  -12.650  2.850
NODE     13      15.000  -14.430  2.850
NODE     14      20.000  -12.650  2.850
NODE     15      20.000  -14.430  2.850
NODE     16      10.000  -12.650  3.155
NODE     17      10.375  -9.250  3.155
NODE     18      15.000  -9.250  3.155
NODE     19      15.000  -12.650  3.155
NODE     20      20.000  -9.250  3.155
NODE     21      20.000  -12.650  3.155
NODE     22      15.000  -9.250  3.800
NODE     23      20.000  -9.250  3.800
NODE     24      10.000  -12.650  3.805
NODE     25      10.375  -9.250  3.800
NODE     26      15.000  -12.650  3.805
NODE     27      20.000  -12.650  3.805
NODE     29      15.000  -14.430  4.800
NODE     30      20.000  -14.430  4.800
NODE     31      10.000  -12.650  4.800
NODE     36      10.375  -9.250  4.800
NODE     38      10.375  -9.930  4.800
NODE     39      10.375  -10.610  4.800
NODE     40      10.375  -11.290  4.800
NODE     41      10.375  -11.970  4.800
NODE     42      10.375  -12.650  4.800
NODE     43      12.688  -9.250  4.800
NODE     44      12.688  -12.650  4.800
NODE     46      15.000  -9.250  4.800
NODE     47      15.000  -9.930  4.800
NODE     48      15.000  -10.610  4.800
NODE     49      15.000  -11.290  4.800
NODE     50      15.000  -11.970  4.800
NODE     51      15.000  -12.650  4.800
NODE     52      15.000  -13.350  4.800
```

NODE	55	17.500	-9.250	4.800						
NODE	56	17.500	-12.650	4.800						
NODE	58	20.000	-9.250	4.800						
NODE	59	20.000	-9.930	4.800						
NODE	60	20.000	-10.610	4.800						
NODE	61	20.000	-11.290	4.800						
NODE	62	20.000	-11.970	4.800						
NODE	63	20.000	-12.650	4.800						
NODE	64	20.000	-13.350	4.800						
NODE	67	19.700	-9.250	4.800	0	1	0	0	0	0
NODE	68	15.600	-9.250	4.800	0	1	0	0	0	0
NODE	69	14.400	-9.250	4.800	0	1	0	0	0	0
NODE	70	10.675	-9.250	4.800	0	1	0	0	0	0
NODE	73	10.375	-13.350	4.800						
NODE	74	10.375	-14.430	0.850						
NODE	76	10.375	-14.430	4.800						
NODE	77	10.375	-14.050	4.800						
NODE	79	15.000	-14.050	4.800						
NODE	80	20.000	-14.050	4.800						
NODE	81	12.688	-9.250	3.155						
NODE	82	17.500	-9.250	3.155						
NODE	900	12.688	-9.250	10.000	1	1	1	1	1	1
NODE	901	12.688	-9.250	9.800	1	1	0	1	1	1
NODE	902	12.688	-9.250	7.800	1	1	0	1	1	1

	Elem ID	np1	np2	material	geom	lcoor	ecc1	ecc2
BEAM	1	2	17	1	30183			
BEAM	2	17	25	1	30183			
BEAM	3	25	36	1	30183			
BEAM	4	1	10	1	30073			
BEAM	5	10	16	1	30073			
BEAM	6	16	24	1	30073			
BEAM	7	24	31	1	30073			
BEAM	8	18	3	1	30183			
BEAM	9	22	18	1	30183			
BEAM	10	46	22	1	30183			
BEAM	11	4	12	1	30073			
BEAM	12	12	19	1	30073			
BEAM	13	19	26	1	30073			
BEAM	14	26	51	1	30073			
BEAM	15	20	5	1	30183			
BEAM	16	23	20	1	30183			
BEAM	17	58	23	1	30183			
BEAM	18	6	14	1	30073			
BEAM	19	14	21	1	30073			
BEAM	20	21	27	1	30073			
BEAM	21	27	63	1	30073			
BEAM	22	11	74	1	20343			
BEAM	23	76	11	1	20343			
BEAM	25	13	8	1	20343			
BEAM	26	29	13	1	20343			
BEAM	28	15	9	1	20343			
BEAM	29	30	15	1	20343			
BEAM	32	43	69	1	20376			
BEAM	33	46	68	1	20376			
BEAM	34	55	67	1	20376			
BEAM	35	47	38	1	500			
BEAM	36	47	59	1	500			
BEAM	37	48	39	1	500			
BEAM	38	48	60	1	500			
BEAM	39	49	40	1	500			

BEAM	40	49	61	1	500
BEAM	41	50	41	1	500
BEAM	42	50	62	1	500
BEAM	43	31	42	1	20376
BEAM	44	42	44	1	20376
BEAM	45	44	51	1	20376
BEAM	46	51	56	1	20376
BEAM	47	56	63	1	20376
BEAM	48	52	73	1	500
BEAM	49	52	64	1	500
BEAM	52	79	77	1	20376
BEAM	53	80	79	1	20376
BEAM	56	13	11	1	20343
BEAM	57	15	13	1	20343
BEAM	58	8	74	1	20343
BEAM	59	9	8	1	20343
BEAM	62	36	38	1	20376
BEAM	63	38	39	1	20376
BEAM	64	39	40	1	20376
BEAM	65	40	41	1	20376
BEAM	66	41	42	1	20376
BEAM	71	46	47	1	20376
BEAM	72	47	48	1	20376
BEAM	73	48	49	1	20376
BEAM	74	49	50	1	20376
BEAM	75	50	51	1	20376
BEAM	80	58	59	1	20376
BEAM	81	59	60	1	20376
BEAM	82	60	61	1	20376
BEAM	83	61	62	1	20376
BEAM	84	62	63	1	20376
BEAM	88	11	10	1	20343
BEAM	89	12	13	1	20343
BEAM	90	14	15	1	20343
BEAM	99	39	25	1	30037
BEAM	100	24	40	1	30037
BEAM	102	22	48	1	30037
BEAM	103	26	49	1	30037
BEAM	105	23	60	1	30037
BEAM	106	27	61	1	30037
BEAM	108	67	58	1	20376
BEAM	109	68	55	1	20376
BEAM	110	69	46	1	20376
BEAM	111	36	70	1	20376
BEAM	112	70	43	1	20376
BEAM	113	42	73	1	20376
BEAM	114	73	77	1	20376
BEAM	115	77	76	1	20376
BEAM	116	51	52	1	20376
BEAM	117	52	79	1	20376
BEAM	118	79	29	1	20376
BEAM	119	63	64	1	20376
BEAM	120	64	80	1	20376
BEAM	121	80	30	1	20376
BEAM	122	11	42	1	20343
BEAM	123	13	51	1	20343
BEAM	124	15	63	1	20343
BEAM	125	20	18	1	500
BEAM	126	18	17	1	500
BEAM	127	16	19	1	500
BEAM	128	19	21	1	500
BEAM	129	25	24	1	500

BEAM 141 5 18 1 500
 BEAM 151 6 19 1 500

	Geom ID	H	T-web	W-top	T-top	W-bot	T-bot	Sh_y	Sh_z
IHPROFIL	20343	0.171	0.006	0.180	0.009	0.180	0.009		
IHPROFIL	20376	0.300	0.0110	0.300	0.019	0.300	0.019		

	Geom ID	H	T-sid	T-bot	T-top	Width	Sh_y	Sh_z
BOX	30037	0.100	0.006	0.006	0.006	0.100		
BOX	30073	0.200	0.010	0.010	0.010	0.200		
BOX	30183	0.150	0.010	0.010	0.010	0.150		
BOX	100	0.040	0.006	0.006	0.006	0.040		
BOX	101	0.150	0.010	0.010	0.010	0.150		
BOX	500	0.100	0.004	0.004	0.004	0.100		

	Loc-Coo	dx	dy	dz
UNITVEC	1	0.000	0.000	0.000

	Mat ID	E-mod	Poiss	Yield	Density	ThermX
MISOIEP	1	2.050E+11	3.000E-01	3.550E+08	7.831E+03	1.200E-05

	Load Case	Elem ID	L O A D	I N T E N S I T Y
--	-----------	---------	---------	-------------------

'===== Live load =====

BEAMLOAD	2	32	0.00000E+00	0.00000E+00	-5.10000E+03
BEAMLOAD	2	33	0.00000E+00	0.00000E+00	-5.10000E+03
BEAMLOAD	2	34	0.00000E+00	0.00000E+00	-5.10000E+03
BEAMLOAD	2	35	0.00000E+00	0.00000E+00	-1.02000E+04
BEAMLOAD	2	36	0.00000E+00	0.00000E+00	-1.02000E+04
BEAMLOAD	2	37	0.00000E+00	0.00000E+00	-1.02000E+04
BEAMLOAD	2	38	0.00000E+00	0.00000E+00	-1.02000E+04
BEAMLOAD	2	39	0.00000E+00	0.00000E+00	-1.02000E+04
BEAMLOAD	2	40	0.00000E+00	0.00000E+00	-1.02000E+04
BEAMLOAD	2	41	0.00000E+00	0.00000E+00	-1.02000E+04
BEAMLOAD	2	42	0.00000E+00	0.00000E+00	-1.02000E+04
BEAMLOAD	2	44	0.00000E+00	0.00000E+00	-1.02000E+04
BEAMLOAD	2	45	0.00000E+00	0.00000E+00	-1.02000E+04
BEAMLOAD	2	46	0.00000E+00	0.00000E+00	-1.02000E+04
BEAMLOAD	2	47	0.00000E+00	0.00000E+00	-1.02000E+04
BEAMLOAD	2	48	0.00000E+00	0.00000E+00	-1.02000E+04
BEAMLOAD	2	49	0.00000E+00	0.00000E+00	-1.02000E+04
BEAMLOAD	2	52	0.00000E+00	0.00000E+00	-5.10000E+03
BEAMLOAD	2	53	0.00000E+00	0.00000E+00	-5.10000E+03
BEAMLOAD	2	108	0.00000E+00	0.00000E+00	-5.10000E+03
BEAMLOAD	2	109	0.00000E+00	0.00000E+00	-5.10000E+03
BEAMLOAD	2	110	0.00000E+00	0.00000E+00	-5.10000E+03
BEAMLOAD	2	111	0.00000E+00	0.00000E+00	-5.10000E+03
BEAMLOAD	2	112	0.00000E+00	0.00000E+00	-5.10000E+03

'===== Wind =====

' BEAMLOAD	3	62	1.50000E+03	0.00000E+00	0.00000E+00
' BEAMLOAD	3	63	1.50000E+03	0.00000E+00	0.00000E+00
' BEAMLOAD	3	64	1.50000E+03	0.00000E+00	0.00000E+00
' BEAMLOAD	3	65	1.50000E+03	0.00000E+00	0.00000E+00
' BEAMLOAD	3	66	1.50000E+03	0.00000E+00	0.00000E+00
' BEAMLOAD	3	113	1.50000E+03	0.00000E+00	0.00000E+00
' BEAMLOAD	3	114	1.50000E+03	0.00000E+00	0.00000E+00
' BEAMLOAD	3	115	1.50000E+03	0.00000E+00	0.00000E+00

Appendix B – Input files to nonlinear (dynamic) analysis - Method 2

B.1 Control file

```

HEAD                               Laydown Area DOP
                                U S F O S Dynamic Analysis
                                GEM Install Scale Inh Cab & Pump Skid 2/4M
,
,
,
      ncnods
CNODES      1
,
      nodex   idof   dfact
      43      3     1.
,
      End_Time  D_t    dT_Res  dT_pri
Dynamic  20.00   1.0    5.0    5.0
Dynamic  20.76   0.005  0.1    0.1
Dynamic  20.90   0.001  0.001  0.001
Dynamic  22.00   0.005  0.005  0.005
Dynamic  24.00   0.01   0.1    0.1
,
'==== Input used in method 1, for comparison ====
,
      End_Time  D_t    dT_Res  dT_pri
'Dynamic  20.00   1.0    5.0    5.0
'Dynamic  20.76   0.005  0.1    0.1
'Dynamic  20.90   0.0001  0.0002  0.0001
'Dynamic  22.00   0.005  0.005  0.005
'Dynamic  24.00   0.01   0.1    0.1
=====
,
      Load_case  time_histID
LOADHIST      1      1
LOADHIST      2      1
,
TIMEHIST 1  Points
,
      Time      Factr
      0.0      0.0
      10.0     1.0
      40.0     1.0
,
      Rat1  Rat2  Freq1 [Hz]  Freq2 [Hz]
DampRatio 0.02  0.02   0.01    20.0
,
,
Dynres_G  Wt
Dynres_G  Wk
Dynres_G  Wi
Dynres_G  Wext
Dynres_G  Wplast
Dynres_N  vel      43  3
Dynres_N  vel      43  1
Dynres_N  Acc      43  3
Dynres_N  Acc      43  1
,

```

```

'          Type (=Local)
Eq_corr Local

CITER

'          max_on/off
CUNFAL          2

```

B.2 Model file

HEAD FE Model Created from STAAD model

```

'
Node ID          X          Y          Z          Boundary code
NODE           1          10.000         -12.650         0.000         1 1 1 0 0 0
NODE           2          10.375         -9.250         0.000         1 1 1 0 0 0
NODE           3          15.000         -9.250         0.000         1 1 1 0 0 0
NODE           4          15.000        -12.650         0.000         1 1 1 0 0 0
NODE           5          20.000         -9.250         0.000         1 1 1 0 0 0
NODE           6          20.000        -12.650         0.000         1 1 1 0 0 0
NODE           8          15.000        -14.430         0.850
NODE           9          20.000        -14.430         0.850
NODE          10          10.000        -12.650         2.850
NODE          11          10.375        -14.430         2.850
NODE          12          15.000        -12.650         2.850
NODE          13          15.000        -14.430         2.850
NODE          14          20.000        -12.650         2.850
NODE          15          20.000        -14.430         2.850
NODE          16          10.000        -12.650         3.155
NODE          17          10.375         -9.250         3.155
NODE          18          15.000         -9.250         3.155
NODE          19          15.000        -12.650         3.155
NODE          20          20.000         -9.250         3.155
NODE          21          20.000        -12.650         3.155
NODE          22          15.000         -9.250         3.800
NODE          23          20.000         -9.250         3.800
NODE          24          10.000        -12.650         3.805
NODE          25          10.375         -9.250         3.800
NODE          26          15.000        -12.650         3.805
NODE          27          20.000        -12.650         3.805
NODE          29          15.000        -14.430         4.800
NODE          30          20.000        -14.430         4.800
NODE          31          10.000        -12.650         4.800
NODE          36          10.375         -9.250         4.800
NODE          38          10.375         -9.930         4.800
NODE          39          10.375        -10.610         4.800
NODE          40          10.375        -11.290         4.800
NODE          41          10.375        -11.970         4.800
NODE          42          10.375        -12.650         4.800
NODE          43          12.688         -9.250         4.800
NODE          44          12.688        -12.650         4.800
NODE          46          15.000         -9.250         4.800
NODE          47          15.000         -9.930         4.800
NODE          48          15.000        -10.610         4.800
NODE          49          15.000        -11.290         4.800
NODE          50          15.000        -11.970         4.800
NODE          51          15.000        -12.650         4.800
NODE          52          15.000        -13.350         4.800

```

NODE	55	17.500	-9.250	4.800						
NODE	56	17.500	-12.650	4.800						
NODE	58	20.000	-9.250	4.800						
NODE	59	20.000	-9.930	4.800						
NODE	60	20.000	-10.610	4.800						
NODE	61	20.000	-11.290	4.800						
NODE	62	20.000	-11.970	4.800						
NODE	63	20.000	-12.650	4.800						
NODE	64	20.000	-13.350	4.800						
NODE	67	19.700	-9.250	4.800	0	1	0	0	0	0
NODE	68	15.600	-9.250	4.800	0	1	0	0	0	0
NODE	69	14.400	-9.250	4.800	0	1	0	0	0	0
NODE	70	10.675	-9.250	4.800	0	1	0	0	0	0
NODE	73	10.375	-13.350	4.800						
NODE	74	10.375	-14.430	0.850						
NODE	76	10.375	-14.430	4.800						
NODE	77	10.375	-14.050	4.800						
NODE	79	15.000	-14.050	4.800						
NODE	80	20.000	-14.050	4.800						
NODE	81	12.688	-9.250	3.155						
NODE	82	17.500	-9.250	3.155						

	Elem ID	np1	np2	material	geom	lcoor	ecc1	ecc2
BEAM	1	2	17	1	30183			
BEAM	2	17	25	1	30183			
BEAM	3	25	36	1	30183			
BEAM	4	1	10	1	30073			
BEAM	5	10	16	1	30073			
BEAM	6	16	24	1	30073			
BEAM	7	24	31	1	30073			
BEAM	8	18	3	1	30183			
BEAM	9	22	18	1	30183			
BEAM	10	46	22	1	30183			
BEAM	11	4	12	1	30073			
BEAM	12	12	19	1	30073			
BEAM	13	19	26	1	30073			
BEAM	14	26	51	1	30073			
BEAM	15	20	5	1	30183			
BEAM	16	23	20	1	30183			
BEAM	17	58	23	1	30183			
BEAM	18	6	14	1	30073			
BEAM	19	14	21	1	30073			
BEAM	20	21	27	1	30073			
BEAM	21	27	63	1	30073			
BEAM	22	11	74	1	20343			
BEAM	23	76	11	1	20343			
BEAM	25	13	8	1	20343			
BEAM	26	29	13	1	20343			
BEAM	28	15	9	1	20343			
BEAM	29	30	15	1	20343			
BEAM	32	43	69	1	20376			
BEAM	33	46	68	1	20376			
BEAM	34	55	67	1	20376			
BEAM	35	47	38	1	500			
BEAM	36	47	59	1	500			
BEAM	37	48	39	1	500			
BEAM	38	48	60	1	500			
BEAM	39	49	40	1	500			
BEAM	40	49	61	1	500			
BEAM	41	50	41	1	500			
BEAM	42	50	62	1	500			
BEAM	43	31	42	1	20376			

BEAM	44	42	44	1	20376
BEAM	45	44	51	1	20376
BEAM	46	51	56	1	20376
BEAM	47	56	63	1	20376
BEAM	48	52	73	1	500
BEAM	49	52	64	1	500
BEAM	52	79	77	1	20376
BEAM	53	80	79	1	20376
BEAM	56	13	11	1	20343
BEAM	57	15	13	1	20343
BEAM	58	8	74	1	20343
BEAM	59	9	8	1	20343
BEAM	62	36	38	1	20376
BEAM	63	38	39	1	20376
BEAM	64	39	40	1	20376
BEAM	65	40	41	1	20376
BEAM	66	41	42	1	20376
BEAM	71	46	47	1	20376
BEAM	72	47	48	1	20376
BEAM	73	48	49	1	20376
BEAM	74	49	50	1	20376
BEAM	75	50	51	1	20376
BEAM	80	58	59	1	20376
BEAM	81	59	60	1	20376
BEAM	82	60	61	1	20376
BEAM	83	61	62	1	20376
BEAM	84	62	63	1	20376
BEAM	88	11	10	1	20343
BEAM	89	12	13	1	20343
BEAM	90	14	15	1	20343
BEAM	99	39	25	1	30037
BEAM	100	24	40	1	30037
BEAM	102	22	48	1	30037
BEAM	103	26	49	1	30037
BEAM	105	23	60	1	30037
BEAM	106	27	61	1	30037
BEAM	108	67	58	1	20376
BEAM	109	68	55	1	20376
BEAM	110	69	46	1	20376
BEAM	111	36	70	1	20376
BEAM	112	70	43	1	20376
BEAM	113	42	73	1	20376
BEAM	114	73	77	1	20376
BEAM	115	77	76	1	20376
BEAM	116	51	52	1	20376
BEAM	117	52	79	1	20376
BEAM	118	79	29	1	20376
BEAM	119	63	64	1	20376
BEAM	120	64	80	1	20376
BEAM	121	80	30	1	20376
BEAM	122	11	42	1	20343
BEAM	123	13	51	1	20343
BEAM	124	15	63	1	20343
BEAM	125	20	18	1	500
BEAM	126	18	17	1	500
BEAM	127	16	19	1	500
BEAM	128	19	21	1	500
BEAM	129	25	24	1	500
BEAM	141	5	18	1	500
BEAM	151	6	19	1	500

	Geom ID	H	T-web	W-top	T-top	W-bot	T-bot	Sh_y	Sh_z
IHPROFIL	20343	0.171	0.006	0.180	0.009	0.180	0.009		
IHPROFIL	20376	0.300	0.0110	0.300	0.019	0.300	0.019		

	Geom ID	H	T-sid	T-bot	T-top	Width	Sh_y	Sh_z
BOX	30037	0.100	0.006	0.006	0.006	0.100		
BOX	30073	0.200	0.010	0.010	0.010	0.200		
BOX	30183	0.150	0.010	0.010	0.010	0.150		
BOX	100	0.040	0.006	0.006	0.006	0.040		
BOX	101	0.150	0.010	0.010	0.010	0.150		
BOX	500	0.100	0.004	0.004	0.004	0.100		

	Loc-Coo	dx	dy	dz
UNITVEC	1	0.000	0.000	0.000

	Mat ID	E-mod	Poiss	Yield	Density	ThermX
MISOIEP	1	2.050E+11	3.000E-01	3.550E+08	7.831E+03	1.200E-05

Load Case Elem ID L O A D I N T E N S I T Y

==== Live load =====

BEAMLOAD	2	32	0.00000E+00	0.00000E+00	-5.10000E+03
BEAMLOAD	2	33	0.00000E+00	0.00000E+00	-5.10000E+03
BEAMLOAD	2	34	0.00000E+00	0.00000E+00	-5.10000E+03
BEAMLOAD	2	35	0.00000E+00	0.00000E+00	-1.02000E+04
BEAMLOAD	2	36	0.00000E+00	0.00000E+00	-1.02000E+04
BEAMLOAD	2	37	0.00000E+00	0.00000E+00	-1.02000E+04
BEAMLOAD	2	38	0.00000E+00	0.00000E+00	-1.02000E+04
BEAMLOAD	2	39	0.00000E+00	0.00000E+00	-1.02000E+04
BEAMLOAD	2	40	0.00000E+00	0.00000E+00	-1.02000E+04
BEAMLOAD	2	41	0.00000E+00	0.00000E+00	-1.02000E+04
BEAMLOAD	2	42	0.00000E+00	0.00000E+00	-1.02000E+04
BEAMLOAD	2	44	0.00000E+00	0.00000E+00	-1.02000E+04
BEAMLOAD	2	45	0.00000E+00	0.00000E+00	-1.02000E+04
BEAMLOAD	2	46	0.00000E+00	0.00000E+00	-1.02000E+04
BEAMLOAD	2	47	0.00000E+00	0.00000E+00	-1.02000E+04
BEAMLOAD	2	48	0.00000E+00	0.00000E+00	-1.02000E+04
BEAMLOAD	2	49	0.00000E+00	0.00000E+00	-1.02000E+04
BEAMLOAD	2	52	0.00000E+00	0.00000E+00	-5.10000E+03
BEAMLOAD	2	53	0.00000E+00	0.00000E+00	-5.10000E+03
BEAMLOAD	2	108	0.00000E+00	0.00000E+00	-5.10000E+03
BEAMLOAD	2	109	0.00000E+00	0.00000E+00	-5.10000E+03
BEAMLOAD	2	110	0.00000E+00	0.00000E+00	-5.10000E+03
BEAMLOAD	2	111	0.00000E+00	0.00000E+00	-5.10000E+03
BEAMLOAD	2	112	0.00000E+00	0.00000E+00	-5.10000E+03

==== Wind =====

'BEAMLOAD	3	62	1.50000E+03	0.00000E+00	0.00000E+00
'BEAMLOAD	3	63	1.50000E+03	0.00000E+00	0.00000E+00
'BEAMLOAD	3	64	1.50000E+03	0.00000E+00	0.00000E+00
'BEAMLOAD	3	65	1.50000E+03	0.00000E+00	0.00000E+00
'BEAMLOAD	3	66	1.50000E+03	0.00000E+00	0.00000E+00
'BEAMLOAD	3	113	1.50000E+03	0.00000E+00	0.00000E+00
'BEAMLOAD	3	114	1.50000E+03	0.00000E+00	0.00000E+00
'BEAMLOAD	3	115	1.50000E+03	0.00000E+00	0.00000E+00
'BEAMLOAD	4	56	0.00000E+00	1.50000E+03	0.00000E+00
'BEAMLOAD	4	57	0.00000E+00	1.50000E+03	0.00000E+00
'BEAMLOAD	4	58	0.00000E+00	1.50000E+03	0.00000E+00
'BEAMLOAD	4	59	0.00000E+00	1.50000E+03	0.00000E+00

```

'
'
'
NodeID      Mass
NODEMASS    43      0      0      6000

'
Type      Time      Vx      Vy      Vz      rVx      rVy      rVz      Id_1      Id_2
Ini_Velo  node      20.75    0      0      -7.67    0      0      0      0      43

'
Load Case   Acc_X      Acc_Y      Acc_Z
GRAVITY     1          0.0000E+00  0.0000E+00 -9.8066E+00
    
```

Appendix C – Input file to static analysis for determination of stiffness

```

STAAD SPACE
START JOB INFORMATION
ENGINEER DATE 01-Jun-09
END JOB INFORMATION
INPUT WIDTH 79
UNIT METER KN
JOINT COORDINATES
1 10 0 12.65; 2 10.375 0 9.25; 3 15 0 9.25; 4 15 0 12.65; 5 20 0 9.25;
6 20 0 12.65; 8 15 0.85 14.43; 9 20 0.85 14.43; 10 10 2.85 12.65;
11 10.375 2.85 14.43; 12 15 2.85 12.65; 13 15 2.85 14.43; 14 20 2.85 12.65;
15 20 2.85 14.43; 16 10 3.155 12.65; 17 10.375 3.155 9.25; 18 15 3.155 9.25;
19 15 3.155 12.65; 20 20 3.155 9.25; 21 20 3.155 12.65; 22 15 3.8 9.25;
23 20 3.8 9.25; 24 10 3.805 12.65; 25 10.375 3.8 9.25; 26 15 3.805 12.65;
27 20 3.805 12.65; 29 15 4.8 14.43; 30 20 4.8 14.43; 31 10 4.8 12.65;
36 10.375 4.8 9.25; 38 10.375 4.8 9.93; 39 10.375 4.8 10.61;
40 10.375 4.8 11.29; 41 10.375 4.8 11.97; 42 10.375 4.8 12.65;
44 12.6875 4.8 12.65; 46 15 4.8 9.25; 47 15 4.8 9.93; 48 15 4.8 10.61;
49 15 4.8 11.29; 50 15 4.8 11.97; 51 15 4.8 12.65; 52 15 4.8 13.35;
55 17.5 4.8 9.25; 56 17.5 4.8 12.65; 58 20 4.8 9.25; 59 20 4.8 9.93;
60 20 4.8 10.61; 61 20 4.8 11.29; 62 20 4.8 11.97; 63 20 4.8 12.65;
64 20 4.8 13.35; 67 19.7 4.8 9.25; 68 15.6 4.8 9.25; 73 10.375 4.8 13.35;
74 10.375 0.85 14.43; 76 10.375 4.8 14.43; 77 10.375 4.8 14.05;
79 15 4.8 14.05; 80 20 4.8 14.05;
MEMBER INCIDENCES
1 2 17; 2 17 25; 3 25 36; 4 1 10; 5 10 16; 6 16 24; 7 24 31; 8 18 3; 9 22 18;
10 46 22; 11 4 12; 12 12 19; 13 19 26; 14 26 51; 15 20 5; 16 23 20; 17 58 23;
18 6 14; 19 14 21; 20 21 27; 21 27 63; 22 11 74; 23 76 11; 25 13 8; 26 29 13;
28 15 9; 29 30 15; 33 46 68; 34 55 67; 35 47 38; 36 47 59; 37 48 39; 38 48 60;
39 49 40; 40 49 61; 41 50 41; 42 50 62; 43 31 42; 44 42 44; 45 44 51; 46 51 56;
47 56 63; 48 52 73; 49 52 64; 52 79 77; 53 80 79; 56 13 11; 57 15 13; 58 8 74;
59 9 8; 62 36 38; 63 38 39; 64 39 40; 65 40 41; 66 41 42; 71 46 47; 72 47 48;
73 48 49; 74 49 50; 75 50 51; 80 58 59; 81 59 60; 82 60 61; 83 61 62; 84 62 63;
88 11 10; 89 12 13; 90 14 15; 99 39 25; 100 24 40; 102 22 48; 103 26 49;
105 23 60; 106 27 61; 108 67 58; 109 68 55; 113 42 73; 114 73 77; 115 77 76;
116 51 52; 117 52 79; 118 79 29; 119 63 64; 120 64 80; 121 80 30; 122 11 42;
123 13 51; 124 15 63; 125 20 18; 126 18 17; 127 25 24; 128 5 18; 129 19 16;
130 21 19; 131 6 19;
*****
***** MATERIAL PROPERTIES *****
*****
DEFINE MATERIAL START
ISOTROPIC STEEL
E 2.05e+008
POISSON 0.3
DENSITY 76.8195
ALPHA 1.2e-005
DAMP 0.03
END DEFINE MATERIAL
*****
***** SECTION PROPERTIES *****
*****
MEMBER PROPERTY EUROPEAN
33 34 43 TO 47 52 53 62 TO 66 71 TO 75 80 TO 84 108 109 113 TO 120 -
121 TABLE ST HE300B
22 23 25 26 28 29 56 TO 59 88 TO 90 122 TO 124 TABLE ST HE180A
UNIT MMS KN

```

```

MEMBER PROPERTY EUROPEAN
4 TO 7 11 TO 14 18 TO 21 TABLE ST TUB20020010
MEMBER PROPERTY BRITISH
1 TO 3 8 TO 10 15 TO 17 TABLE ST TUB15015010.0
UNIT METER KN
MEMBER PROPERTY AMERICAN
35 TO 42 48 49 99 100 102 103 105 106 125 TO 131 TABLE ST TUB1001004
*****
***** CONSTANTS *****
*****
UNIT MMS KN
CONSTANTS
BETA 90 MEMB 56 TO 59
BETA 0 MEMB 1
MATERIAL STEEL ALL
*****
***** SUPPORTS, MEMB SPECS, OFFSETS, ETC *****
*****
MEMBER TRUSS
99 100 102 103 105 106 122 TO 124
SUPPORTS
1 TO 6 PINNED
67 68 FIXED BUT FX FY MX MY MZ
*****
***** DEAD LOAD *****
*****
*LOAD 1 DEAD LOAD
*SELFWEIGHT Y -1.1 LIST 1 TO 23 25 26 28 29 33 TO 49 52 53 56 TO 59 62 TO 66 -
*71 TO 75 80 TO 84 88 TO 90 99 100 102 103 105 106 108 109 113 TO 124
***** Unit loads *****
UNIT METER KN
LOAD 7 UNIT LOAD
JOINT LOAD
36 FX 1
46 FX -1
*****
***** LIVE LOAD LAYDOWN AREA *****
*****
*LOAD 2 LIVE LOAD
*MEMBER LOAD
*35 TO 42 UNI GY -10.2
*44 TO 49 UNI GY -10.2
*33 34 52 53 108 109 UNI GY -5.1
*****
PERFORM ANALYSIS
PARAMETER 9
CODE AISC
PERFORM ANALYSIS PRINT ALL
FINISH
    
```